2018

Chromodomain Helicase DNA Binding Protein 1 (Chd1) is required for orofacial development in Xenopus

Brent Wyatt

Chromodomain Helicase DNA Binding Protein 1 (Chd1) is required for orofacial development in *Xenopus*

A dissertation submitted in partial fulfillment of the requirements for the degree of Doctor of Philosophy at Virginia Commonwealth University

by

BRENT HARDIN WYATT
B.S. Biology, East Carolina University 2009
M.S. Molecular Biology and Biotechnology 2013

Director: Amanda Jane Dickinson, Ph.D.
ASSOCIATE PROFESSOR
DEPARTMENT OF BIOLOGY

Virginia Commonwealth University
Richmond, Virginia
May, 2018

ACKNOWLEDGEMENTS

There are no words that can truly express my gratitude to the following people for all the help and support they have provided during my time here at VCU.

My mentor Dr. Amanda Dickinson. She has been a very caring and supportive mentor and has provided me with invaluable advice on research, writing, and presentations. She was a continual source of encouragement and helped me do things I never thought I would be capable of.

My committee members Dr. Greg Walsh, Dr. Jim Lister, Dr. Rita Shiang, Dr. Laura Mathies, and Dr. Shirley Taylor for their advice on research and writing.

My lab members were like family. Nathalie Houssin is one of the kindest people I have ever met and she taught me many of the techniques that I learned here. I regularly asked Stacey Wahl and Allyson Kennedy twenty questions a day and they never turned me away. Nav Bharathan was always happy to help me troubleshoot experiments and provided a lot of positive encouragement during the stressful period of writing my dissertation and preparing for my defense. Deborah Howton was my best friend here and her support helped me continue to strive to better myself.

My family have always been there to support me and I cannot thank them enough for everything they have done for me.

My friend Crystal Beckvold. She reminds me not to give up no matter how hard things seem.

TABLE OF CONTENTS

LIST OF TABLES

LIST OF FIGURES

LIST OF ABBREVIATIONS

ACF	ATP-utilizing chromatin assembly and remodeling factor 1
AP	Alkaline phosphatase
ATP	Adenosine triphosphate
BCIP	5-bromo-4-chloro-3-indolyl-phosphate
Bh	Basihyal
BSA	Bovine serum albumin
C	Celsius
$CaCl_2$	Calcium chloride
cDNA	Complementary Dioxyribonucleic acid
C. elegans	*Caenorhabditis elegans*
Ch	Ceratohyal
Chd	Chromodomain helicase DNA binding protein
ChIP	Chromatin immunoprecipitation
ChIP-seq	Chromatin immunoprecipitation sequencing
Ct	Threshold cycle
CVA	Canonical variate analysis
DFA	Discriminant function analysis

DIG	Digoxigenin
D. melanogaster	*Drosophila melanogaster*
DMSO	Dimethyl sulfoxide
DNA	Dioxyribonucleic acid
D. rerio	*Danio rerio*
DSIF	DRB-sensitivity inducing factor
EDTA	Ethylenediaminetetraacetic acid
ESC	Embryonic stem cell
Eth	Ethmoid
FACT	Facilitates chromatin transcription
GAPDH	Glyceraldehyde 3-phosphate dehydrogenase
HCl	Hydrochloric acid
HDAC	Histone deacetylation
hpf	Hours post fertilization
H. sapiens	*Homo sapiens*
kb	Kilobase
kD	Kilodalton
M	Molar
MAB	Maleic acid buffer
MBS	Modified Barth’s saline
$MgCl_2$	Magnesium chloride
Mk	Meckel’s
µg	Microgram

µl	Microliter
µm	Micrometer
µM	Micromolar
mg	Milligram
ml	Milliliter
mM	Millimolar
M. musculus	*Mus musculus*
MO	Morpholino
NaCl	Sodium chloride
NBT	Nitroetrazolium blue chloride
NCoR	Nuclear receptor corepressor
PAF	Polymerase association factor
PBT	Phosphate buffered saline with tween-20
PFA	Paraformaldehyde
Pq	Palatoquadrate
PVA	Polyvinyl alcohol
qRT-PCR	Quantitative reverse transcription polymerase chain reaction
RAR	Retinoic acid receptor
RARE	Retinoic acid response element
RNA	Ribonucleic acid
rpm	Revolutions per minute
RT-PCR	Reverse transcription polymerase chain reaction
S. cerevisiae	*Saccharomyces cerevisiae*

SMRT	Silencing mediator for retinoid or thyroid hormone receptors
SSC	Saline sodium citrate
TAE	Tris base, acetic acid, ethylenediaminetetraacetic acid
TBP	TATA binding protein
UTR	Untranslated region
WSTF	Williams syndrome transcription factor
X. laevis	*Xenopus laevis*
ZGA	Zygotic gene activation

ABSTRACT

CHROMODOMAIN HELICASE DNA BINDING PROTEIN 1 (CHD1) IS REQUIRED FOR OROFACIAL DEVELOPMENT IN *XENOPUS*

By Brent Hardin Wyatt, PhD.

A dissertation submitted in partial fulfillment of the requirements for the degree of Doctor of Philosophy at Virginia Commonwealth University

Virginia Commonwealth University, 2018

Major Director: Amanda Dickinson, PhD.
Associate Professor, Department of Biology

Abnormalities affecting orofacial development are some of the most common, expensive, and devastating birth defects. Children born with such defects may experience difficulties with eating, breathing, and speech and in addition, these defects often require multiple surgeries to correct them. Therefore, it is critical to understand how the orofacial region develops in order to better treat and prevent these types of birth defects. *Xenopus*

laevis has emerged as a strong model in which to examine orofacial development and was utilized here to investigate the cellular and molecular mechanisms underlying the complex development of the orofacial region. Retinoic acid is one signal involved in orchestrating orofacial development and accomplishes this in part by regulating the nucleosome structure of target genes. The work presented here characterizes the role of an ATP-dependent chromatin remodeler, chromodomain helicase DNA binding protein 1 (Chd1), in orofacial development in *X. laevis.* The spatial expression of Chd1 supports its role in orofacial development and reduced expression of Chd1 resulted in abnormal facial development. Closer examination of Chd1 morphant embryos revealed that Chd1 is required for the expression of important neural crest and cartilage genes that are necessary for proper development of the face. In addition, there was an increase in apoptosis in regions consistent with migrating neural crest and neural crest derived structures. As a consequence, many of the facial cartilages do not form properly in morphant embryos resulting in a smaller face. Further, this work presents evidence that Chd1 may cooperate with retinoic acid to regulate orofacial development in *X. laevis*.

CHAPTER 1 THE ROLE OF CHROMODOMAIN HELICASE DNA BINDING PROTEIN 1 (CHD1) IN OROFACIAL DEVELOPMENT

The face is one of the most important features of humans and is necessary for eating, breathing, communication, and social recognition. Therefore, birth defects affecting the face can be devastating. In addition, such defects can also affect the psychological development of the children born with them (Centers for Disease Control and Prevention, 2018). Some facial defects can be surgically corrected, however, such procedures can be difficult, and usually requires a team of medical professionals and multiple surgeries, resulting in thousands of dollars in healthcare costs. Therefore, it is important to understand how the orofacial region develops to help prevent these defects from occurring.

In this chapter, *X. laevis* was utilized to investigate Chromodomain helicase DNA binding protein 1 (Chd1), a chromatin remodeler that is critical for early development and has been difficult to study in an embryo due to the severity of knockout of this gene (Guzman-Ayala et al., 2015). Therefore, the expression of Chd1 was reduced with titratable antisense oligos in *Xenopus laevis* embryos to characterize the role of Chd1 in orofacial development. This is the first study to elucidate the role of Chd1 during the development of this region. Further, this chapter also presents findings that suggest the possibility of a cooperation between Chd1 and retinoic acid.

INTRODUCTION

Midface and palate development

The developing orofacial region is carefully crafted by the growth and merging of facial prominences through an orchestration of apoptosis, cell division, and cell movements. Such orchestration is regulated by a complex network of signals, transcription factors, and epigenetic factors. In addition, both genetic and environmental factors can impact orofacial development (Chai and Maxson, 2006; Cordero et al., 2011; Jiang et al., 2006; Szabo-Rogers et al., 2010). The orofacial region and surrounding midface tissues are composed of the mouth, primary palate, upper lip, philtrum, nose, and the area between the eyes (Sperber et al., 2010). These structures are created by the growth and fusion of the facial prominences, which include the frontonasal prominence, the paired medial nasal prominences, the paired lateral nasal prominences, and the paired maxillary prominences.

This process of the growth and fusion of the facial prominences begins with the thickening of the ectoderm of the frontonasal prominence to form the nasal placodes. The nasal placodes continue to develop and form the nasal pits and in addition, the medial and lateral nasal prominences arise from cell proliferation around the nasal placodes.

Next, the maxillary prominences push the nasal pits and the medial nasal prominences toward the midline. Following this process, the upper lip forms from the fusion of the maxillary and medial nasal prominences. The distal part of the medial nasal prominence forms the intermaxillary segment, which grows into the oral cavity to form the primary palate. The maxillary prominences will fuse with the primary palate to form the secondary palate (Jiang et al., 2006; Suzuki et al., 2016). Defects in the growth or fusion of these prominences can result in orofacial clefts, midface hypoplasia, or hypertelorism (Suzuki et al., 2016). In non-amniotes such as *Xenopus* and zebrafish, the fusion of these prominences appears to occur directly without a midline epithelial seam that occurs in amniotes (Dudas et al., 2007; Iseki, 2011; Kennedy and Dickinson, 2012; Swartz et al., 2011). Additionally, amniotes form a secondary palate that separates the oral and nasal cavities and fuses with the primary palate, while, non-amniotes do not form a secondary palate, but instead, the primary palate grows posteriorly (Ferguson, 1988). Regardless of these differences between amniotes and non-amniotes, the signaling processes involved in directing the growth and merging of the facial prominences are well conserved (Szabo-Rogers et al., 2010).

Using *Xenopus* to investigate orofacial development

X. laevis has proven to be a valuable tool to study the cellular and molecular mechanisms regulating orofacial development (Dickinson, 2016). *X. laevis* produces large clutches of embryos that develop *ex-utero*, thus, making the face easily visualized throughout development. Further, *X. laevis* embryos do not display head flexure that can make visualization of the orofacial region difficult in other models, such as zebrafish,

mouse, and chick embryos. In addition, orofacial development is well conserved in this species (Dickinson and Sive, 2007). *X. laevis* has long been used in classical embryological studies and the ease of chemical treatments make *Xenopus* a useful model to study chemical genetics. Further, many modern techniques are applicable in *Xenopus*. For instance, molecular loss and gain of function experiments are routine and face transplants are amenable in *X. laevis* (Dickinson, 2016; Dickinson and Sive, 2009; Jacox et al., 2014).

Retinoic acid signaling

The development of the facial prominences is guided in part by retinoic acid signaling (Mark et al., 2004), which regulates proliferation, differentiation, and apoptosis during embryogenesis (Finnell et al., 2004). Retinoic acid is important for the development of the neural crest cells (Brickell and Thorogood, 1997), which contribute to the establishment of the facial primordia. In addition, retinoic acid is necessary for the development of the neural crest derived branchial arches that give rise to head structures (Mark et al., 2004). Over- or under-exposure to retinoic acid during fetal development can disrupt closure of the neural tube and lead to developmental defects, such as orofacial clefts. During palatogenesis, excess retinoic acid can disturb palatal shelf outgrowth, palatal shelf elevation, and shelf fusion, by interfering with cell proliferation and growth factors (Ackermans et al., 2011). When chick embryos are exposed to excess retinoic acid during early stages of development, the upper beak does not form, while the lower beak develops normally (Wedden et al., 1988). Further, the lower jaw forms abnormally into upper jaw-like structures in mice exposed to excess retinoic acid at E8.5, when neural

crest cells are migrating (Abe et al., 2008). The development of neural crest derived craniofacial skeletal elements are also disrupted in mice with compound null mutations of retinoic acid receptors (Lohnes et al., 1994) and ablation of retinoic acid receptors in neural crest cells in mice leads to severe defects in derivatives of branchial arch structures (Dupe and Pellerin, 2009).

Retinoic acid is derived from vitamin A via two oxidation reactions. In the first reaction, alcohol and retinol dehydrogenases oxidize retinol to retinaldehyde. In the second reaction, retinaldehyde dehydrogenase converts retinaldehyde to retinoic acid. In the cell, retinoic acid binds to receptors found in the nucleus to regulate transcription of target genes. These receptors include RARs and RXRs that usually bind as a heterodimer to DNA binding sites called retinoic acid response elements (RAREs) that are found in the regulatory region of target genes. These receptors cooperate with co-repressors and co-activators to regulate the genes targeted by retinoic acid (Niederreither and Dolle, 2008; Rhinn and Dolle, 2012).

When retinoic acid receptors are bound to RAREs in the absence of retinoic acid, the receptors recruit corepressors including nuclear receptor co-repressor (NCoR) and silencing mediator for retinoid or thyroid hormone receptors (SMRT). The corepressors help recruit histone modifiers and chromatin remodelers to stabilize the nucleosome structure so that DNA is inaccessible to the transcriptional machinery (Fig. 1.1A). One such category of a histone modifier recruited by the corepressors are histone deacetyltransferases (HDACs) (Niederreither and Dolle, 2008). HDACs remove acetyl groups from histone proteins resulting in an increase in the positive change of histone tails and encourage stronger interaction between the histones and DNA (Haberland et

al., 2009b). Another category of histone modifiers recruited by the corepressors are histone methyltransferases that methylate lysine residues of histone tails that are associated with transcriptional repression, including H3K9, H3K27, and H4K20. In addition, ATP dependent chromatin remodelers, such as members of the SMARCA family and SWI/SNF complexes, are recruited to further aid in stabilizing the nucleosome structure (Bastien and Rochette-Egly, 2004; Niederreither and Dolle, 2008; Rosenfeld et al., 2006).

When retinoic acid binds to the receptors, the receptors undergo a conformational change that releases the corepressors and creates a binding surface for coactivators, including members of the SRC/p160 family, p300/CBP, and CARM-1. These coactivators destabilize the nucleosome structure also via histone modification and recruitment of ATP-dependent chromatin remodelers (Fig. 1.1B). One such modification is histone acetylation (Bastien and Rochette-Egly, 2004; Niederreither and Dolle, 2008; Rosenfeld et al., 2006), which adds acetyl groups to lysine residues of histone tails and neutralizes the positive charge of these histone tails. This weakens the interaction between histones and DNA (Haberland et al., 2009b). Additionally, histone methyltransferases modify methylation of lysine residues on the histone tails to remove methylation that is associated with transcriptional repression and methylate lysine residues that are associated with transcriptional activation, including H3K4. The coactivators can also interact with the basal transcriptional machinery. (Niederreither and Dolle, 2008; Rosenfeld et al., 2006). Retinoic acid targets numerous genes including Hox genes, signaling factors and hormones, receptors, enzymes, and genes involved in the retinoid pathway (Rhinn and Dolle, 2012).

Retinoic acid is important for midface and palate development in *X. laevis* (Kennedy and Dickinson, 2012). More specifically, decreased retinoic acid signaling during a specific window of orofacial development results in a median cleft in *X. laevis* and mice (Dupe and Pellerin, 2009; Kennedy and Dickinson, 2012). An expression and pathway analysis was utilized to gain insight into how retinoic acid regulates midface development (Kennedy and Dickinson, 2012; Wahl, in prep). In this analysis, embryos were exposed to a RAR inhibitor from stage 24-30 (26-37.5 hpf). After exposure to the RAR inhibitor, the orofacial region of the embryos was dissected and this was followed by isolation of RNA from these orofacial tissues. A microarray analysis was utilized to examine the isolated RNA to identify targets of retinoic acid. One class of genes identified in this work were transcriptional regulators including histone and chromatin modifiers. This prompted the hypothesis that retinoic acid signaling is required for the expression of the transcriptional machinery necessary to perpetuate this signal.

Chromodomain helicase DNA binding protein 1

One gene altered in the expression analysis that may represent a novel regulator of orofacial development was chromodomain helicase DNA binding protein 1, or Chd1. This gene encodes a member of the chromodomain helicase DNA binding protein family and is conserved in metazoans from yeast to humans. There are three domains important for Chd1 function. 1) A pair of N-terminally located chromodomains that function to bind to nucleosomes, 2) a centrally located ATP dependent SNF2-like helicase domain that helps to disrupt the interaction between DNA and histone proteins, and 3) a C-terminally located DNA binding domain that binds preferentially to A+T rich regions. Together, these

domains function to modify chromatin structure to regulate transcription (Hall and Georgel, 2007; Marfella and Imbalzano, 2007).

Most often, Chd1 is associated with active transcription. For example, Chd1 binds to methylated H3K4, which is associated with promoters of active genes in mammals and *Drosophila* (Eissenberg et al., 2007; Flanagan et al., 2005; Sims et al., 2005). Additionally, Chd1 localizes to the interband and puff regions of *Drosophila* polytene chromosomes, which are associated with extended chromatin and high transcriptional activity respectively (Stokes et al., 1996). Further, Chd1 interacts with Rtf1, a subunit of the polymerase association factor (PAF) complex, and Spt5, a component of DRB-sensitivity inducing factor (DSIF) in yeast, both of which are integral for transcriptional elongation (Simic et al., 2003). In addition, Chd1 also interacts with proteins that function to rearrange nucleosomes. One of which is Pob3, a component of the FACT (facilitates chromatin transcription) complex in yeast, and the Pob3 homologue, SSRP1, in mammalian nuclei and drosophila polytene chromosomes (Kelley et al., 1999; Simic et al., 2003). Overall, the role of Chd1 in active transcription is an important part of metazoan development.

On the cellular level, Chd1 is necessary for open chromatin and stem cell pluripotency in mouse embryonic stem cells (Gaspar-Maia et al., 2009). With the complete loss of Chd1, mouse embryos arrest developmentally prior to gastrulation. Further investigation into the cause of the developmental arrest revealed that Chd1 is necessary to facilitate a high transcriptional output. Without this high transcriptional output, the embryo is not capable of generating the cell population that is necessary to progress through the complex morphogenesis and rapid growth of this early developmental phase (Guzman-Ayala et al., 2015). Furthermore, Chd1 is needed to

activate *hmgpi* and *klf5* at zygotic gene activation (ZGA) to control initiation of cell fate specification (Suzuki et al., 2015). An investigation using a conditional knockout of Chd1 specifically in endothelial cells in mouse embryos revealed that Chd1 is important for definitive erythropoiesis. Without Chd1 in endothelial cells, mouse embryos die due to anemia early during development (Koh et al., 2015). While these studies elegantly reveal a critical role for Chd1 during embryonic development in mammals, additional studies are required to better understand the later developmental roles of Chd1, specifically during orofacial development.

Epigenetics modifiers are important for craniofacial development

While there is little information about a potential role for Chd1 during craniofacial development, other epigenetic modifiers are important for craniofacial development (summarized in table 1.1). This includes other members of the CHD family. One such example is Chd7, which is associated with CHARGE syndrome, and can include craniofacial defects such as a square-shaped face, a broad nasal bridge, a small mouth, and cleft lip and/or cleft palate (Zentner et al., 2010). Using cell culture and *Xenopus* embryos, it was shown that Chd7 is important for neural crest specification and migration (Bajpai et al., 2010). Furthermore, this isn't the only member of the CHD protein family associated with craniofacial development. Mutations in Chd8 can result in macrocephaly, hypertelorism, down-slanted palpebral fissures, broad nose, pointed chin, and a broad forehead with prominent supraorbital ridge in humans (Bernier et al., 2014). Macrocephaly was also observed in *Chd8*$^{+/-}$ mouse embryos, and this work revealed that Chd8 regulates cell cycle and histone modification (Platt et al., 2017). Together this data

highlights an important role for CHD proteins in craniofacial development. In addition, there is also a large body of data now emerging that epigenetic modifiers in general are instrumental in coordinating the complex development of neural crest and the embryonic face.

These epigenetic modifiers include other chromatin remodelers such as ATRX. Mutations in ATRX can lead to telecanthus, midface hypoplasia, and a tented upper lip (Gibbons and Higgs, 2000). In addition, mutations in Williams syndrome transcription factor (WSTF), a subunit found in WINAC, WICH, and BWICH chromatin remodelers, is associated with Williams-Beuren syndrome (Lu et al., 1998). These mutations can lead to a broad forehead, flat nasal bridge, a wide mouth, malar flattening, and full cheeks (Burn, 1986; Metcalfe, 1999). Another example is the chromatin organizer CFDP1. It has been suggested that mutations in *CFDP1* may be associated with microcephaly (Messina et al., 2017). Certainly, chromatin modifiers are not the only category of epigenetic modifiers that are important for craniofacial development.

Another category is histone modifiers, such as HDACs and histone methyltransferases. Mutations in Hdac8 can lead to Cornelia De Lange syndrome 5 (Kaiser et al., 2014), which is characterized by dysmorphic facial features including microcephaly, flat midface, downturned corners of the mouth, and micrognathia (Boyle et al., 2015). Additional investigations of HDACs, including Hdac1 and Hdac4, have demonstrated that these proteins are important for formation of the craniofacial cartilage and bone in animal models (DeLaurier et al., 2012; Haberland et al., 2009b; Pillai et al., 2004). Histone methyltransferases and polycomb repressive complexes that have histone methyltransferase activity are also important for the development of the craniofacial

cartilage and bone. For example, the histone methyltransferase, Phf8, is necessary for proper jaw development in zebrafish (Qi et al., 2010). Further, Ezh2, a member of the polycomb repressive complex 2, is important for neural crest positional identity (Minoux et al., 2017) and cartilage and bone formation in mice (Schwarz et al., 2014). In humans, mutations in Ezh2 are associated with Weaver syndrome, which can be characterized by macrocephaly and hypertelorism (Gibson et al., 2012). Another polycomb repressive complex member, Ring1b/Rnf2, is necessary for the development of the craniofacial cartilage, bone, and musculature in zebrafish (van der Velden et al., 2013).

Finally, another factor involved are proteins such as Rai1, which is a protein that interacts with chromatin and is thought to function as a histone code reader (Darvekar et al., 2013). Rai1 has been associated with Smith-magenis syndrome (Carmona-Mora et al., 2010), which can lead to brachycephaly, midface hypoplasia, bow shaped mouth, and prognathism (De Leersnyder, 2013). Investigations into the role of Rai1 during development in *X. laevis* revealed that loss of Rai1 function results in defects in neural crest migration and development of the facial cartilage (Tahir et al., 2014). Together, these studies highlight the importance of epigenetic modifiers in craniofacial development.

Given the complexity of craniofacial development, it was predicted that transcription and epigenetic factors are specifically required for the precise interpretation of signals and the coordination of gene expression necessary for the formation of this structure. Therefore, the purpose of this study is to test the effects of perturbing epigenetic regulators, in particular Chd1, on orofacial development, and further, to determine whether Chd1 cooperates with retinoic acid signaling during midface development.

METHODS

1. Animals

Xenopus laevis embryos were obtained using standard procedures (Sive et al., 2000) approved by the VCU Institutional Animal Care and Use Committee (IACUC protocol number AD20261). Embryos were staged according to Nieuwkoop and Faber (Nieuwkoop and Faber, 1994).

2. Table of Genes

The genes included in this table were identified from an expression analysis conducted on embryos treated with the retinoic acid receptor inhibitor BMS-453. The embryos were treated with 10μM BMS-453 from stages 24-30 (26-35 hpf). Following treatment, the orofacial region was dissected from these embryos for RNA isolation and microarray analysis (Kennedy and Dickinson, 2012) (Wahl in prep). The genes that were decreased by 1.5 fold or greater in this expression analysis were analyzed manually. The accession numbers were used to search the NCBI database to identify the gene name. Then, the gene name was used to search the GeneCards human gene database

(http://www.genecards.org) to identify the function of the protein encoded by these genes. Any genes that were identified to play a role in chromatin regulation, histone modification, transcriptional initiation, or transcriptional elongation were included in the table.

3. Chemical Treatments

a. Transcriptional regulation inhibitors

Stock solutions of the transcriptional elongation inhibitor leflunomide (Sigma L5025), 100uM in DMSO) and the histone deacetylase inhibitor trichostatin A (Sigma T8552, 100mM in DMSO) were created. The stock solution of trichostatin A was further diluted to a concentration of 0.1mM in DMSO. Treatments were performed in 2ml of 0.1X modified Barth's saline (MBS) with 1% DMSO in a 12-well plate. 10 embryos per well were incubated in 200µM leflunomide or 0.1µM trichostatin A from stage 24 (26-27.5 hpf) to stage 29-30 (35-37.5 hpf) at 15°C. Control treated embryos were raised in 0.1X Modified Barth's saline (MBS) with 1% DMSO from stage 24 (26-27.5 hpf) to stage 29-30 (35-37.5 hpf) at 15°C. Embryos were removed from the treatment at stage 29-30 (35-37.5 hpf) and raised to stage 43 (87-92 hpf) in 0.1X MBS, at which point they were fixed in 4% paraformaldehyde (PFA) overnight at 4°C. This was followed by three washes in phosphate buffered saline with tween-20 (PBT).

b. RAR Inhibitor

A stock solution of an RAR inhibitor (BMS-453, Tocris 3409, 10mM in DMSO) was created. This stock solution was further diluted to a concentration of 1mM in DMSO. Treatments were performed in 4ml of 0.1X MBS with 1% DMSO in a 6-well plate. 10

embryos per well were bathed in 1µM BMS-453 from the 2-cell stage (1.5-2 hpf) to stage 43 (87-92 hpf). Control treated embryos were raised in 4ml of 0.1X MBS with 1% DMSO from the 2-cell stage (1.5-2 hpf) to stage 43 (87-92 hpf). The media was refreshed each day during treatment. At the end of treatment, embryos were fixed in 4% PFA overnight at 4°C. This was followed by three washes in PBT.

c. RAR Agonist

A stock solution of the RAR agonist (TTNPB, Tocris 0761, 10mM in DMSO) was created. Treatments were performed in 4ml of 0.1X MBS with 1% DMSO in a 6-well plate. 10 embryos per well were bathed in 2.5µM TTNP at stage 23 (25-26.5 hpf) for four hours at room temperature. Control treated embryos were bathed in 4ml of 0.1X MBS with 1% DMSO at stage 23 (25-26.5 hpf) for four hours at room temperature. At the end of treatment, embryos were placed in 1ml of Trizol for RNA isolation as described in 6b.

4. Imaging

a. Whole embryos

Whole embryos were imaged in a petri dish containing PBT using a dark background. Embryos were imaged using a Zeiss Discovery V8 stereoscope fitted with a Zeiss Axiocam MRc camera.

b. Faces

To obtain images of the face, the head was removed from the body of fixed embryos with a scalpel. This was done by first making a cut through the body at the

posterior end of the gut to remove internal pressure while making the second cut to remove the head. A second cut at the anterior end of the gut was used to remove the head. The heads were positioned in dishes lined with clay and filled with PBT. A glass pipette tool was used to create a depression in the clay in which to place the embryo head. This glass pipette tool was created by first heating the very tip of the pipette over a flame. As the glass soften and began to curve, the pipette was removed from the flame to create a roughly 90° bend. Two pairs of forceps were used to push the clay around the head to hold it in place. Embryos were imaged using a Zeiss Discovery V8 stereoscope fitted with a Zeiss Axiocam MRc camera.

c. In situ

Fixed embryos were placed through a glycerol series. Beginning in PBT, the embryos were incubated in 50% glycerol in PBT, then 75% glycerol in PBT, and finally 100% glycerol. The embryos were incubated at each step of the series until they sank to the bottom of the tube. Whole embryos were imaged in a petri dish containing 100% glycerol on a white background as described in section 4A. To obtain images of the face, the head was removed in PBT as described in section 4B. Next, the heads were placed through the same glycerol series as whole embryos. Finally images were taken as described in section 4B in a dish lined with clay and filled with glycerol. The exception to this is the image of the face at stage 40 (66-76 hpf). These embryos were sectioned using a Leica VT1000P vibrotome to section heads mounted in low melt agarose.

5. Computational analysis of Chd1 gene and protein sequences

The full length sequences for *chd1* for *Homo sapiens* (AF006513.1), *Mus musculus* (NM_007690.3), *Xenopus laevis* L (XM_018264496.1), *Xenopus laevis* S (XM_018244340.1), *Danio rerio* (NM_001128298.2), *Drosophila melanogaster* (NM_057849.5), *Caenorhabditis elegans* (NM_059593.6), and *Saccharomyces cerevisiae* (NM_001179054.1) were retrieved from NCBI. The sequences were aligned with Clustal Omega to determine the percent identity with *H. sapiens*.

Full length sequences for the Chd1 protein for *Homo sapiens* (AAB87381.1), *Mus musculus* (NP_031716.2), *Xenopus laevis* L (XP_018119985.1), *Xenopus laevis* S (XP_018099827.1), *Danio rerio* (NP_001121770.2), *Drosophila melanogaster* (NP_477197.1), *Caenorhabditis elegans* (NP_491994.2), and *Saccharomyces cerevisiae* (NP_011091.1) were retrieved from NCBI. The sequences were aligned with Clustal Omega to determine the percent identity with *H. sapiens*.

The sequence corresponding to the chromodomains and helicase domain for *H. sapiens, M. musculus, D. rerio, D. melanogaster, C. elegans, and S. cerevisiae* were identified by accessing the Chd1 sequence on the NCBI protein database and choosing the graphics format to determine the position of these domains within the sequence. The helicase domain was represented by the span of sequence that included the SNF2 family N-terminal domain and the helicase conserved C-terminal domain. The full length protein sequences for Chd1 in all species mentioned above were aligned with the full length protein sequence for Chd1 in *X. laevis* by utilizing Clustal Omega. The overlapping region corresponding to the chromodomains and helicase domains from the analyzed species was used to determine the position of the chromodomains and helicase domain in *X.*

laevis. The percent identity with *H. sapiens* for the chromodomains and helicase domain for each species was determined with the multiple alignment in Clustal Omega.

The DNA binding domain was identified in *M. musculus* (Delmas et al., 1993). The sequence corresponding to the DNA binding domain in the other species was identified by performing a multiple alignment with Clustal Omega between the full length Chd1 protein for *M. musculus* and the full length Chd1 protein sequence for the other analyzed species. The percent identity was determined with the multiple alignment in Clustal Omega.

6. RT-PCR to detect chd1 expression levels and splicing defects in morphants

a. Isolating tissues

To determine if *chd1* was expressed at various stages of development, RNA was isolated from 10 whole embryos that were at the unfertilized, 1-cell, blastocyst, and gastrulation stages. To investigate *chd1* expression at stages 24 (26-27.5 hpf), 30 (35-37.5 hpf), 35 (50-53.5 hpf), and 40 (66-76 hpf), RNA was isolated from 15 embryo heads at each stage. The heads were removed from the body of fixed embryos with a scalpel. This was done by first making a cut through the body at the posterior end of the gut. Then the head was removed with a second cut at the anterior end of the gut.

To determine the efficiency of Chd1-MO1, RNA was isolated from 10 whole embryos at stage 26 (29.5-31 hpf).

b. RNA extraction and cDNA synthesis

Isolated tissues were collected in 1ml of Trizol (Ambion 15596026). The tissues were mechanically homogenized with a sterile, disposable pestle. The solution was centrifuged at 14,800g for 10 minutes at 4°C to separate the soluble and insoluble portions. The soluble portion was moved to a clean tube and the insoluble portion was discarded. 200µl of chloroform was mixed with the soluble portion. The mixture was centrifuged at 12,000g for 30 minutes at 4°C to separate the phases. The aqueous phase was moved to a clean tube, while the remaining phase was discarded. 500µl of isopropyl alcohol was added to the aqueous phase to precipitate the RNA. This mixture was centrifuged at 12,000g for 20 minutes at 4°C to collect the precipitated RNA at the bottom of the tube. The isopropyl alcohol was removed and the precipitated RNA was washed with 1ml of 70% ethanol. This was centrifuged at 7500g for 10 minutes at 4°C to collect the precipitated RNA at the bottom of the tube. The ethanol was removed and the RNA was resuspended in 50µl of nuclease free water. The resuspended RNA was mixed with 25µl of a lithium chloride solution (Ambion AM9480) and incubated overnight at -20°C. This mixture was centrifuged at 14,800g for 30 minutes at 4°C. The lithium chloride solution was removed and discarded. The RNA was washed in 1ml of 70% ethanol. This was centrifuged at 14,800g for 30 minutes at 4°C. The ethanol was removed and the RNA was resuspended in 20µl of nuclease free water.

1µg of RNA was used to synthesize cDNA using the Qiagen quantitect reverse transcription kit (Qiagen 205311) or the biosystems high capacity cDNA reverse transcription kit (Thermofisher 4368814).

c. RT-PCR

RT-PCR was performed with Apex 2x hotstart taq master mix (Cat. Number 42-144) on a BioRad MJ Mini Personal Thermocycler. Primers were designed to target the 3' end of *chd1* to determine expression of *chd1*. These primer sequences were Chd1-F: GGTCAGTTCCCATGAAGAAG and Chd1-R: ATGAGCAGCTTTGGTGTG.

Primers were designed to target exon 1 and exon 3 of *chd1* to determine the efficiency of Chd1-MO1 to block splicing. Chd1MO1-F: GCGATGAAGACAATGTAAGC targeted exon 1 and Chd1MO1-R: CATCTGAGCCACTGTTTGAA targeted exon 3 of *chd1*. Exon 2 was predicted to be absent in the product of this reaction. To translate the predicted product, exon 2 of *chd1* was identified on xenbase.com and the *chd1* sequence without exon 2 was translated using A Plasmid Editor software.

The PCR products were analyzed on a 2% agarose gel prepared with molecular grade agarose (Bioline BIO-41025) in TAE buffer.

d. qRT-PCR of craniofacial genes

RNA was isolated from 30 embryo heads using the Trizol method followed by a lithium chloride precipitation as described in section 6B. cDNA was prepared using the applied biosystems high capacity cDNA reverse transcription kit (Thermofisher 4368814). qRT-PCR was performed with SensiFAST SYBR No-Rox (Bioline BIO-98002) on a Bio-Rad CFX96 Real Time PCR system. The relative amounts of amplification were calculated using the delta-delta CT method and were normalized to expression levels of GAPDH. Primer sequences are in table 1.2.

e. qRT-PCR for Chd1 expression after exposure to RAR agonist

qRT-PCR was performed as described in section 6d. The relative amounts of amplification were calculated using the delta-delta CT method and were normalized to expression levels of actin. Primer sequences are in table 1.2.

7. In situ hybridization

a. Probe preparation

DIG labeled RNA probes for Chd1 were prepared using a plasmid template containing a partial sequence for *Xenopus* Chd1 from Dharmacon (Catalog #: MXL1736-202727035, Clone ID: 6643113, Genbank #: BC094094). This sequence targeted the 3' end of chd1 including a portion of the 3' UTR generating a probe that was 2894 base pairs in length. BLAST (NCBI) analysis suggested this sequence was specific to Chd1 and not well conserved with other CHD proteins.

The plasmid was linearized with SacI (NEB R0156S) for synthesis of the antisense probe. While the plasmid was linearized with MluI (NEB R0198S) for synthesis of the sense probe. The restriction digest reactions were purified by gel extraction (Qiagen Qiaquick gel extraction kit, Qiagen 28706). 2µg of template DNA was used in a 20µl reaction containing 1X transcription buffer (NEB B9012S), 1X DIG RNA labeling mix (Roche 11277073910), 40 units RNAsin (Bioline BIO-65027), and 1X T7 RNA polymerase (NEB M0251S) for the antisense probe, or 1X SP6 RNA polymerase (NEB M0207S) for the sense probe. The reactions were incubated in a 37°C water bath for 5 hours. After incubation, 30µl of nuclease free water and 25µl of a lithium chloride solution (Ambion AM9480) were added to the reaction tube and incubated overnight at -20°C. This mixture

was centrifuged at 14,800g for 30 minutes at 4°C. The lithium chloride solution was removed and discarded. The RNA was washed in 1ml of 70% ethanol. This was centrifuged at 14,800g for 30 minutes at 4°C. The ethanol was removed and the RNA was resuspended in 20µl of nuclease free water. Since the probe was large (3894 base pairs) and did not work well in preliminary experiments, hydrolyzation was utilized to create shorter fragments of the probe (expected to be about 300 base pairs) (Sive et al., 2000). To do this, 1µg of probe was hydrolyzed in 40mM sodium bicarbonate and 60mM sodium carbonate for 60 minutes at 60°C. The hydrolyzed probe was precipitated in a solution containing 200µl water, 25µl 3M sodium acetate, and 600µl ethanol. The solution was centrifuged at 14,800g for 10 minutes. After centrifugation, the supernatant was removed and the probe was resuspended in 20µl of nuclease free water.

b. Hybridization and visualization

In situ hybridization was performed as described in (Sive et al., 2000), omitting the proteinase K treatment. Embryos were fixed in 4% PFA overnight at 4°C. After three washes in PBT, embryos were dehydrated in a methanol series in PBT: 25% to 50% to 70% to 80% to 90% to 100%. Once in 100% methanol, embryos were incubated overnight at -20°C. The embryos were rehydrated by reversing the methanol series and ending in PBT. After three washes in PBT, embryos were rinsed twice in 0.1M triethanolamine. The embryos were then incubated in a mixture of 12.5µl acetic anhydride and 4ml of 0.1M triethanolamine and this was repeated twice. Next, the embryos were washed three times in PBT and bleached (1.5% hydrogen peroxide and 5% formamide in 2X SSC) on a light box. Embryos were washed in 2X SSC followed by two washes in PBT. Next, embryos

were incubated in hybridization buffer (50% formamide, 5X SSC, 5mg/ml torula RNA, 0.1% tween-20, and 50µg/ml heparin) at 60°C overnight. The embryos were incubated with the hydrolyzed probe in hybridization buffer overnight at 60°C. Unbound probe was washed out by first incubating in warm hybridization buffer at 60°C, then four washes in 2X SSC at 60°C, followed by four washes in 0.2X SSC at 60°C for 45 minutes each. There was an additional wash in 0.2X SSC at room temperature and then three washes in maleic acid buffer (MAB) (150mM maleic acid, 100mM NaCl, 0.1% tween-20, 7.9g/L NaOH, pH 7.5) for 30 minutes each. This was followed by an incubation in block solution (10% Blocking reagent (Roche 11096176001), 10% lamb serum, 80% MAB) for 3 hours at room temperature. Embryos were incubated overnight at 4°C in 0.63µl of anti-Digoxigenin-AP (Roche 11093274910) diluted in 1ml of block solution. The embryos were washed six times in MAB and two times in alkaline phosphatase (AP) buffer (50mM Tris pH 9.5, 50mM NaCl, 25mM MgCl2, 0.05% tween-20, 20g/L PVA) for 30 minutes each. Finally, bound probe was detected with NBT/BCIP (36µl 50mg/ml NBT (Promega S380C) and 28µl 50mg/ml BCIP (Promega S381C)) in 10ml of AP buffer with 1mM levamisole (Acros Organics 187870100). The staining reaction was stopped with two washes in AP buffer followed by two washes in PBT. Embryos were fixed in 4% PFA overnight at 4°C and then washed three times in PBT. Embryos were imaged as described in section 4C.

8. Morpholino knockdown

Antisense morpholinos were purchased from GeneTools; Chd1MO1: CTAGTCACTTTACCTCTTGCTCCATC Chd1MO2: CTTCATCGCTATGTCCATTCATTGT. A standard control morpholino was obtained from

GeneTools. Microinjections were performed using an Eppendorf femtojet microinjector and a Zeiss Discovery V8 stereoscope. Embryos were placed in a dish lined with nylon Spectra mesh (1000 µm opening and 1350 µm thickness) at the bottom to hold embryos in place and filled with 3% Ficoll 400 (Fisher Bioreagents BP525) dissolved in 0.1X MBS. The injections were performed at the 1-cell stage. After injection, embryos were moved to a dish containing 0.1X MBS and raised to stage 43 (87-92 hpf) at 15°C. Embryos were fixed in 4% PFA overnight at 4°C and were then washed three times in PBT. Images were taken as described in section 4 A-B.

9. Measurements and morphometrics

Measurements were performed with Axiovision40 software (Zeiss) based on the method described in (Kennedy and Dickinson, 2014a, b). Face height was determined on frontal views of embryo faces by measuring the distance from the top of the eyes to the top of cement gland along the midline. The intercanthal distance was determined by measuring the distance between the eyes. Measurements are expressed in µm.

Twenty-seven landmarks were chosen to represent the shape of the face for geometric morphometric analysis. These landmarks were placed on images of the embryo faces by utilizing the pointpicker plugin of ImageJ software (NIH). The coordinates of these landmarks were entered into MorphoJ software (Klingenberg et al., 2010) to align the data by procrustes fit and eliminate information about scale, size, position, and orientation. A canonical variate analysis (CVA) was used to determine the variance between groups relative to the variance within each group. This analysis converted variance into components. These components, also known as canonical variates, were

displayed in a scatter plot to illustrate the relationship between the analyzed groups. The further the distance between canonical variates, the more different those groups were. This data was also displayed as a three dimensional transformation grid for Chd1-MO1 morphants to show the relative changes of the landmark positions of the morphants compared to control embryos. A discriminate function analysis (DFA) was utilized to examine the relationship between embryos treated with the RAR inhibitor (BMS-453), Chd1-MO1 morphants, and their respective controls. The output of the DFA was displayed on a three dimensional transformation grid.

10. Alcian blue staining

Cartilages were stained using standard protocols (Taylor and Van Dyke, 1985) with some modifications. Embryos were fixed in Bouins fixative overnight at 4°C. The fixative was washed out in 70% ethanol. Next, embryos were immersed in alcian blue stain (0.1mg/ml alcian blue (Sigma A-5268) in 1 part acetic acid and 4 parts ethanol) for 4 days at room temperature. Embryos were washed in 1% HCl in 70% ethanol four times. Next, the embryos were rehydrated through an ethanol series in PBT: 70% ethanol to 50% ethanol to 25% ethanol to 100% PBT. Embryos were fixed in 4% PFA for two hours followed by three washes in PBT. Next, the embryos were bleached (1.5% hydrogen peroxide and 5% formamide in 2X SSC) on a light box. After three washes in PBT, the embryos were incubated in 2% KOH three times. Finally, the embryos were cleared in a series of 2% KOH and glycerol: 50% KOH and 50% glycerol to 40% KOH and 60% glycerol to 20% KOH and 80% glycerol to 100% glycerol. Facial cartilages were imaged in 100% glycerol.

11. Flow Cytometry

50 embryo heads were dissected as described in section 6A and collected in 1X MBS on ice. Single cells were obtained using a protocol adapted from (Lee et al., 2012). The tissues were mechanically digested in 0.5X calcium free Ringer's solution (58 mM NaCl, 1.45 mM KCl, 2.5 mM HEPES, pH 7.2). The cells were washed three times in 0.5X calcium free Ringer's solution and two times in 1X PBS. Cells were dissociated by incubating them in 0.25% Trypsin/EDTA (Sigma T4049) and 5 mg/mL collagenase type 2 (Worthington LS004174) for 20 minutes at 37°C. The suspension was passed through a 40µm cell strainer (Greiner Bio-One 542040) and centrifuge at 3000 rpm for 2 minutes at 4°C. Cells were resuspended in 5% goat serum in 1X PBS and centrifuged at 3000 rpm for 2 minutes at 4°C. Finally, cells were labeled with propidium iodide staining solution (100 mM Tris pH 7.5, 154 mM NaCl, 1 mM CaCl2, 0.5 mM MgCl2, 0.2% Bovine Serum Albumin (BSA), 0.1% Nonidet P-40, 86 µg/mL RNAse A (Thermoscientific EN0531), and 20 µg/mL propidium iodide) for 1 hour. Cells were passed through a cell strainer prior to analysis on the flow cytometer. Cells were analyzed with a Canto - BD FACSCanto II Analyzer.

12. Immunohistochemistry

Embryos were fixed in 4% PFA for two hours at room temperature. After three washes in PBT, embryos were dehydrated in a methanol series: 25% to 50% to 70% to 80% to 90% to 95% to 100%. Next, embryos were bleached (1% hydrogen peroxide in

methanol) for several days until bleached. After rehydrating the embryos through the reverse of the methanol series, the embryos were washed three times in PBT. Endogenous alkaline phosphatases were inactivated by incubating embryos in hybridization buffer (50% formamide, 5X SSC, 5mg/ml torula RNA, 0.1% tween-20, and 50µg/ml heparin) for three hours at 65°C. After five washes in PBT, embryos were incubated in block solution (1% goat serum, 5% BSA, 0.1% triton) overnight at 4°C. Next, the embryos were incubated with anti-rabbit cleaved caspase 3 antibody (Cell Signaling 9661S) diluted 1:1000 in PBT overnight at 4°C. After three washes in PBT, embryos were incubated in goat anti-rabbit AP secondary (Cat. # 0751-1506) diluted 1:500 in PBT overnight at 4°C. The embryos were washed three times in PBT and then three times in AP buffer (50mM Tris pH 9.5, 50mM NaCl, 25mM MgCl2, 0.05% tween-20, 20g/L PVA) with 2mM levamisole. The color was developed by incubating embryos with NBT/BCIP (Roche 11697471001) in AP buffer. The coloration reaction was stopped by washing the embryos two times in AP buffer then two times in PBT with 5mM EDTA. Embryos were fixed in 4% PFA and then imaged after three washes in PBT.

13. RARE analysis

The 10kb sequence upstream of the transcription start site for each gene was retrieved from xenbase.org. These sequences were examined for transcription factor binding sites using PATCH public 1.0 software. The parameters were set to scan vertebrate sites with a minimum site length of 6 and 0 mismatches. The mismatch penalty was set at 100 with a lower score boundary of 87.5. The output was examined for the frequency of RAR binding sites.

14. Statistical analysis

Chi-square test was utilized to determine if differences in phenotype prevalence were statistically significant. Kruskal-Wallis test by ranks was utilized to determine if differences in facial size measurements were statistically significant. Student's t-test was utilized to determine if differences in expression based on qRT-PCR analysis were statistically significant.

RESULTS

1. Transcriptional regulators are required for orofacial development

Orofacial development is a complex process involving multiple signals to shape this region. With the multifaceted nature of this signaling network, it takes an intricate system of transcription and epigenetic factors to regulate a cell's response (Chai and Maxson, 2006; Jiang et al., 2006; Szabo-Rogers et al., 2010). Retinoic acid is one signal involved and was used here to investigate changes to transcriptional regulators during a specific time window of orofacial development (Kennedy and Dickinson, 2012).

a. Inhibition of retinoic acid receptor function results in decreased expression of transcriptional regulators

Inhibition of retinoic acid receptors during early orofacial development results in embryos with a median cleft (Kennedy and Dickinson, 2012). Expression analysis of the orofacial tissues of these embryos revealed that transcriptional regulators represented the group that was most altered in response to decreased RAR function (Wahl in prep). This data was analyzed to identify genes that were decreased by at least 1.5 fold and

were also involved in 1) chromatin regulation, 2) histone modification, 3) transcriptional elongation, or 4) transcriptional initiation (summarized in table 1.3). This analysis revealed twelve chromatin regulators which included seven ATP-dependent chromatin remodelers, four histone chaperones, and one chromatin organizer. In addition, nine histone modifiers which included two histone acetyltransferases, one histone deacetyltransferase, five histone methylases, and one histone demethylase were identified. Finally, three transcriptional elongation factors and one transcriptional initiation factor were identified.

Further scrutiny of these proteins revealed that a subset are involved in regulation of retinoic acid receptor function. Histone deacetylases and SWI/SNF chromatin remodeling complexes are known to be recruited by corepressors and coactivators bound to retinoic acid receptors to regulate retinoic acid signaling (Niederreither and Dolle, 2008). The identification of a histone deacetylase and members of the SWI/SNF family in the expression analysis suggest that retinoic acid receptor function may be necessary to maintain expression of genes encoding proteins essential for its own regulation. Further, this analysis may also indicate novel players such as CHD proteins in the regulation of retinoic acid receptor function.

b. Inhibition of transcriptional regulators during early orofacial development can cause midface defects

Next, two of the identified transcriptional processes were perturbed to determine if they are generally required during early orofacial development. To test this, embryos were exposed to pharmacological inhibitors that target transcriptional elongation and histone

deacetylation. These embryos were treated using the same experimental procedure as those embryos treated with the retinoic acid receptor inhibitor (Kennedy and Dickinson, 2012). In brief, embryos were treated with a pharmacological inhibitor from stage 24 (26-27.5 hpf) to 30 (35-37.5 hpf). After the treatment, the embryos were removed from the antagonist and were then raised to stage 42-43 (80-92 hpf) for analysis (Fig. 1.2A).

One prominent category identified in the expression analysis was transcriptional elongation. This included the genes *tceb3*, *rtf1*, and *isw1*, and additionally, the chromatin regulators *chd1* and *spt16* that also function to facilitate this process were identified as well. To inhibit transcriptional elongation, leflunomide, which has been shown to effectively inhibit transcriptional elongation and cause craniofacial defects in zebrafish (White et al., 2011) was utilized. Leflunomide works by inhibiting dihydroorotate, an enzyme involved in the biosynthesis of pyrimidine, thus, reducing the nucleotide pool (McLean et al., 2001). Results revealed that 100% of embryos exposed to leflunomide had smaller faces indicated by a reduced intercanthal distance of at least 25% (n=20, 2 biological replicates, p-value = 2.5E-10; Fig. 1.2B, D, F, H). This result suggests that transcriptional elongation is an important process during this early stage of facial development. Since transcriptional elongation occurs in a chromatin environment in a cell, this raised the question of the importance of chromatin regulation during this process.

Another prominent category identified was histone modification, therefore the effect of repressive histone modifications, namely histone deacetylation, on early facial development was investigated. Histone deacetylation by HDACs causes a tighter association between histones and DNA, thereby inhibiting transcription (de Ruijter et al., 2003). These proteins play a role in transcriptional repression of genes targeted by

retinoic acid in the absence of retinoic acid binding to receptors (Urvalek and Gudas, 2014). Inhibition of histone deacetylation with the HDAC inhibitor, Trichostatin A, has been shown to result in histone hyperacetylation and inhibition of the cell cycle in zebrafish (Ignatius et al., 2013). Trichostatin A inhibits class I, II, and IV HDACs (Yoshida et al., 1995) and works through an interaction with zinc ion at the catalytic active site, thereby chelating this metal ion that is necessary for nucleophilic attack on the substrate employed by HDACs to hydrolyze acetyl-L-lysine side chains in histone proteins (Finnin et al., 1999; Lombardi et al., 2011). Results revealed that 100% of embryos exposed to Trichostatin A had a smaller face, mouth, and eyes (n=20, 2 biological replicates, p-value = 2.5E-10; Fig. 1.2C, E, G, I). Furthermore, these embryos had abnormally shaped mouths that were more round in shape compared to controls suggesting that proper regulation of histone acetylation and deacetylation is necessary for early orofacial development. Together, these results highlight that the transcriptional processes of elongation and histone deacetylation are generally required during early orofacial development.

2. Chd1 is important for facial development in *Xenopus laevis*

The results in the previous section suggested that not surprisingly, transcriptional regulation is indeed critical for orofacial development. Next, the focus was turned to one particular regulator, Chd1, which was identified in a microarray expression analysis of face tissues that were deficient in retinoic acid signaling and was among the most highly altered genes in this analysis. This gene represented a novel regulator that has not been previously examined in orofacial development. Previous work in the lab has also validated

this microarray expression analysis using RT-PCR with two different primer sets (unpublished and Wahl et al in prep). To determine whether Chd1 is required for orofacial development, a series of classic developmental experiments was performed. First, a multiple alignment was utilized to establish whether Chd1 was conserved between frogs and other species. Next, the localization of *chd1* expression was investigated with *in situ* hybridization. Finally, Chd1 expression levels were reduced to gain insight into the role of this chromatin remodeler. Further, the changes in the face of embryos with reduced Chd1 expression were quantified through traditional measurements and geometric morphometric analysis.

a. The Chd1 gene and protein is well conserved across vertebrates

Evidence from yeast, flies, mice, and humans suggest Chd1 functions as a chromatin remodeler across metazoans (Hall and Georgel, 2007). If this protein has similar functions across such phyla, then it would be expected that the gene, protein, and domain structure would be well conserved. To test this hypothesis, gene, protein and domain sequence alignments were performed. The open reading frame of the *chd1* gene from *Mus musculus, Xenopus laevis, Danio rerio, Caenorhabditis elegans, Drosophila melanogaster, and Saccharomyces cerevisiae* was aligned with *Homo sapiens*.

First, the L and S forms of chd1 in *X. laevis* were aligned. These two forms are the result of a genome duplication that resulted in allotetraploidy in *X. laevis*. This alignment revealed that the L and S forms are 95% identical. Next, both the L and S forms were compared with the other species and this alignment revealed that the *chd1* gene is well

conserved. The L and S forms of *X. laevis chd1* were 77.63% and 78.12% identical to human *CHD1* respectively. This was 10% less than mice and 7% more than zebrafish. Overall, this represents conservation among vertebrates. There was, as expected, less similarity with the invertebrate species. *D. melanogaster* was 53.20% identical, *C. elegans* was 54.86% identical, and *S. cerevisiae* was 50.37% identical to human *chd1* (Table 1.4).

Next, the Chd1 protein was compared between these species. First, the L and S forms of *X. laevis* Chd1 were aligned and this analysis revealed that they were 96% identical. Next, these sequences were aligned with the other species. The L and S forms of *X. laevis* Chd1 were 84.93% and 85.46% identical to human Chd1. This was 11% less identical than mouse Chd1 and 5% more identical than zebrafish Chd1. There was less conservation with the invertebrate species. *D. melanogaster* was 49.48% identical, *C. elegans* was 47.11% identical, and *S. cerevisiae* was 38.43% identical to human Chd1 (Table 1.4). This result prompted a closer examination of the functional domains of Chd1.

The chromodomains, helicase domain, and DNA binding domains are presumably critical for the function of Chd1 and conservation of these would be further evidence of conserved function. The organization of the protein domains were analyzed and this revealed that the organization was similar between these species (Fig. 1.3). Next, a multiple alignment of these domains was performed to determine the identity between the species. The L and S forms of *X. laevis* chromodomain 1 was 78% and 80% identical to human chromodomain 1. This was 17% less than mouse and 7% less than zebrafish. *D. melanogaster* was 57.14% identical, *C. elegans* was 51.11% identical, and *S. cerevisiae* was 56.10% identical to human chromodomain 1. The L and S forms of chromodomain 2 were both 90.74% identical to human chromodomain 2. This was 4% less than mouse

and only 0.17% more than zebrafish. *D. melanogaster* was 48.08% identical, *C. elegans* was 34.04% identical, and *S. cerevisiae* was 28.85% identical to human chromodomain 2 (Table 1.4).

Next, the helicase domain was aligned and this revealed that this domain was the most conserved between these species. The L and S forms of *X. laevis* were 94.51% and 93.56% identical with the human helicase domain. This was 5% less than human and 1% more than zebrafish. *D. melanogaster* was 74.22% identical, *C. elegans* was 69.78% identical, and *S. cerevisiae* was 54.89% identical with the human helicase domain (Table 1.4).

Finally, the DNA-binding domain was aligned and this revealed that there was strong conservation among vertebrates. The L and S forms of the *X. laevis* DNA binding domain were 90.75% and 91.67% identical to human DNA binding domain. This was 7% less than mouse and 3% more than zebrafish. *D. melanogaster* was 48.66% identical, *C. elegans* was 38.35% identical, and *S. cerevisiae* was 30.35% identical to the human DNA binding domain sequence (Table 1.4). Together, these results suggest that Chd1 is conserved across phyla and likely has a similar function in these species.

b. Chd1 is expressed during early development in the head and presumptive heart of X. laevis embryos

Next, the spatiotemporal expression of Chd1 during *X. laevis* development was investigated. The temporal expression of *chd1* was examined by utilizing reverse

transcription polymerase chain reaction (RT-PCR) at various stages of development. Next, the spatial expression of *chd1* was examined by utilizing RNA in situ hybridization.

The expression of *chd1* was examined with RT-PCR at eight different stages to determine when *chd1* is expressed during early development in *X. laevis*. Expression was examined in whole embryos at the unfertilized, 1-cell, blastula, and gastrulation stages. Further, expression was also examined in embryonic heads at stages 24 (26-27.5 hpf), 30 (35-37.5 hpf), 35 (50-53.5 hpf), and 40 (66-76 hpf). This analysis revealed that *chd1* was expressed at all eight of these stages of development (Fig. 1.4A). In agreement with these results, mouse chd1 is expressed maternally and through pre-implantation development (Guzman-Ayala et al., 2015). Together, these results suggest that Chd1 has an important role during early embryonic development in *X. laevis*.

Next, the spatial localization of *chd1* at various stages was examined by utilizing RNA in situ hybridization to gain more insight into the role of Chd1 during early embryonic development. At stage 24-25 (26-29.5 hpf), *chd1* was expressed throughout the head with enriched expression in the eye and a stripe under the eye. Expression was absent in other areas of the embryo at this stage (Fig. 1.4Bi, i', ii). At stage 29-30 (35-37.5 hpf), *chd1* was expressed in the face with an enrichment in the developing eye, otic vesicle, and in the branchial arches. During early tadpole stages (stage 34-35, 44.5-53.5 hpf) *chd1* expression was localized in regions around the eye, the brain, the anterior face, and the presumptive heart (Fig. 1.4Bv, v', vi). Finally, at stage 40 (66-76 hpf), *chd1* was localized to the head and face, with enriched expression around the eye and in the brain ventricles (Fig. 1.4Bvii, vii', viii). The expression on the dorsal side of the tail observed at stages 34-35 (44.5-53.5 hpf) and 40 (66-76 hpf) was also observed faintly in the respective sense

controls. Therefore, the expression observed in the tail may not be specific to *chd1* expression. Together, these results suggest Chd1 could have a role in craniofacial development and prompted further investigation into this possibility.

c. Decreased Chd1 results in developmental defects including abnormal orofacial development

To investigate the role of Chd1 in the development of the face, an antisense oligo (Morpholino (MO), Gene Tools) was utilized to reduce Chd1 levels and evaluate the effect. Chd1-MO1 was designed to bind to the splice donor site at the exon 2 - intron 2 boundary and inhibit access of the splicing machinery to this region of the pre-mRNA. It was predicted that this would result in a splicing defect that would lead to the deletion of exon 2. To test this, RT-PCR was utilized to determine whether this MO could in fact cause a splicing defect. More specifically, this RT-PCR assay was designed to determine whether binding of this MO would result in the deletion of exon 2. RNA was extracted from embryos injected with 65-75ng of Chd1-MO1 or an equal amount of a standard control morpholino (Fig. 1.5A). The RNA was isolated from the embryo heads at stage 29-30 (35-37.5 hpf). Primers specific to exon 1 and exon 3 of *chd1* were used to determine whether exon 2 was present based on the size of the amplified PCR product. A PCR product of 339 base pairs would indicate that exon 2 was still present and Chd1-MO1 did not block splicing as expected. However, a PCR product of 152 base pairs would indicate exon 2 was deleted and Chd1-MO1 effectively blocked splicing. The result of this PCR assay revealed that the smaller 152 base pair product was present in RNA from Chd1-

MO1 morphants, therefore suggesting that exon 2 was deleted in these morphant embryos (Fig. 1.5A-B). Translation of the chd1 sequence without exon 2 revealed numerous stop codons beginning with one in exon 3. This suggests that the altered chd1 sequence would not likely produce a functional Chd1 protein.

Next, the effect of reduced Chd1 levels was examined by injecting embryos with Chd1-MO1 at the 1-cell stage. Embryos injected with 15-25ng of Chd1-MO1 developed normally and embryos injected with 35-45ng of Chd1-MO1 had a mild reduction in the size of the embryo head. Embryos injected with 65-75ng of Chd1-MO1 displayed several developmental defects and this amount was chosen for use in further investigations. Chd1 expression was reduced by injecting 65-75ng of Chd1-MO1 at the 1-cell stage and examining embryos at stage 43 (87-92 hpf). This morpholino was fluorescently tagged so that the embryo could be visually assessed after injection. The injected embryos were manually sorted based on similar fluorescence intensity and similar expression pattern of the fluorescence through the embryo. Embryos with similar intensity and expression pattern of fluorescence would indicate that these embryos received a similar amount of Chd1-MO1, and thereby, reducing the amount of variability in the morphants. 100% of Chd1-MO1 morphants were smaller than embryos injected with control morpholino. Further, the tail curved ventrally in 55% of Chd1-MO1 morphants. There was also edema observed in the anterior ventral region, near the developing heart and gut, in 85% of Chd1-MO1 morphants. In 55% of Chd1-MO1 morphants, there was blistering in the skin along the edges of the tail (Fig. 1.5C-D).

Closer inspection of the face revealed that 100% of Chd1-MO1 morphants had narrower faces. The mouth was smaller and more circular in shape in 88% of Chd1-MO1

morphants compared to control embryos. Furthermore, in a subset of these morphant embryos, the mouth was missing. Finally, there were eye defects in 36% of Chd1-MO1 morphants. These defects included smaller eyes, abnormally shaped eyes, and in some cases, missing eyes (Fig. 1.5C-D). The variability may have been due to the difficulty of injecting the exact same amount of morpholino into every embryo. While careful sorting of the injected embryos based on fluorescence can reduce variability, it does not completely eliminate the variability. Together, these results suggest Chd1 is important for development of the face. Further, the narrowing of the face prompted me to quantify the changes in the size and shape of the face in Chd1 morphants.

The narrowing of the face in Chd1-MO1 morphants may be the result of defects in the development of the midface. Tissue deficiencies in midface development can lead to median craniofacial hypoplasia. This may result in defects in the development of the forebrain, the nasal structures, and the palate (Allam et al., 2011). The intercanthal distance, or distance between the eyes, and the face height were measured to investigate whether there were deficiencies in the development of the midface in Chd1-MO1 morphants.

The intercanthal distance was decreased by 52% in Chd1-MO1 morphants when compared to controls (p-value < 0.001, $n = 33$, 3 biological replicates Fig 1.6A). While the face height was increased by 21% in Chd1-MO1 morphants compared to controls (p-value < 0.001, $n = 33$, 3 biological replicates Fig 1.6A). Further, the intercanthal to face height ratio in control embryos was 2.10, while the ratio in Chd1-MO1 morphants was 0.80. Therefore, the intercanthal distance was twice the face height in control embryos, while the intercanthal distance was less than the face height in Chd1-MO1 morphants.

These results suggest that the faces of Chd1-MO1 morphants were quantitatively narrower. The next question was whether the faces of Chd1-MO1 morphants were simply smaller or if there was a change in the shape of the face in these embryos as well.

Therefore, geometric morphometric analysis was utilized to examine the shape the face of Chd1-MO1 morphants. Twenty-seven landmarks were chosen to represent the shape of the face (Fig. 1.6B). These landmarks were aligned using MorphoJ software to eliminate differences in the size of the embryos. Canonical variant analysis was utilized on the data generated from this alignment to determine how loss of Chd1 affected the shape of the face. This analysis revealed variability in Chd1-MO1 morphants, while there was less variability in control embryos. Additionally, there was a statistically significant difference between control and Chd1-MO1 morphant embryos (p-value < 0.0001) (Fig. 1.6C). This difference was highlighted when vectors showing the changes in landmark position were superimposed on a transformation grid (Fig. 1.6D). This revealed that landmarks were shifted inward toward the midline and outward toward the dorsal and ventral regions of the head in Chd1 morphants. Together, these results suggest a role for Chd1 in the development of the face.

d. The defects in morphants are specific to loss of Chd1

A second morpholino, Chd1-MO2, was utilized to ensure the phenotypic changes in Chd1-MO1 morphants were specifically the result of reduced expression of Chd1. If two different morpholinos resulted in similar phenotypic changes in morphant embryos, then this would suggest that the changes were due to reduced expression of the targeted

gene and not due to off target effects. This is because it is unlikely that two different morpholinos would have the same off target effects, assuming these off target effects were the cause of the phenotype.

Chd1-MO2 was designed to block translation by overlapping the translation start site. Embryos were injected with 30-40ng of Chd1-MO2 at the 1-cell stage and examined at stage 43 (87-92 hpf) (Fig. 1.7A-B). 35% of Chd1-MO2 morphants were smaller than embryos injected with an equal amount of control morpholino. Further, in 25% of Chd1-MO2 morphants, there was curvature in the tail. In some cases, this was similar to the ventral curvature observed in Chd1-MO1 morphants. In other cases, the tail curved dorsally, or appeared crooked and curved dorsally and then back ventrally. There was also edema observed in the anterior ventral region near the developing heart and gut similar to Chd1-MO1 morphants in 20% of Chd1-MO2 morphants. Also like Chd1-MO1 morphants, there was blistering of the skin along the edges of the tail in 20% of Chd1-MO2 morphants (Fig. 1.7C-D).

Examination of the face revealed that 35% of Chd1-MO2 morphants had narrower faces. Further, 55% of Chd1-MO2 morphants had smaller and misshapen mouths. The shape was more circular compared to controls. Finally, 40% of Chd1-MO2 morphants had eye defects. These defects included smaller eyes and misshapen eyes (Fig. 1.7C-D). Together, these phenotypes were similar to those observed in Chd1-MO1 morphants. However, there were differences in the percentage of morphant embryos displaying these phenotypes. This may have been due to (1) the different type of morpholino used and (2) the different amount of morpholino that was injected into embryos. Chd1-MO2 was a translation blocking morpholino and this type of morpholino can sometimes have a

stronger effect on embryos. This is because translation blocking morpholinos can bind to maternally expressed messenger RNAs (mRNAs) and thereby, prevent translation of these maternal transcripts. However, splice blocking morpholinos, such as Chd1-MO1, will only bind to unspliced RNA and therefore, not have the early effect on maternally expressed transcripts. The initial injections of Chd1-MO2 at higher concentrations caused high incidences of embryonic death in injected embryos. Therefore, the amount that was injected was reduced. Taken together, these two conditions may have contributed to observed differences in the percentages of affected morphant embryos. Overall, the similarities between Chd1-MO1 and Chd1-MO2 morphants suggest that the phenotypes are the result of loss of Chd1 and not off target effects.

3. Decreased Chd1 results in changes in orofacial genes and cartilage development

The data in the previous section strongly suggested that reduced expression of Chd1 resulted in changes in the size and shape of the developing face. This prompted me to investigate potential mechanisms that may contribute to these changes. Since Chd1 is a transcriptional regulator, the changes in Chd1 morphants may be due to changes in gene expression in these embryos. Furthermore, the craniofacial cartilage and bone provides structure to the face and changes in the facial cartilages may result in changes in the size and shape of the face.

a. Decreased Chd1 results in changes in orofacial genes

Chd1-MO1 morphants and embryos injected with a standard control morpholino were raised to stage 29-30 (35-37.5 hpf) and then the heads of these embryos were dissected for RNA isolation. Quantitative reverse transcription polymerase chain reaction (qRT-PCR) was utilized to investigate the relative transcript levels of a subset of genes highly expressed in the face and that were also downregulated upon RAR inhibition (Fig. 1.8A). These genes were normalized to *gapd*h expression to determine relative changes in their expression. This analysis revealed that *lhx8* expression was unaffected by reduced expression of Chd1, while the expression of *alx4* and *pdgfra* was slighted elevated. Expression of the homeobox transcription factor, *msx2*, was reduced. Further, expression of the neural crest gene, *ap2*, and the cartilage genes, *has2* and *six2*, were also reduced (Fig. 1.8B). This was an interesting result, especially considering that the neural crest is known to contribute to craniofacial cartilage and bone development (Mayor and Theveneau, 2013). The reduced expression of *ap2*, together with the reduced expression of *has2* and *six2*, may indicate that there are changes in the facial cartilages in Chd1-MO1 morphants. Therefore, the facial cartilages in Chd1-MO1 morphants were examined next.

b. Decreased Chd1 results in reduced and missing cartilages

The craniofacial cartilage helps provide the underlying structure as the base of the shape of the face. Therefore, any changes in the development of the facial cartilage

could lead to changes in facial shape. To investigate cartilage, Alcian blue staining was utilized to compare the cartilages in Chd1 morphants and control embryos. Embryos were injected at the 1-cell stage with 65-75ng of Chd1-MO1 or an equal amount of control morpholino. Embryos were allowed to develop until stage 45 (98-106 hpf) when the cartilages in the face have formed (Fig. 1.8C). The cartilages were well formed in control embryos. However, the cartilages were reduced or missing in Chd1 morphants. This was apparent in the reduced size of the ceratohyal and Meckel's cartilages. The ceratohyal cartilage helps form the floor of the mouth (Rose, 2009) and the Meckel's cartilage helps form the lower jaw (Altig and McDiarmid, 1999). Additionally, the ethmoid cartilage that forms the roof of the oral cavity (Altig and McDiarmid, 1999) was missing in many Chd1 morphants (Fig. 1.8D). The changes in the cartilages were consistent with the reduced size and defects observed Chd1 morphants.

4. Decreased Chd1 results in increased cell death

Decreases in cell proliferation or increases in cell death could also be a contributing factor to the decreased size observed in Chd1 morphants. In mice there are defects in the cell cycle and increased apoptosis in *Chd1*$^{-/-}$ embryos (Guzman-Ayala et al., 2015). To investigate if this is also true in frogs, flow cytometry was utilized to characterize the cell cycle profile in Chd1 morphants. Immunohistochemistry was also utilized to detect phospho-histone H3, a marker for chromatin condensation of cells entering into the mitotic phase (Hendzel et al., 1997), and cleaved caspase 3, a marker for apoptotic cells (Elmore, 2007), to examine whether there were changes in cell death in Chd1 morphants.

a. Decreased Chd1 results in an increased number of cells in the sub-G1 fraction

The initial analysis began with investigating the cell cycle in Chd1 morphants. To do this embryos were injected with 65-75ng of Chd1-MO1 or an equal amount of control morpholino at the 1-cell stage. The heads of injected embryos were dissected and collected at stage 29-30 (35-37.5 hpf) for cell dissociation and isolation. The cells were labeled with propidium iodide for flow cytometry (Fig. 1.9A). There were small decreases in the G0/G1, S, and G2/M phases of the cell cycle in stage 29-30 (35-37.5) Chd1-MO1 morphants, suggesting little change in cell proliferation (Fig. 1.9B). Consistent with this, there was no change in phospho-histone H3 labeling in Chd1 morphants (Fig. 1.9C). Interestingly, there was a larger proportion of cells in the sub-G1 fraction in Chd1-MO1 morphants (Fig. 1.9B). This fraction contains cells that have lost some of their DNA, which happens primarily when cells are undergoing apoptosis (Arends et al., 1990; Nagata, 2000; Nagata et al., 2003). These results suggested that there may be an increase in cell death in Chd1-MO1 morphants, and perhaps, this may also be a contributing factor to the reduction in the size of morphant embryos.

b. Decreased Chd1 results in an increase in cleave caspase 3 positive cells

To investigate cell death further, immunohistochemistry was utilized to detect cleaved caspase 3. To do this, Chd1-MO1 morphants were raised to stage 29-30 (35-37.5 hpf). Next, a colormetric assay was used to detect bound cleaved caspase 3

antibody in Chd1-MO1 morphants (Fig. 1.10A). There was a dramatic increase in the number of cleaved caspase 3 positive cells in Chd1 morphants compared to control embryos. These cleaved caspase 3 positive cells were enriched in the face, eyes, brain region, and along the back of the embryo near the neural tube (Fig. 1.10B). Furthermore, the regions containing an enrichment of cleaved caspase 3 positive cells are similar to the regions containing an enrichment of chd1 expression (Fig. 1.4B). Together, these results suggest that reduced Chd1 expression leads to increased apoptosis.

5. Chd1 cooperates with retinoic acid during orofacial development

Retinoic acid signaling is necessary for the development of the orofacial region. Since inhibition of retinoic acid receptor function resulted in decreased levels of *chd1*, this prompted me to investigate a potential connection between retinoic acid and Chd1. The aim of this analysis was to determine whether the changes in facial development in Chd1 morphants was similar to embryos treated with a retinoic acid receptor inhibitor. In addition, a bioinformatic approach was utilized to search for the presence of retinoic acid receptor binding sites upstream of the Chd1 transcription start site.

a. Some changes in the facial shape are similar between Chd1 morphants and embryos exposed to the RAR inhibitor

The size and shape of the face in *X. laevis* are altered when either Chd1 expression is decreased or RAR function is inhibited. This prompted an investigation of how similar the changes were between these two groups. To do this, embryos were

injected with 65-75ng of Chd1-MO1 or a standard control morpholino at the 1-cell stage and raised to stage 43 (87-92 hpf), or exposed to 1μM of the RAR inhibitor from the 2-cell stage (1.5-2 hpf) to stage 43 (87-92 hpf) (Fig. 1.11A). The treatment strategy with the RAR inhibitor was extended, compared to the treatment strategy used in previous experiments, so that it was more closely comparable to injection of Chd1-MO1. Next, the intercanthal distance and face height were measured for both of these treatment groups. The intercanthal distance was reduced by 52% and the face height was increased by 26% in Chd1 morphants compared to controls. In embryos exposed to the RAR inhibitor, the intercanthal distance was reduced by 45% and the face height was increased by 20% compared to controls (Fig. 1.11B-C). These results indicate that the face is narrower in embryos with decreased Chd1 expression or exposure to a RAR inhibitor. Next, these embryos were examined with morphometric analysis to determine if the changes in the shape of the face were also similar.

Chd1 morphants and embryos exposed to the RAR inhibitor were analyzed using 27 landmarks that represented the shape of the face (Fig. 1.12A-B). The landmarks were aligned by Procrustes fit and then examined with canonical variant analysis to determine the similarity between the treatment groups. Canonical variate 1 accounted for 63.962% and illustrates that Chd1 morphants and embryos exposed to the RAR inhibitor are different from controls, which is indicated by the greater distance between clusters on the canonical variate 1 axis. The clusters for Chd1 morphants and embryos exposed to the RAR inhibitor are separated by a shorter distance along the canonical variate 1 axis, suggesting that the faces of these embryos are more similar to each other than they are to controls. Canonical variate 2 accounted for 30.891% and suggests that there are some

differences between the faces of Chd1 morphants and embryos exposed to the RAR inhibitor, based on the greater distance between clusters on the canonical variate 2 axis. Canonical variate 3 accounted for 5.146% and illustrates that the faces of Chd1 morphants and embryos exposed to the RAR inhibitor are very similar based on the short distance between clusters on the canonical variate 3 axis. Next, a discriminate function analysis was utilized to examine the differences between Chd1 morphants and embryos exposed to the RAR inhibitor. The results were presented as vectors superimposed on a transformation grid in order to visualize the changes in the landmarks between these two groups. There was not much difference between many of the landmarks, indicated by short vectors, especially in the superior region of the face and in the midface. There were some longer vectors in the inferior region of the face, near where the lower jaw develops. Together, these results suggest that there are some similarities in the changes that occur in the size and shape of Chd1 morphants and embryos exposed to the RAR inhibitor.

b. Retinoic acid binding sites are enriched in the 10,000 base pairs upstream of the Chd1 TSS

Chd1 may be regulated by retinoic acid directly. Therefore, a bioinformatics approach was utilized to identify possible binding sites for RARs. RARs bind to retinoic acid response element (RARE) sites and the presence of these in the region upstream of the Chd1 transcription start site would support the potential for direct regulation of Chd1 by retinoic acid. The RARE consensus sequence is 5'-(A/G)G(G/T)TCA-3' and is the binding site for retinoic acid receptors (Rhinn and Dolle, 2012). PATCH software was

utilized to identify RARE sites in the 10,000 base pairs upstream of the Chd1 transcription start site. 53 RARE sites were found in this region (Fig 1.13). It is possible that the core hexameric sequence could occur by chance alone. However, it would only be expected for the sequence to occur by chance alone about 10 times in 10,000 base pairs. This suggests that RARE sites are present in the region upstream of the Chd1 transcription start site about 5X more than by chance alone. Other genes that are known to be targets of retinoic acid, such as Fgf8 and Rai1 (Abe et al., 2008; Imai et al., 1995), have 41 and 46 sites respectively in the 10,000 base pairs upstream of their transcription start sites (Fig. 1.13A-D). Therefore, the frequency of RARE sites upstream of Chd1 is similar to known targets of retinoic acid.

RARE sites usually occur as a direct repeat spaced 1, 2, or 5 base pairs apart. Therefore, a more stringent analysis was utilized to determine if any of the RARE upstream of Chd1 occurred as a direct repeat. This analysis revealed that the RARE sites upstream of Chd1 did not occur as direct repeats. Next, an alternative consensus sequence, 5'-(A/G)G(G/T)T(G/C), was considered. This consensus motif was identified from the alignment of known RARE motifs found in retinoic acid target genes that are spaced five base pairs apart. This alignment included RARE motifs found in the promoters of human and mouse genes involved in retinoic acid metabolism, retinoic acid signaling, and in development (Lalevee et al., 2011). Analysis with this sequence revealed the presence of one site that occurred as a repeat spaced 5 base pairs apart that was located 6212 base pairs upstream of the Chd1 transcription start site (5'-AGTTGAtttatAGGTGA-3'), and may represent a site that is bound directly by retinoic acid receptors.

c. Exposure to a RAR agonist increases Chd1 expression

The presence of a potential RARE site upstream of the Chd1 transcription start site suggested the possibility that retinoic acid may directly regulate Chd1. To investigate this further, stage 23 (25-26.5 hpf) embryos were exposed to 2.5μM an RAR agonist (TTNPB) for four hours. At the end of treatment, RNA was isolated from these embryos and analyzed with qRT-PCR. The results of this analysis revealed that the expression of Chd1 doubled in response to exposure to the RAR agonist (Fig. 1-14A). This result suggests that retinoic acid is upstream of Chd1, and together with a potential RARE site upstream of the Chd1 transcription start site, supports the possibility that retinoic acid directly regulates Chd1.

d. Comparison of expression of Chd1 and RARγ

The similarities in the face shape changes in Chd1 morphants and embryos with reduced RAR function prompted further comparisons between these two groups. First, comparison of Chd1 and RARγ expression revealed that there was enriched expression of Chd1 in a region under the eye that was similar to the expression of RARγ at stage 29-31 (35-40 hpf). Further, this expression is in a region that surrounds the developing future mouth. At stage 40 (66-76 hpf), there was similar expression both under the eye and in a region in the midface between the eye and the developing brain (Fig. 1-14B). Together, the similarities in spatial localizations supports that Chd1 and retinoic acid may cooperate to regulate gene expression.

e. Comparison of cartilage defects between Chd1 morphants and embryos deficient in RARγ function

The changes in the shape of the face between these two treatments may be explained by similar changes in the craniofacial cartilages. To gain insight into whether the changes in the cartilages were similar, embryos were exposed to 1μM of the RAR inhibitor, BMS453, from the 2-cell stage (1.5-2 hpf) to stage 45 (98-106 hpf) or injected with 65-75ng of Chd1-MO1 at the 1-cell stage and raised to stage 45 (98-106 hpf). Overall, the cartilage defects were more severe in embryos exposed to the RAR inhibitor. However, there were some similarities, particularly, in the more severe Chd1 morphants. In embryos exposed to the RAR inhibitor, the ceratohyal and Meckel's cartilages were severely reduced and many of the other facial cartilages were missing and indiscernible. This was similar to Chd1 morphants in which the ceratohyal and Meckel's cartilages were reduced and many of the other facial cartilages were missing and indiscernible (Fig. 1.14C). In the less severe Chd1 morphants, the ceratohyal and Meckel's cartilages were also reduced, but not as severely as these cartilages were in embryos exposed to the RAR inhibitor. Together, the abnormalities in development of the craniofacial cartilages between Chd1 morphants and embryos deficient in RARγ function further support the possibility that Chd1 and retinoic acid cooperate to regulate gene expression.

DISCUSSION

This study is the first to examine the role of Chd1 specifically in orofacial development. Reduced Chd1 expression results in a narrower face, which correlates with missing or smaller facial cartilages. Such defects could be caused by an increase in cell death and defects in expression of genes required for neural crest development and cartilage differentiation. Further, Chd1 may cooperate with retinoic acid to regulate orofacial development.

Chd1 is required for craniofacial development in *X. laevis*

In mice, knockout of Chd1 results in embryonic arrest following implantation, ultimately leading to the death and resorption of the embryo (Guzman-Ayala et al., 2015). Therefore, the role of Chd1 in later developmental events, such as facial development, could not be assessed in these studies. Here, titratable morpholinos were utilized to reduce the levels of Chd1 and allow the embryo to proceed through early development. By doing so, embryos did indeed have many defects beyond early development such as defects in gut coiling, edema around the heart, skin blisters, general overall smaller size, and craniofacial defects. Specifically, decreasing Chd1

expression resulted in embryos with smaller mouths that were more circular in shape compared to control embryos. The faces of Chd1 morphants were consistently narrower with a reduced intercanthal distance. Further analysis utilizing geometric morphometrics revealed significant changes in the shape of morphant embryo faces. Together, these changes in the size and shape suggest defects in the development of the midface in Chd1 morphants. These midface defects may represent changes in the growth and merging of the facial prominences that form the orofacial region, resulting in the defects observed in Chd1 morphants. Further, these defects may arise from changes in important factors necessary for facial development.

Complete loss of Chd1 in mice leads to embryonic death before craniofacial development can occur (Guzman-Ayala et al., 2015). However, other CHD family members, specifically Chd7 and Chd8 are necessary for craniofacial development in mice and humans (Basson and van Ravenswaaij-Arts, 2015; Platt et al., 2017; Sperry et al., 2014). Chd7 is associated with CHARGE syndrome, which has features that are similar to known neurocristopathies and can include defects such as orofacial clefts (Pauli et al., 2017). Chd7 is expressed in premigratory and migratory neural crest cells in *Xenopus* and in mice (Bajpai et al., 2010; Fujita et al., 2014). In addition, Chd7 is expressed in the branchial arches in chick embryos (Aramaki et al., 2007). Using morpholinos to reduce expression of Chd7 in *X. laevis* resulted in decreased expression of the migratory neural crest specifiers *Twist, Slug,* and *Sox9*. This inhibited neural crest cell migration *in vivo* resulting in reduced craniofacial cartilages and a decrease in the distance between the eyes (Bajpai et al., 2010). Deletion of Chd7 in migrating neural crest cells in mice also resulted in reduced craniofacial cartilages, including reductions

in the ethmoid bones, and a decrease in the intercanthal distance. Further, the Chd7 knockout mice exhibited palatal shelf hypoplasia resulting in some mice with complete clefting of the palate (Sperry et al., 2014). These results are similar to some of those observed in Chd1 morphants. Specifically, the decreased intercanthal distance and reductions in the craniofacial cartilages. Further, the ethmoid cartilage was missing in many Chd1 morphants similar to the hypoplastic ethmoids bones in Chd7 conditional knockout mice. Chd8 mutations are associated with a subtype of autism with features including macrocephaly, wide-set eyes, broad nose, and pointed chin (Bernier et al., 2014). *Chd8*$^{+/-}$ mice also display macrocephaly (Platt et al., 2017). Together, these results demonstrate the importance of CHD family members in craniofacial development. Therefore, the role of Chd1 was examined further to better understand the changes that occur with reduced Chd1 expression.

Chd1 is required for neural crest and cartilage development

Craniofacial defects can occur when the development of the underlying structures are disrupted, and often, these defects arise from problems with neural crest development. Cranial neural crest cells migrate into the face to form cartilage, bone, peripheral nerves, and connective tissues (Betancur et al., 2010). In addition, neural crest cells have inductive roles in the development of other tissues, such as the head muscle and skin (Rinon et al., 2007; Simoes-Costa and Bronner, 2015). This raised the question of whether Chd1 deficiency results in craniofacial defects due to the disruption of neural crest development. The spatial localization of Chd1 did indeed support a role in the development of neural crest cells. Chd1 was present in regions behind the eye

that were consistent with the timing and location of migrating neural crest cells. Later, Chd1 was expressed in the branchial arches and midface regions consistent with the locations of neural crest cells after their migration is complete. Additionally, in Chd1 morphants, expression of the neural crest regulatory gene, Ap2, was decreased, and dying cells were localized in regions consistent with neural crest. Further, the craniofacial cartilage, a derivative of neural crest cells, was reduced. Together, these results indeed point to a role for Chd1 in neural crest development.

Neural crest specification and migration seem to be very susceptible to defects when epigenetic regulators are perturbed. For instance, loss of the histone demethylase JmjD2A results in the downregulation of expression of neural crest specifier genes including Sox10, Sox8, FoxD3, Snail2, and Wnt1. JmjD2A acts by removing the repressive H3K9me3 mark at the appropriate developmental time for the specification of neural crest cells (Strobl-Mazzulla et al., 2010). HDAC repressive complexes also play a role in regulating neural crest development. Knockdown of Hdac4 with morpholinos in zebrafish results in the disruption of migration of cranial neural crest cells labeled with a *sox10:EGFP* transgene. This disruption occurred in a subset of cranial neural crest cells that contribute to the development of the medial ethmoid plate. This resulted in the loss of cartilage from the ethmoid plate and clefting in the palatal skeleton (DeLaurier et al., 2012). Hdac8 is also important for cranial neural crest development. The deletion of Hdac8 from neural crest derived tissues resulted in defects in the development of the frontal and interparietal bones in mice. This was similar to global deletion of Hdac8. Loss of Hdac8 leads to the upregulation of homeobox genes such as Lhx1 and Otx2 that would normally be repressed in cranial neural crest cells, resulting in the disruption

of skull patterning and formation (Haberland et al., 2009a; Haberland et al., 2009b). Hox gene expression and craniofacial osteochondrogenesis is also influenced by Ezh2, a component of the polycomb repressive complex 2. Knockout of Ezh2 in pre-migratory neural crest cells in mice leads to severe craniofacial defects including missing jaw and nasofrontal plate structures. These phenotypes arose from the impaired differentiation of neural crest derived cartilage and bone. This was due to the upregulation of hox genes in derivatives of cranial neural crest cells in Ezh2 mutant mice (Schwarz et al., 2014). Similarly, Ring1b/Rnf2, a component of the polycomb repressive complex 1 is also required for chondrocyte differentiation of cranial neural crest cells. In zebrafish *ring1b/rnf2* mutants, almost all of the craniofacial cartilages, including the jaw cartilages, and craniofacial muscles are missing (van der Velden et al., 2013). Since Chd1 is also required for epigenetic regulation of transcription, it is not unexpected that it also regulates neural crest development.

Neural crest contribute to the development of a diverse range of derivatives including the craniofacial bone and cartilage. The craniofacial skeleton provides the underlying structure to form the size and shape of the face. Examination of the craniofacial cartilages in Chd1 morphants revealed that there were reduced and missing cartilages. These changes may be due in part to defects in neural crest development. In addition, the expression of Has2 was also reduced in Chd1 morphants. Has2 synthesizes hyaluronan, which is a structural component of cartilage, skin, smooth muscle, and other connective tissues (Spicer and Tien, 2004). Knockout of Has2 in mice results in embryonic death at midgestation (E9.5-10), thus establishing that Has2 is critical for development (Camenisch et al., 2000). Has2 is expressed in areas of

migrating neural crest and in craniofacial structures such as the developing lower jaw, including the Meckel's cartilage, and in the ascending palatal shelf in mice (Tien and Spicer, 2005). In *X. laevis*, Has2 morphants have reduced and missing cartilages. Such changes occurred in the palatoquadrate, Meckel's, and ceratohyal cartilages (Casini et al., 2012). These cartilages were also missing or reduced in Chd1 morphants, suggesting that the changes in the facial cartilages in Chd1 morphants may be due to the reduced expression of Has2. In addition, Has2 is necessary for the migration and survival of pre-chondrogenic cranial neural crest cells in *X. laevis*. In Has2 morphants, migration of cranial neural crest cells is impaired and there is an increase in the number of apoptotic cells in branchial arches where neural crest cells will differentiate into chondrocytes (Casini et al., 2012). Similarly, there was also an increase in apoptotic cells in the area of the branchial arches in Chd1 morphants. In summary, Chd1 is required for proper development of neural crest cells and the craniofacial cartilages, and defects in these tissues could account for the craniofacial defects in Chd1 morphants.

Reduced Chd1 expression does not affect cell division

In addition to neural crest defects, the small size of the face of Chd1 morphants could also be explained by decreased cell proliferation. The cell cycle was examined in detail in the craniofacial cells using flow cytometry. These results indicate only a small change in the mitotic phase consistent with no dramatic change in phospho-histone H3 labeling, which is associated with chromatin condensation of cells entering into the mitotic phase (Hendzel et al., 1997). In the mouse E5.5 *Chd1*$^{-/-}$ epiblast, phospho-histone H3 labeling was about 40% higher than in control embryos. This was observed

in combination with no significant changes in the proportion of cells in S phase, suggesting problems with the completion of mitosis in *Chd1*$^{-/-}$ embryos (Guzman-Ayala et al., 2015). The difference between phospho-histone H3 labeling between *Chd1*$^{-/-}$ mouse embryos and *X. laevis* Chd1 morphants may be due to the complete knockout of Chd1 in mice versus knockdown of Chd1 in *X. laevis*. Further, the difference may arise from the difference in timing in which these embryos were examined. The *Chd1*$^{-/-}$ mice embryos were examined prior to the onset of gastrulation, while the Chd1 morphants were examined later in development during a time when the face is forming.

There was a minor decrease in the proportion of cells in the G0/G1 phase. During the G1 phase, transcription and translation occurs, and cells in the G1 phase can respond to differentiation signals and initiate cell fate decisions more quickly than other phases of the cell cycle (Dalton, 2015; Deniz et al., 2016). Chromatin remodelers, such as CHD family members, are involved in transcriptional regulation, both as activators and repressors, and perhaps, Chd1 is necessary for transcriptional regulation during G1. Since RNA synthesis is high during G1, the decrease in the proportion of cells in G0/G1 in Chd1 morphants may be one of the contributing factor that led to the decrease in expression of some genes observed in morphant embryos.

Additionally, Chd1 may be necessary for recognition of DNA replication origins. The replication origins are selected during G1 and selection of origins that will be activated is influenced by cell fate and environmental conditions (Mechali, 2010; Wu and Gilbert, 1996). DNA replication origins are typically found in open chromatin structures (Audit et al., 2009; Cayrou et al., 2010; Field et al., 2008; Zhou et al., 2005) and positioning of a nucleosome at a DNA replication origin can inhibit initiation of

replication at that origin (Simpson, 1990). During G1, the minichromosome maintenance complex is recruited to the origin recognition complex by CDC6 and CDT1 to form the pre-replication complex (Alabert and Groth, 2012). The assembly of this complex occurs in the absence of a repressive chromatin structure. Histone acetylation plays a role in facilitating an open chromatin structure (DePamphilis, 2016; Miotto and Struhl, 2010) and perhaps, Chd1 has a role in facilitating an open chromatin structure as well.

Chd1 loss increases cell death

Most significantly, there was an increase in the proportion of cells in the sub-G1 fraction. This fraction contains cells that have lost some of their DNA, which happens primarily when cells are undergoing apoptosis. These results suggested that there may be increased cell death in Chd1 morphants. This was consistent with the increase in the number of cleaved caspase 3 positive cells in Chd1 morphants. Cleavage of caspase 3 activates this proteolytic enzyme to cleave other key proteins involved in apoptosis. It does this by activating proteins that promote apoptosis or inactivating proteins that would inhibit apoptosis. Once apoptosis is initiated, the cell will undergo changes including the fragmentation of DNA (Elmore, 2007). Similarly, increased apoptotic cells have been observed in *Chd1*$^{-/-}$ mice prior to embryonic arrest (Guzman-Ayala et al., 2015). These apoptotic cells in mice were marked by cleaved poly (ADP-ribose) polymerase (PARP). PARP is cleaved by proteases, such as caspases, and the 24 kD cleaved fragment binds to nicked DNA irreversibly, thus, preventing DNA repair (Chaitanya et al., 2010).

Chd1 has a role in DNA repair of DNA double strand breaks via homologous recombination. Chd1 is recruited to chromatin in response to double strand break induction, where it facilitates opening the chromatin around the double strand break. Further, Chd1 is involved in CtIP recruitment to double strand break sites. CtIP works with MRE11 to initiate end resection. This indicated that Chd1 plays a role in end resection during homologous recombination mediated double strand break repair (Kari et al., 2016).

Cleaved caspase 3 positive cells are localized to regions of neural crest migration, providing some evidence that at least a subset of the dying cells could be neural crest cells. Double labeling these cells with a cleaved caspase 3 marker and a neural crest marker will be necessary to confirm this hypothesis. Taken together, the facial abnormalities in Chd1 morphants are likely to be partially due to increased cell death affecting the neural crest.

Chd1 has multiple roles in orofacial development. First, Chd1 is required for expression of important neural crest and cartilage genes that are necessary for proper development of the face. Second, Chd1 is required to maintain cells in G1 to facilitate transcription of genes that are required at high levels. Third, Chd1 is necessary for proper DNA repair and decreased Chd1 expression can lead to increased apoptosis as a result of errors in repair. As a result, neural crest cells die and many of the facial cartilages do not form properly, and consequently, this results in a smaller face (Fig 1.15).

Chd1 cooperates with retinoic acid to regulate orofacial development

Evidence from this work and other performed in the Dickinson lab provide overwhelming evidence that Chd1 cooperates with retinoic acid in orofacial development. First, Chd1 expression was decreased in orofacial tissues exposed to a RAR inhibitor during a specific time window of orofacial development. This suggested that retinoic acid may play a role in regulating expression of Chd1. Secondly, Chd1 and RAR**γ** expression patterns are similar and both are expressed in craniofacial tissues consistent with neural crest. Retinoic acid is known to be important for neural crest development and the localization of Chd1 suggests that it too may be important for neural crest development. Third, Chd1 morphants and embryos exposed to RAR antagonists have similar craniofacial defects, such as a reduction in facial size suggestive of midface hypoplasia. Further analysis utilizing morphometrics revealed that a subset of facial landmarks change in a similar way in Chd1 morphants and embryos exposed to a RAR inhibitor. The development of similar cartilages was altered in response to decreased Chd1 expression or decreased RAR function, which may account for the changes in the size and shape of the face. These changes may have arisen from the misexpression of the neural crest and cartilage genes Ap2 and Has2 that occurs in Chd1 morphants and embryos exposed to a RAR inhibitor. Together, these results may indicate that retinoic acid and Chd1 cooperate to regulate orofacial development.

Another CHD family member, Chd7, also cooperates with retinoic acid to direct neural stem cell and inner ear development. Chd7 is required to maintain the subventricular zone stem cell niche and the rostral migratory stream. Decreased Chd7

leads to defects in proliferation, self-renewal, and neurogenesis in neural stem and progenitor cells in the subventricular zone. *Nestin*-lineage *Chd7*-deficient neurospheres that were exposed to retinoic acid showed increased neuronal potential. In addition, the inhibition of retinoic acid with citral could partially rescue the defects in the semicircular canals in Chd7 deficient mice. Further analysis revealed that Chd7 binds directly to *Rarβ, Rxrγ,* and *Neurod1*, suggesting that Chd7 regulates retinoic acid signaling and pro-neuronal genes to promote proper development of the inner ear and differentiation of neuroblasts (Micucci et al., 2014). In addition to CHD proteins, retinoic acid is known to cooperate with other epigenetic factors. In *Xenopus*, the histone reader Rai1 is regulated by retinoic acid in craniofacial development. Decreased Rai1 expression alters facial size and shape, and leads to reductions in the ethmoid, infrarostral, Meckel's, and ceratohyal cartilages, which is similar to cartilages that were affected by decreased Chd1. Further, the expression pattern of Ap2 was abnormal in Rai1 morphants (Tahir et al., 2014).

Exposure to a RAR agonist led to increased expression of Chd1 suggesting that retinoic acid is upstream of Chd1. To assess whether retinoic acid may regulate Chd1 directly, the region upstream of the Chd1 transcription start site was examined for the presence of RARE sites. These sites were present 5X more than expected by chance alone. Further, these sites were found in the same regions of the Chd1 promoter in humans, mice, and zebrafish, and at similar density to other genes known to be direct targets of retinoic acid. Many RAREs occur as direct repeats of the core hexameric sequence separated by 1, 2, or 5 base pairs and when this was applied as a more stringent analysis, it revealed that none of the RARE sites in the region upstream of

Chd1 were consistent with this pattern. Although, one site located about 600 base pairs upstream (5'-GGGTCAcTGACCT-3') contained a consensus sequence and a sequence that while not a direct repeat, was one that has been shown to be part of a site bound by RAR-RXR heterodimers in *CrabpII* in mice (Durand et al., 1992). These two sequences were separated by 1 base pair and may represent a potentially functional site that may be bound by a RAR-RXR heterodimer. Further analysis with an alternative consensus sequence, 5'-(A/G)G(G/T)T(G/C)A-3' (Lalevee et al., 2011), revealed the presence of one RARE site that consisted of a repeat spaced 5 base pairs apart located 6212 base pairs upstream of the Chd1 transcription start site. In addition, ChIP-seq experiments have identified many loci in which RAR binding occurred at a half site with no identifiable direct repeat (Delacroix et al., 2010), suggesting the potential that a direct repeat may not be necessary for RAR to bind to Chd1. Unfortunately, the cryptic nature of RAREs present limitations for bioinformatic analysis. An example of this is the *F11r* promotor. ChIP experiments identified a region of the *F11r* promoter that was bound by RARγ and thought to contain a RARE. However, deletion reporter construct analysis revealed that this RARE site was not necessary for retinoic acid induced expression, but a different sequence was necessary, and bioinformatic analysis did not identify a RARE site in this sequence (Savory et al., 2014). There is no evidence that RARs are bound to the Chd1 promoter in ChIP-seq experiments in mouse embryonic fibroblasts and embryonic stem cells (Delacroix et al., 2010). However, these are very different types of cells and thus, ChIP experiments will be necessary in embryos to determine whether Chd1 is directly bound by retinoic acid receptors.

Together, these results suggest that Chd1 cooperates with retinoic acid to regulate orofacial development. This cooperation may consist of the recruitment of Chd1 by the retinoic acid receptors and coactivators to destabilize the nucleosome structure of retinoic acid target genes and activate transcription. Chd1 directly binds to methylated H3K4 (Sims et al., 2005) and retinoic acid increases H3K4me3 when it binds to receptors (Urvalek et al., 2014). Additionally, it is possible that retinoic acid is upstream of Chd1 and may regulate Chd1 expression directly. Alternatively, retinoic acid may regulate Chd1 expression indirectly by directing the expression of some unknown intermediate gene. Or retinoic acid may be necessary for Chd1 expression by some other mechanism.

The expression of another epigenetic modifier, Hdac1, was also decreased in response to exposure to the RAR inhibitor. Further, inhibition of HDAC with trichostatin A resulted in embryos with narrow faces similar to Chd1 morphants. HDACs are known to bind to receptors bound to RAREs of retinoic acid regulated genes in the absence of retinoic acid to regulate stem cell differentiation (Urvalek and Gudas, 2014). Perhaps, retinoic acid is necessary for expression of these regulators so that they can regulate transcription of other genes. For instance, Has2 is a retinoic acid responding gene (Saavalainen et al., 2005) and reduced Chd1 expression resulted in decreased Has2 expression. So it may be possible that retinoic acid regulates transcription of genes necessary for its own function.

If this is the case and retinoic acid regulates Chd1, then Chd1 might be recruited by coactivators to facilitate transcription of retinoic acid target genes. In addition, Chd1 is necessary for proper RNA splicing and DNA repair to ensure the accuracy of these genes

during orofacial development. When RAR function is inhibited, Chd1 is not expressed at sufficient levels to facilitate transcription. This results in the misregulation of genes important for orofacial development, such as Ap2 and Has2. Further, reduced Chd1 expression may lead to defects in RNA splicing and DNA repair leading to abnormal orofacial development (Fig. 1.16).

CONCLUSIONS AND FUTURE DIRECTIONS

Understanding how the orofacial region develops is critical to develop strategies to prevent birth defects affecting this region. The development of the orofacial region is complex and every aspect involved in the development of this important region is not completely understood. Chd1 was examined here for the first time to specifically elucidate the role of this chromatin remodeler in orofacial development. The findings presented in this chapter suggest that Chd1 is important for neural crest and cartilage development in *X. laevis* craniofacial development. Further, this chapter presents evidence that there may be cooperation between Chd1 and retinoic acid signaling to regulate orofacial development. These results only scratch the surface of the importance of Chd1 in orofacial development and potential cooperation with retinoic acid.

An expression analysis of the orofacial tissues of Chd1 morphants would provide insight into which genes are regulated in part by Chd1. A microarray or RNA-seq analysis could be used to examine the orofacial tissues of Chd1 morphants at stage 29-30 (35-37.5 hpf) to obtain a global view of the genes altered in response to reduced Chd1 expression. Additionally, these results could be compared to the results from the expression analysis of the orofacial tissues of embryos exposed to the RAR inhibitor.

This comparison may reveal genes that are altered similarly when either Chd1 expression is reduced or RAR function is inhibited, and this may provide further support for the possibility that Chd1 and retinoic acid are in a common pathway if many genes are similarly altered. In addition, Chd1 is important for regulating RNA splicing and RNA-seq analysis could also reveal whether that are alterations in gene splicing in Chd1 morphants by aligning the sequencing results to determine if Chd1 morphants display defects that are not observed in the sequencing results from control embryos.

The results from this study suggested that Chd1 may be important for neural crest development, however, it is not known specifically what role Chd1 plays during neural crest cell development. This role could be elucidated with RNA *in situ* hybridization by utilizing neural crest cell specification and migration markers to determine if expression of these markers is altered in response to reduced Chd1 expression. This analysis could be performed on embryos injected in 1 cell of the 2-cell stage with Chd1-MO or an equal amount of control morpholino. The expression pattern of Sox9, Twist, and Slug at the neurula stage would reveal whether Chd1 was important for neural crest cell specification based on how these specification markers were expressed on the Chd1 morphant side versus the control side of the injected embryo. Further, the expression of Ap2 in embryos injected in 1 cell of the 2-cell stage at stage 26-28 (29.5-35 hpf) would reveal whether Chd1 is important for neural crest cell migration based on whether Ap2 labeled cells are localized to areas where neural crest cells are known to migrate to, such as the branchial arches. Finally, to assess whether Chd1 regulates neural crest cell differentiation, Chd1 morphants could be analyzed to determine whether cells have differentiated into neural crest cell derivatives such as

cartilage. Col2a1 is involved in making type II collagen that is found primarily in cartilage and could be used as a marker to determine whether reduced Chd1 expression affects neural crest cell differentiation into chondrocytes.

Another question that remains is whether reduced Chd1 expression leads to downregulation of genes such as Ap2 and Has2 as a result of misregulation of transcription or as a result of increased cell death. Therefore, the pan-caspase inhibitor, Z-VAD-FMK, could be used to inhibit cleaved caspase mediated execution of apoptosis in Chd1 morphants. The expression of Ap2 and Has2 could be examined with qRT-PCR stage 29-30 (35-37.5 hpf) in the head tissues of morphant embryos to determine whether their expression is downregulated in response to reduced Chd1 expression. If expression of these genes is still downregulated in embryos exposed to the pan-caspase inhibitor, then this would suggest that reduced expression of Chd1 results in the misregulation of transcription of these genes. Alternatively, if expression of Ap2 and Has2 is not altered in Chd1 morphants exposed to the pan-caspase inhibitor, then this would suggest that it is the increase in cell death that results in reduced expression of these genes in response to loss of Chd1.

The increase in cell death that was observed in Chd1 morphants may be the result of defects in DNA repair in morphant embryos. Chd1 plays a role in the repair of double strand breaks by facilitating the opening of chromatin around double strand breaks to allow access to the DNA for repair. The presence of a phosphorylated form of H2AX, γH2AX, generally reflects the presence of double strand DNA breaks. Therefore, a γH2AX antibody could be utilized to determine if there is more DNA damage present in Chd1 morphant embryos compared to controls. Immunohistological staining utilizing a

γH2AX antibody in embryos injected in 1 cell of the 2-cell stage with Chd1-MO or an equal amount of control morpholino may reveal whether there are more double strand breaks in Chd1 morphants. The presence of an increased number of double strand breaks would suggest that there is an impairment of DNA repair.

Finally, while the results presented here support the possibility that retinoic acid could regulate Chd1, further testing is necessary to determine if RARs bind directly to Chd1. ChIP analysis is often used to examine the relationship between proteins and DNA and an antibody specific to RARγ could be utilized for ChIP to determine the regions of DNA that this protein binds to. Sequencing the DNA sequences bound to RARγ would reveal whether Chd1 is directly bound by RARs. If the region of Chd1 bound by RARs contains a predicted RARE site, then this would strengthen the argument that Chd1 is regulated by retinoic acid.

Together, these investigations will further reveal the role of Chd1 in orofacial development and the importance of this chromatin remodeler in neural crest cell development. Additionally, these experiments will provide insight into whether Chd1 is important for regulating RNA splicing and DNA repair in the faces of *Xenopus* embryos and this may provide a potential mechanism to help explain why there was an increase in cell death in Chd1 morphants. Finally, these investigations may reveal whether Chd1 is directly bound by RARs and further our understanding of the importance of retinoic acid signaling in orofacial development. Overall, this will enhance what is known about how the orofacial region forms and contribute to the development of strategies to prevent orofacial defects.

TABLES AND FIGURES

Table 1.1: *Epigenetic modifiers that are necessary for craniofacial development*

Gene Name	Gene Function	Defect in human/animal models	Reference	OMIM Number
Chd7	Chromatin remodeler	CHARGE syndrome	(Basson and van Ravenswaaij-Arts, 2015)	608892
Chd8	Chromatin remodeler	Subtype of Autism	(Platt et al., 2017)	610528
Atrx	Chromatin remodeler	Alpha-thalassemia syndrome	(Gibbons and Higgs, 2000; Ratnakumar and Bernstein, 2013)	300032
Wstf	Chromatin Remodeler	Williams-Beuren syndrome	(Lu et al., 1998)	605681
Cfdp1	Chromatin organization	Microcephaly (Based on similarities with *MCPH1)*	(Messina et al., 2017)	608108
Hdac1	Histone deacetylase	Craniofacial cartilage defects in zebrafish	(Ignatius et al., 2013)	601241
Hdac4	Histone deacetylase	Palatal defects and shortened face on zebrafish Brachydactyly mental retardation syndrome in humans Non-syndromic oral clefts	(DeLaurier et al., 2012; Park et al., 2006; Williams et al., 2010)	605314

Hdac8	Histone deacetylase	Cornelia De Lange Syndrome 5 Wilson-Turner Syndrome Deletion in mice results in loss of specific cranial skeletal elements	(Haberland et al., 2009a; Harakalova et al., 2012; Kaiser et al., 2014)	300269
Ezh2	Subunit of Polycomb repressive complex 2. PRC2 trimethylates H3K27me3	Craniofacial bone and cartilage defects in mouse Weaver Syndrome	(Gibson et al., 2012; Schwarz et al., 2014)	601573
Ring1b/ Rnf2	E3 ubiquitin-protein ligase, mediates ubiquitination of H2AK119	Required for craniofacial development in zebrafish	(van der Velden et al., 2013)	608958
Rai1	Histone code reader	Smith-Magenis syndrome	(Carmona-Mora et al., 2010)	607642

Table 1.2: *Primer sequences for qRT-PCR*

Primer Name	**Primer Sequence**
Actin-F	GGCCGTACAACTGGTATTG
Actin-R	CATGATGGCATGAGGTAAGG
Alx4-F	CAGAGTGCAGGTTTGGTT
Alx4-R	CGTAGGCAGAGGAGAAGT
Ap2-F	ACGTTGAGGACCAGAGTATC
Ap2-R	GAACACCTCGTTGGGATTG
Has2-F	GGTCTTCATGTCCCTCTACT
Has2-R	CCAACCTGCCTTGTTGAT
Lhx8-F	CTATTCCGCATACGTTCCTC
Lhx8-R	CAATGACTGGAGACCAAGAG
Msx2-F	CTCCAGGAAGCGGAAATAG
Msx2-R	CAGCCTGAATAGGAGAGTTG
Pdgfra-F	GCACAGTTCTCAGACATCAG
Pdgfra-R	GGTCTCATCCTCCCTCTTTA
Six2-F	GACGGAGAAGAGACCAGTTA
Six2-R	GTTGTGGCCGTACCATTC
Gapdh-F	ATCAAGGCCGCCATTAAG
Gapdh-R	CAAAGATGGAGGAGTGAGTG

Table 1.3: *Genes depleted in the orofacial tissues of embryos with a RAR antagonist induced median cleft*

Category	Accession Number	Gene Name	Gene Description	Function	Activate or Repress Transcription
Chromatin remodeling	BC094093.1	chd1	Chromo-domain helicase DNA binding protein 1	Modifies chromatin structure	Activate and repress (Baumgart et al., 2017; Kelley et al., 1999; Stokes et al., 1996; Tai et al., 2003)
	BG018373	chd2l	Chromo-domain helicase DNA binding protein 2-like	Modifies chromatin structure	Activate (Siggens et al., 2015)
	CB943650	atrx	Alpha thalassemia/ mental retardation syndrome X-linked	Transcription regulation and chromatin remodeling	Activate (Levy et al., 2015)
	BU910939	bptf	Nucleosome remodeling factor subunit BPTF-like	Histone binding component of NURF	Activate (Landry et al., 2008)

	BQ885933	smarca2	SWI/SNF related, matrix associated, actin dependent regulator of chromatin, subfamily a, member 2 L homologue	Transcription coactivator cooperating with nuclear hormone receptors	Activate (Muchardt et al., 1996)
	BC073120.1	smarcad1	SWI/SNF related, matrix associated actin dependent regulator of chromatin, subfamily a, containing DEAD/H box 1	Facilitates deacetylation of newly assembled histones. Restoration of heterochromatin organization after replication	Repress (Rowbotham et al., 2011)
	BG016780	baz1a	Bromo-domain adjacent to zinc finger domain protein 1A-like	Subunit of the ATP dependent chromatin assembly factor (ACF). Regulates spacing of nucleosomes	Activate (Collins et al., 2002)
Histone chaperone	BG162673	rsf1	Remodeling and spacing factor 1	Forms complex with SNF2H to remodel and space chromatin	Repress (Zhang et al., 2017)

	AF278538.1	nap1l1	Nucleosome assembly protein 1-like 1	Histone chaperone removes and replaces H2A-H2B histone protein dimer. Facilitates nucleosomal sliding	Activate (Lee et al., 2017)
	BJ094806	supt6h	Suppressor of Ty 6 homologue	Histone chaperone, binds H3, Enhances elongation	Activate (Endoh et al., 2004)
	BC089261.1	spt16	FACT complex subunit SPT16	Component of the FACT complex, a general chromatin factor that acts to reorganize nucleosomes	Activate (Birch et al., 2009)
Chromatin organization	BX847655	Cbx5	Chromobox5	Component of hetero-chromatin, recognizes and binds histone H3 tails methylated at Lys-9 (H3K9me), leading to epigenetic repression	Repress (Bannister et al., 2001)
Histone acetylation	BC070732.1	phf20	PHD finger protein 20	Component of the MOF histone acetyl-transferase protein complex.	Activate (Badeaux et al., 2012)

	BG020636	jade2	E3 ubiquitin protein ligase Jade-2	Histone Acetyl-transferase component of the HBO1 complex	Activate (Panchenko, 2016)
Histone deacetylation	AF020658.1	hdac1	Histone deacetylase 1	Histone deacetylase	Repress (Delcuve et al., 2012)
Histone methylation	BJ639070	ash2l	Absent, small, or homeotic-like	Histone methyl-transferase	Activate (Wan et al., 2013)
	CA986691	setd8	SET domain containing (lysine methyl-transferase) 8	Methyl-transferase, mono-methylates H3K20	Activate and repress (Milite et al., 2016)
	BC100183.1	prdm2	PR domain containing 2, with ZNF domain	Histone methyl-transferase, Methylates H3K9	Repress (Cheedipudi et al., 2015)
	BX850045	nsd1	Histone lysine N-methyl-transferase, H3 lysine-36 and H4 lysine-20 specific	histone methyl-transferase, methylates H3K36 and H3K20	Activate and repress (Huang et al., 1998)
	BP682076	mll	Myeloid/ lymphoid or mixed lineage leukemia (trithorax homolog)	Protein complex, Histone methyl transferase, methylates H3K4	Activate (Milne et al., 2002)

Histone demethylation	BC056031.1	phf8	PHD finger protein 8	Histone lysine demethylase	Activate (Gu et al., 2016; Maina et al., 2017)
Transcription Initiation	BP731934	taf3	Transcription initiation factor TFIID subunit 3 isoform 1	General factor required for accurate and regulated initiation by RNA polymerase II	Activate (Lauberth et al., 2013)
Transcription elongation	BC085215.1	tceb3	Transcription elongation factor B (SIII), polypeptide 3	Suppresses transient pausing of polymerase	Activate (Aso et al., 1995)
	CO382632	rtf1	Rtf1, Paf1/RNA polymerase II complex component, homologue	Component of PAF1 complex, Interacts with Chd1	Activate (Mayekar et al., 2013)
	BC108883.1	iws1	IWS1 homologue	Assembly factor, recruits various factors to the RNAPII elongation complex and is recruited via binding to the transcription elongation factor SUPT6H	Activate (Liu et al., 2007)

Table 1.4: *Chd1 is conserved. Comparison of human Chd1 full length gene and protein sequence and major domains with mice, frogs, zebrafish, flies, worms, and yeast.*

Percent Identity with *Homo sapiens*						
Species	**Gene**	**Protein**	**Chromo-domain 1**	**Chromo-domain 2**	**Helicase**	**DNA Binding**
Mus musculus	88.10	95.84	96.00	94.44	99.52	97.38
Xenopus laevis L	77.63	84.93	78.00	90.74	94.51	90.75
Xenopus laevis S	78.12	85.46	80.00	90.74	93.56	91.67
Danio rerio	70.56	79.65	86.05	90.57	92.12	87.34
Drosophila melanogaster	53.20	49.48	57.14	48.08	74.22	48.66
Caenorhabditis elegans	54.86	47.11	57.11	34.04	69.78	38.35
Saccharomyces cerevisiae	50.37	38.43	56.10	28.85	54.89	30.35

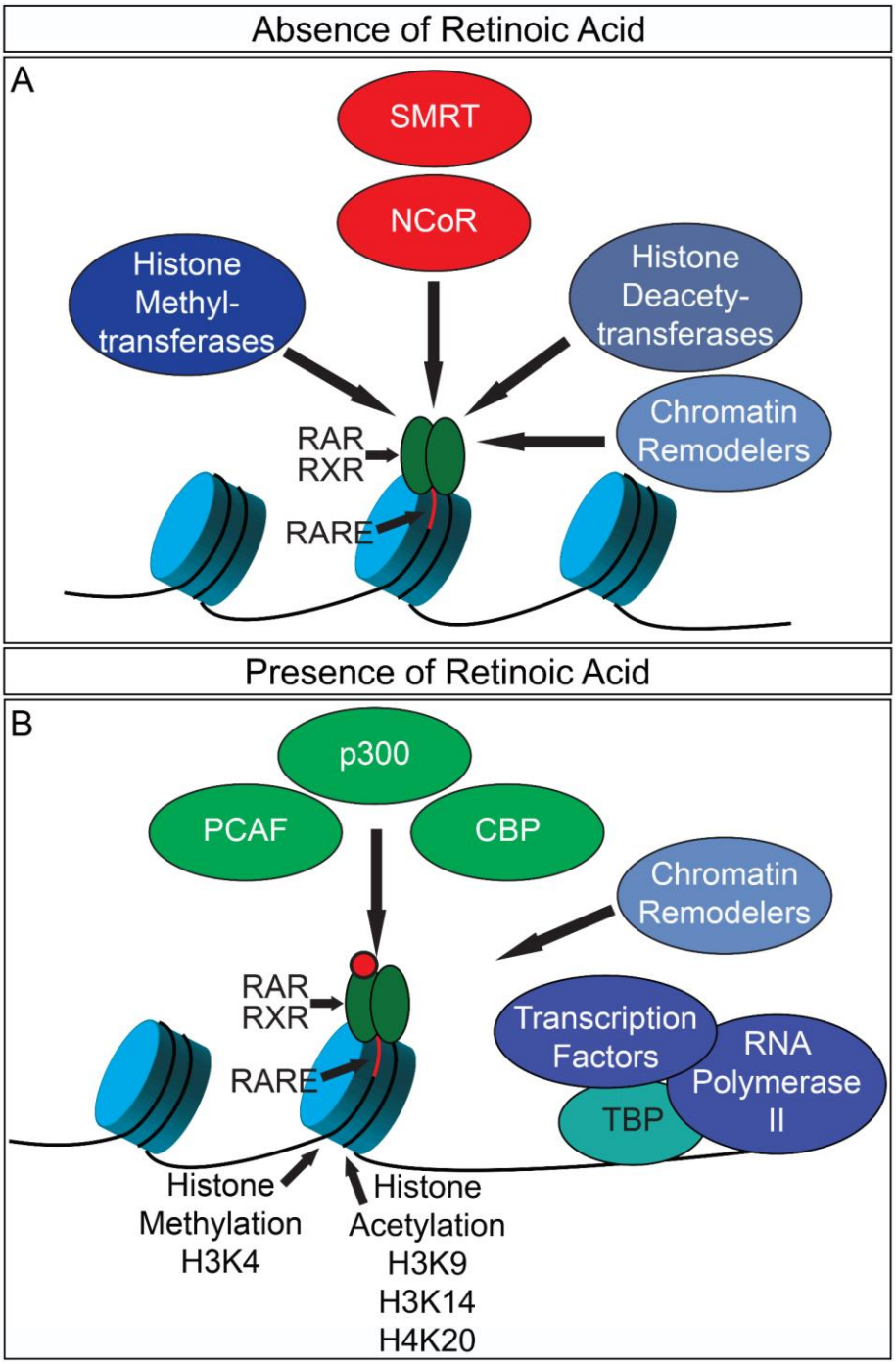

Figure 1.1: *Retinoic acid signaling. (A) Retinoic acid receptors recruit corepressors in the absence of retinoic acid to stabilize the nucleosome structure and repress transcription. (B) Retinoic acid receptors recruit coactivators in the presence of retinoic acid to destabilize the nucleosome structure and activate transcription. TBP=TATA Binding Protein (Adapted from Niederreither and Dolle, 2008)*

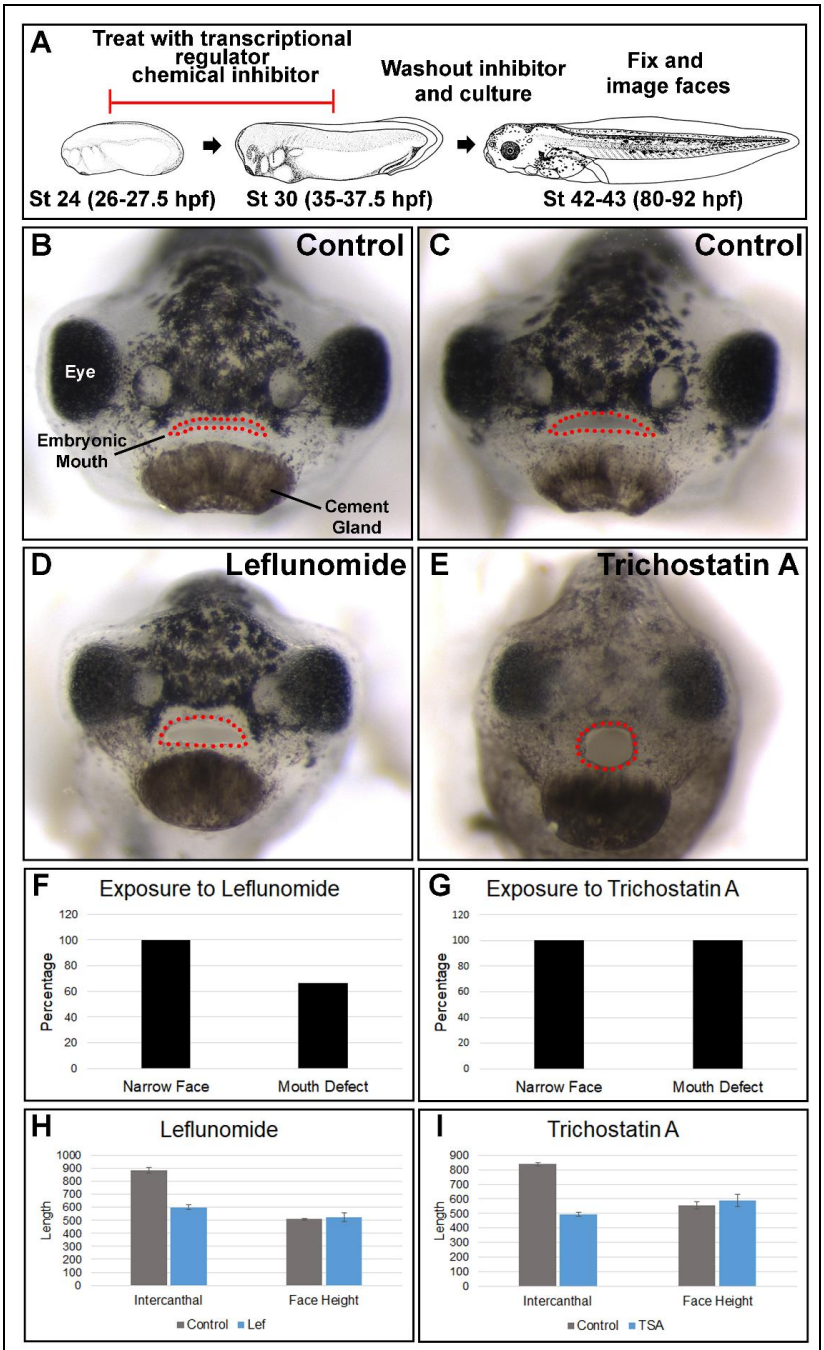

Figure 1.2: *The effects of transcriptional elongation and histone deacetylation on craniofacial development. (A) Schematic of the experimental design for inhibitor treatment. (B-E) Representative frontal views of faces of stage 42-43 embryos treated with DMSO (B-C), 200uM leflunomide (D), or 0.1uM Trichostatin A (E). (F-G) Bar graphs representing frequency of phenotypic defect. (H-I) Measurements of the intercanthal distance and face height of treated embryos.*

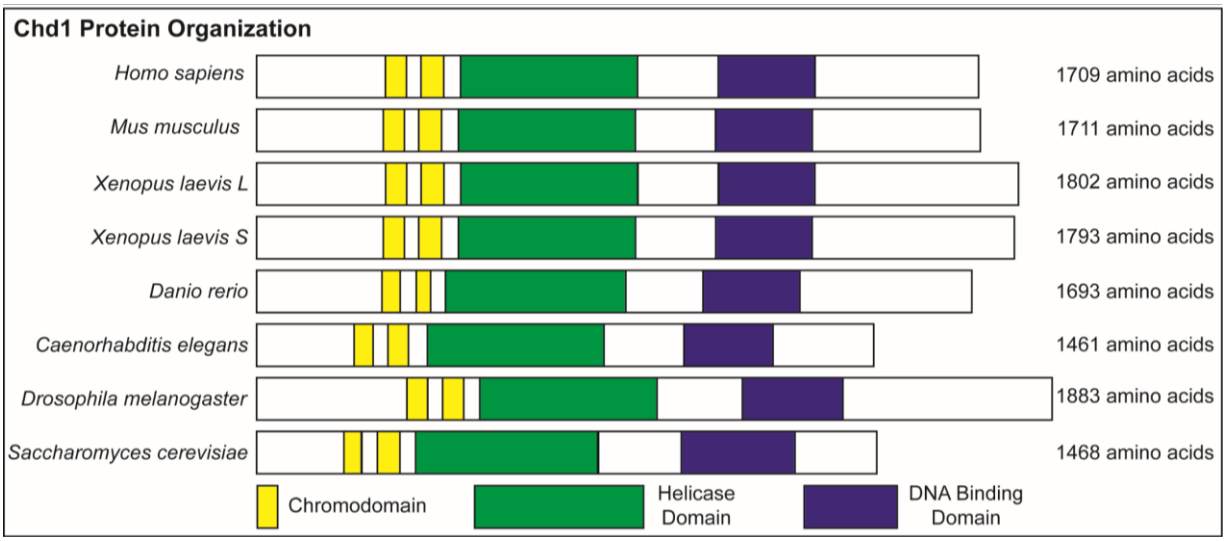

Figure 1.3: *Chd1 protein organization is conserved in metazoans. Schematic representation of the Chd1 protein in human, mouse, frog, zebrafish, flies, worms, and yeast. This shows the organization of the primary domains including the tandem chromodomains, the helicase domain, and the DNA binding domain.*

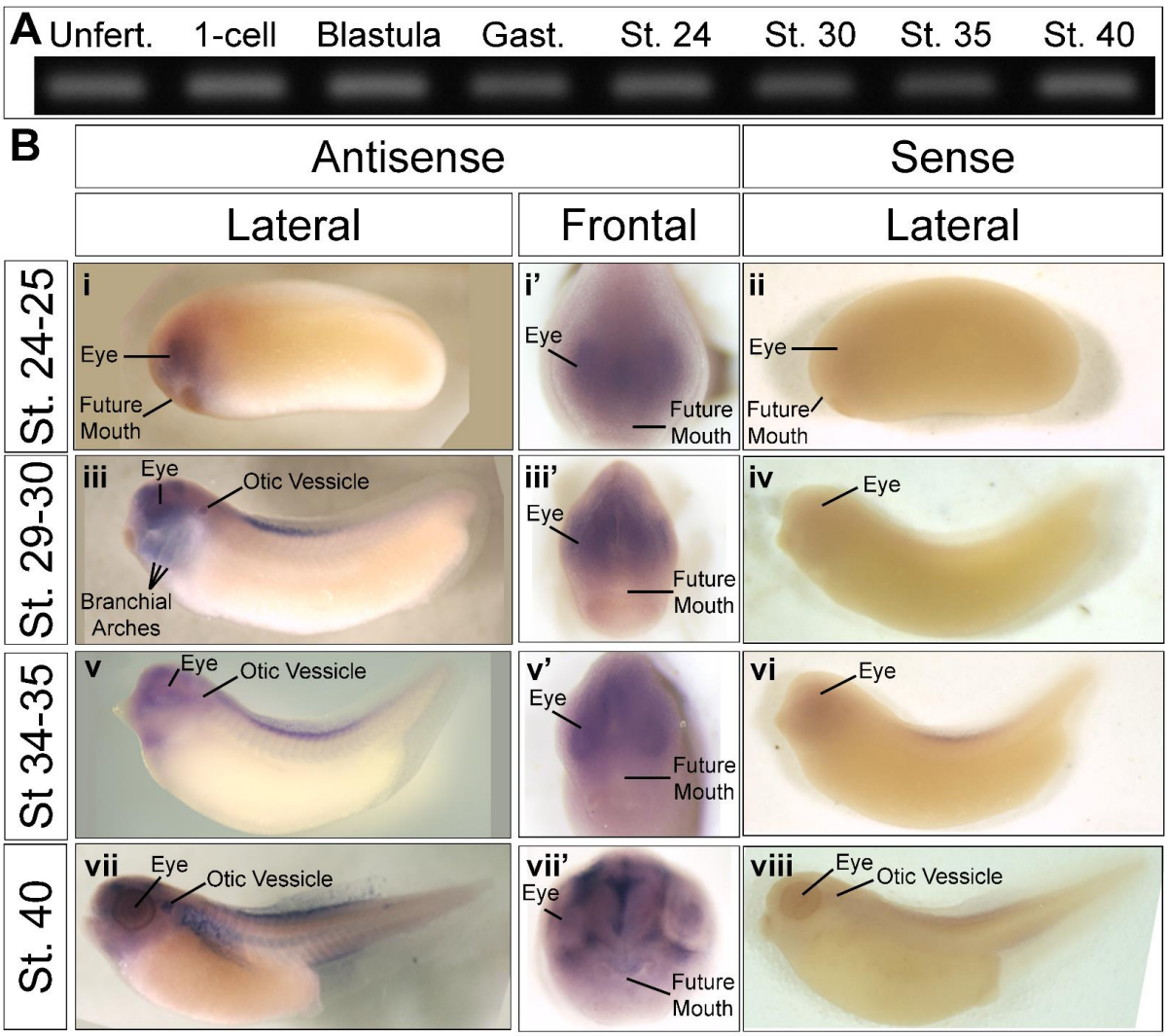

Figure 1.4: *Chd1 is expressed during early development in the head and presumptive heart. (A) RNA isolated from whole embryos (unfertilized, 1-cell, blastula, and gastrulation stage) or embryo heads (st. 24-25 (26-29.5 hpf), st. 29-30 (35-37.5 hpf), st. 34-35 (44.5-53.5 hpf), and st. 40 (66-76 hpf)) was analyzed with PCR using Chd1 specific primers. (B) In situ hybridization for Chd1, lateral and frontal views. Anterior is to the left.*

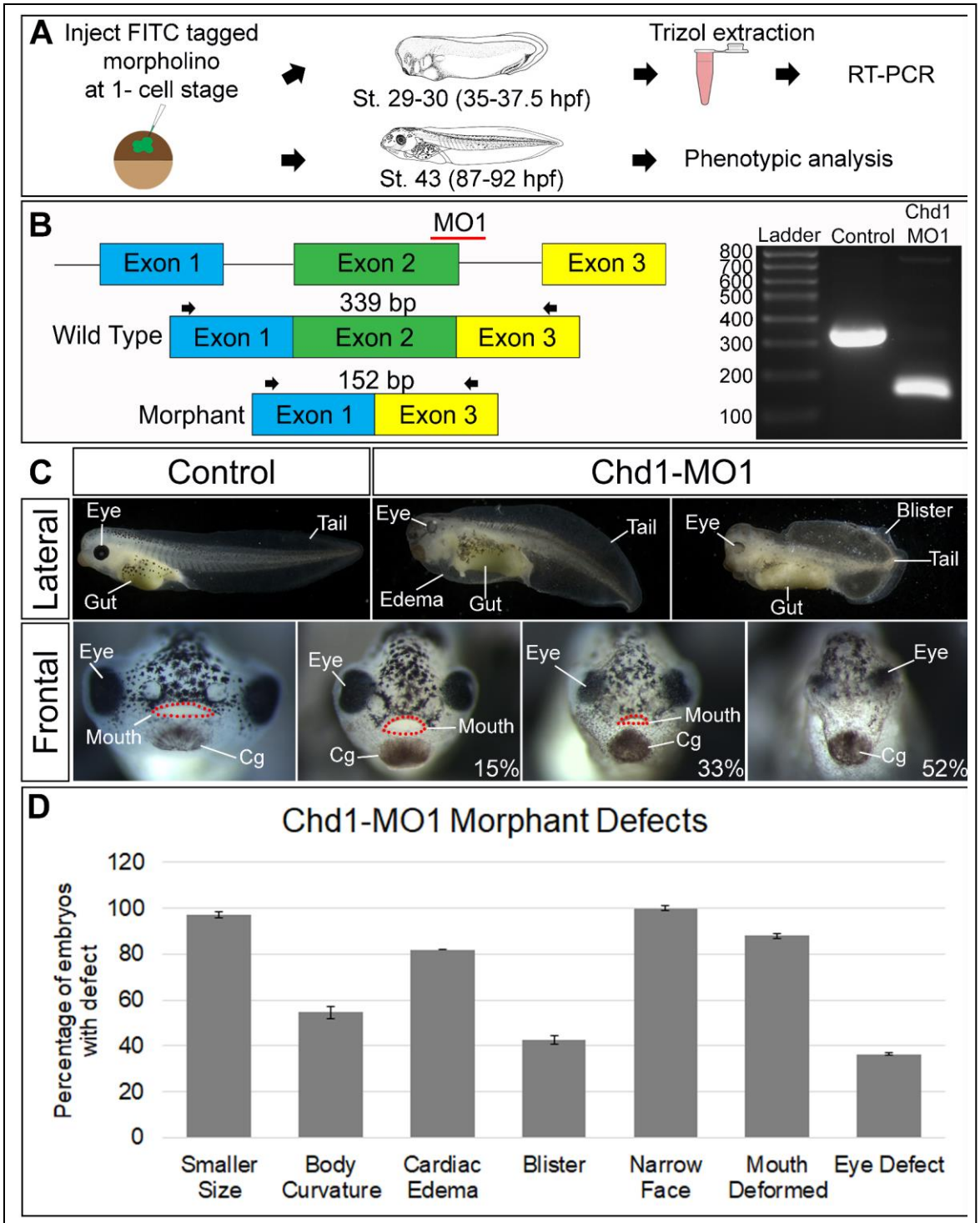

Figure 1.5: *Chd1 morpholino knockdown results in defects in the embryo. (A) Schematic of experimental design. (B)Chd1-MO binds to the exon 2-intron 2 boundary. Deletion of exon 2 was detected with PCR using primers located in exon 1 and exon 3 (arrows). (C) Representative lateral and frontal views of Chd1 morphants. (D) Bar graph represents the defects observed in control and Chd1 morphant embryos.*

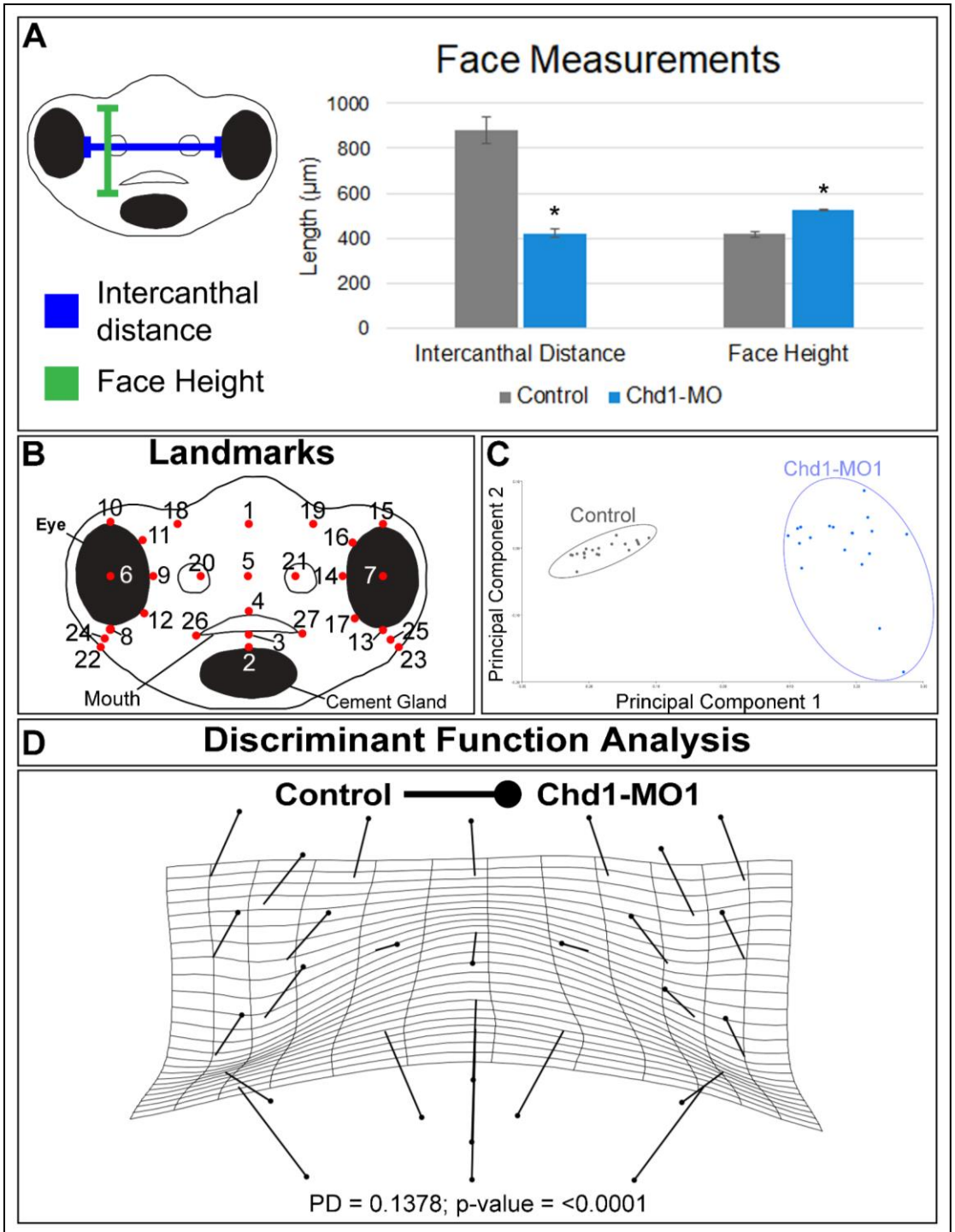

Figure 1.6: *Quantitative analysis of facial size and shape in Chd1 morphants. (A) Facial dimensions for the intercanthal distance and face height were measured and represented as a bar graph. (B) Landmarks for morphometric analysis. (C) Canonical variant analysis of landmark coordinates for control and Chd1 morphant embryos. (D) Transformation grid showing the change in landmark positions between control and Chd1 morphant embryos.*

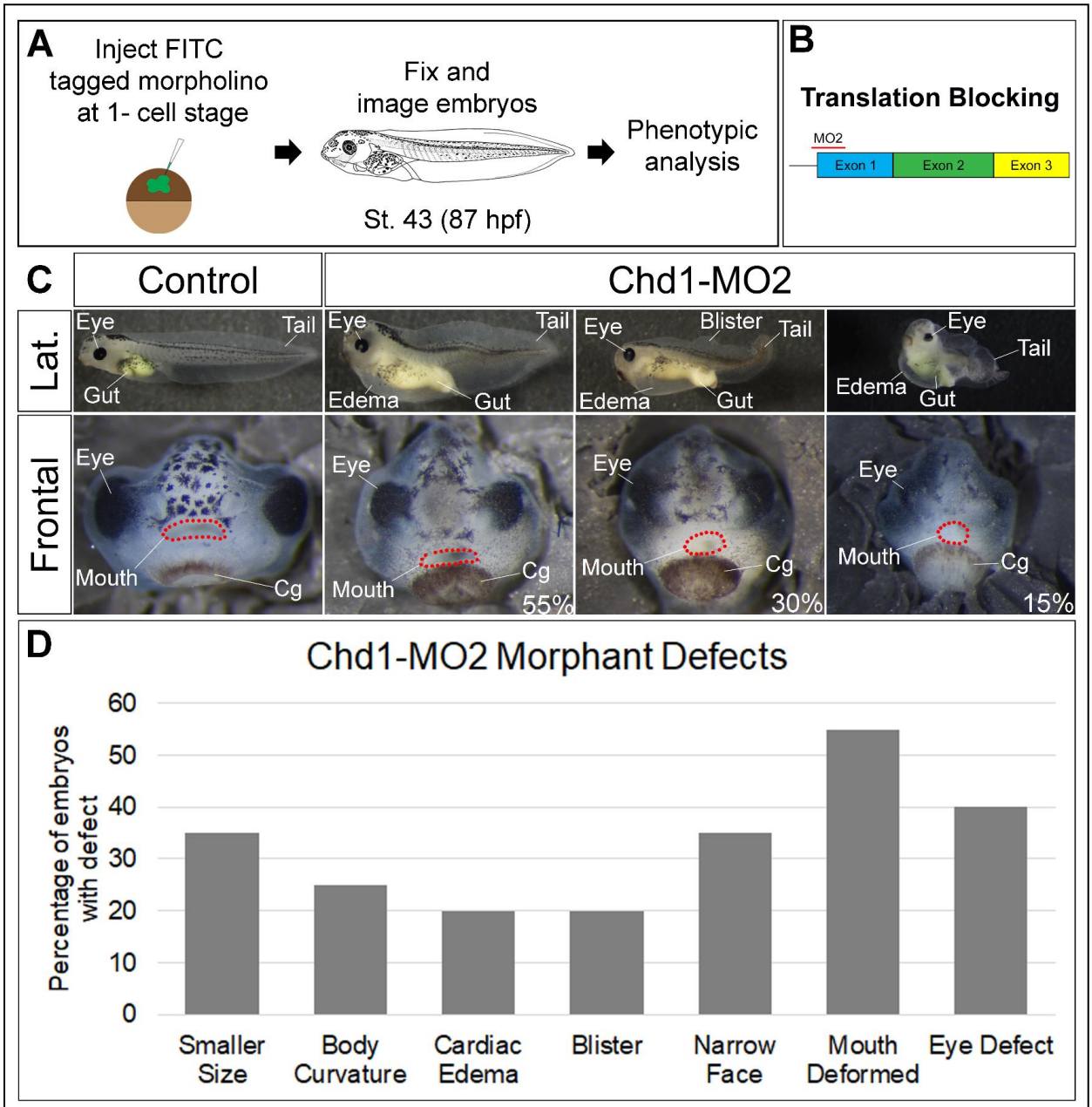

Figure 1.7: *Chd1-MO2 knockdown results in defects in the embryo. (A) Schematic of experimental design. (B) Chd1-MO2 binds to the translation start site. (C) Representative lateral and frontal views of Chd1-MO2 morphants. (D) Bar graph represents the defects observed in control and Chd1 morphant embryos.*

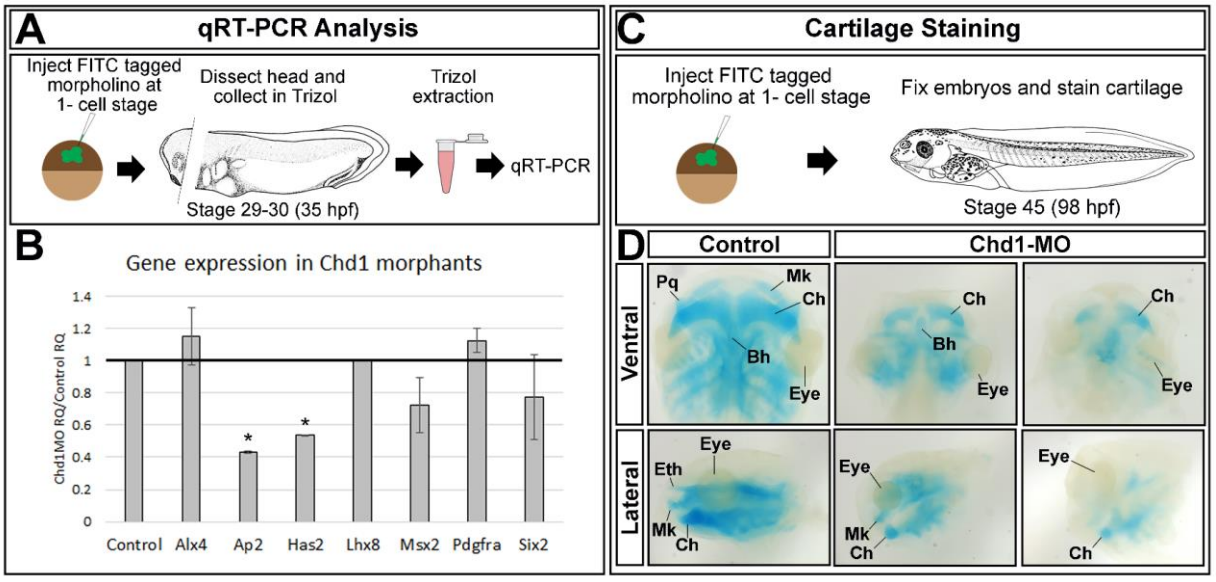

Figure 1.8: *Knockdown of Chd1 alters gene expression, facial cartilage. (A) Schematic of experimental design to test changes in gene expression. (B) qRT-PCR analysis of gene expression in embryo heads reveals decreased expression of genes involved in neural crest and cartilage development. (C) Schematic of experimental design to test changes in cartilage development. (D) Alcian blue staining reveals missing and reduced cartilages in Chd1 morphants. Abbreviations; Bh=Basihyal, Ch=Ceratohyal, Eth=Ethmoid, Mk=Meckel's, Pq=Palatoquadrate.*

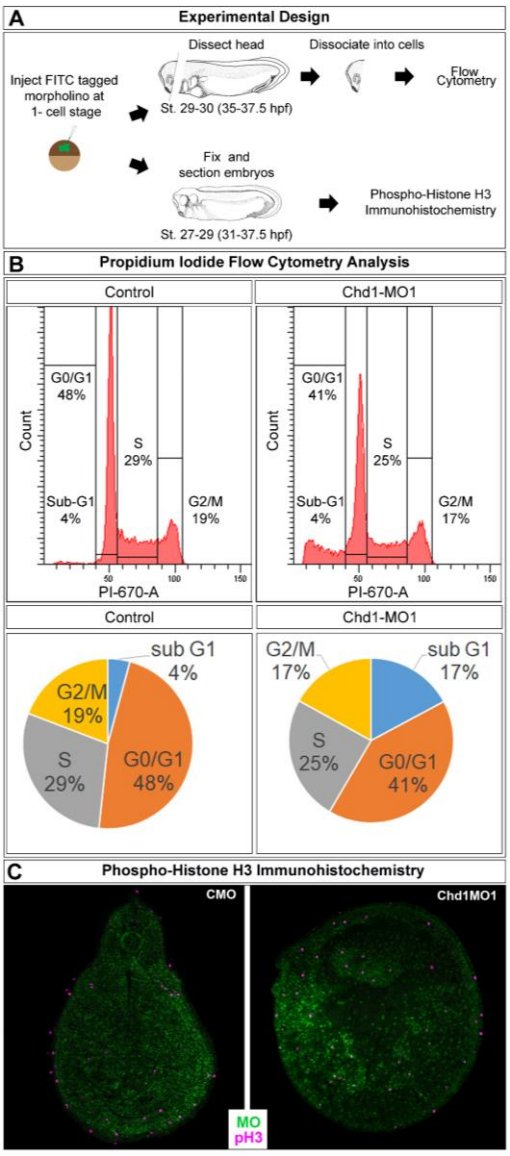

Figure 1.9: *Decreased Chd1 results in an increase in cells in the sub-G1 phase. (A) Schematic of experimental design for investigating cell cycle and cell death. (B) Propidium iodide staining and flow cytometry analysis reveals no change in cell cycle, but an increase in cells falling into the sub-G1 fraction in Chd1 morphants. (C) Phospho-histone H3 immunohistochemistry in control and Chd1 morphant embryo sections shows no change in phospho-histone H3 labeled cells.*

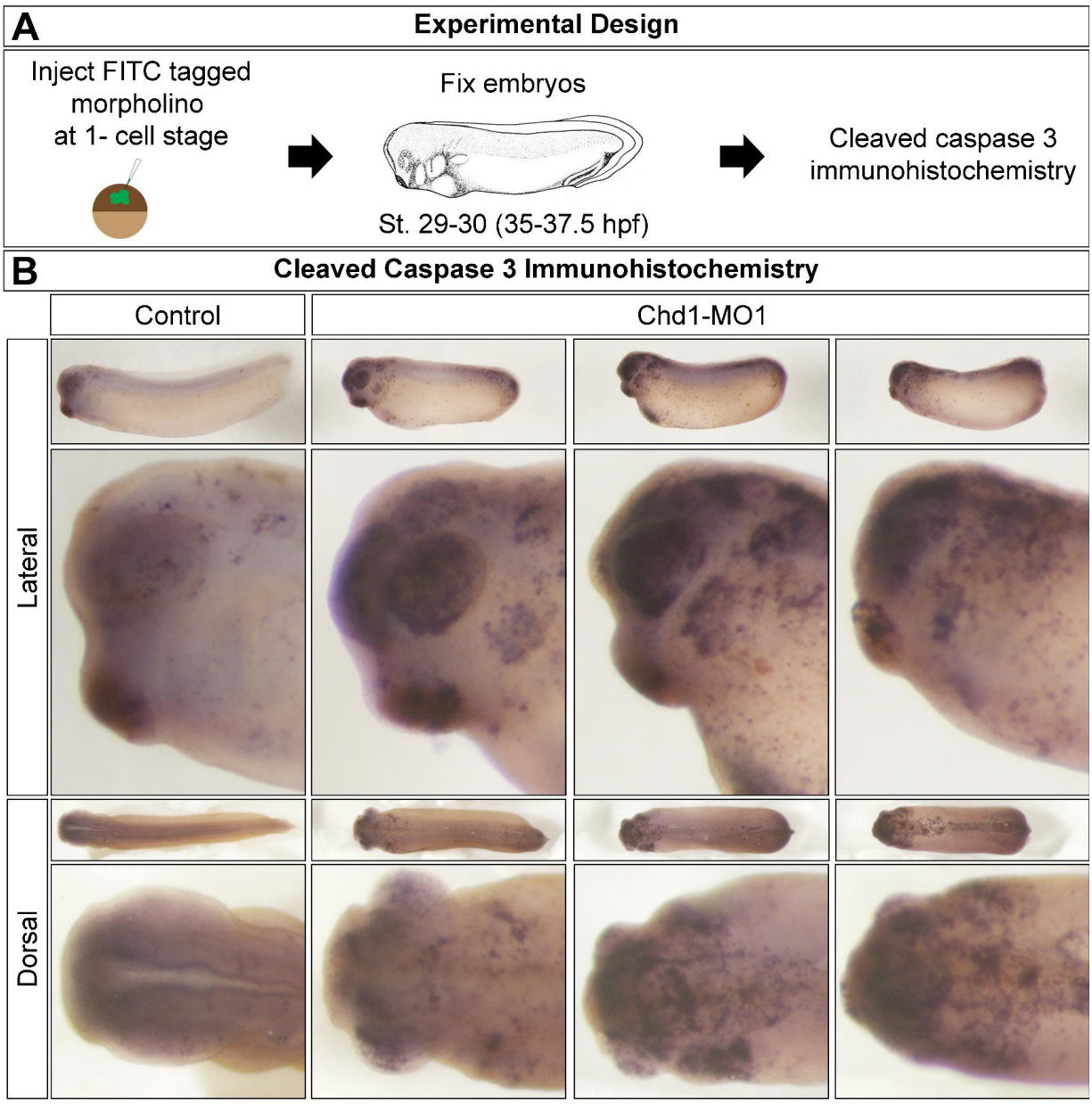

Figure 1.10: *Decreased Chd1 results in increased cell death. (A) Experimental design for assaying cell death in Chd1 morphants. (B) Cleaved caspase 3 IHC reveals an increase in cell death in Chd1 morphants.*

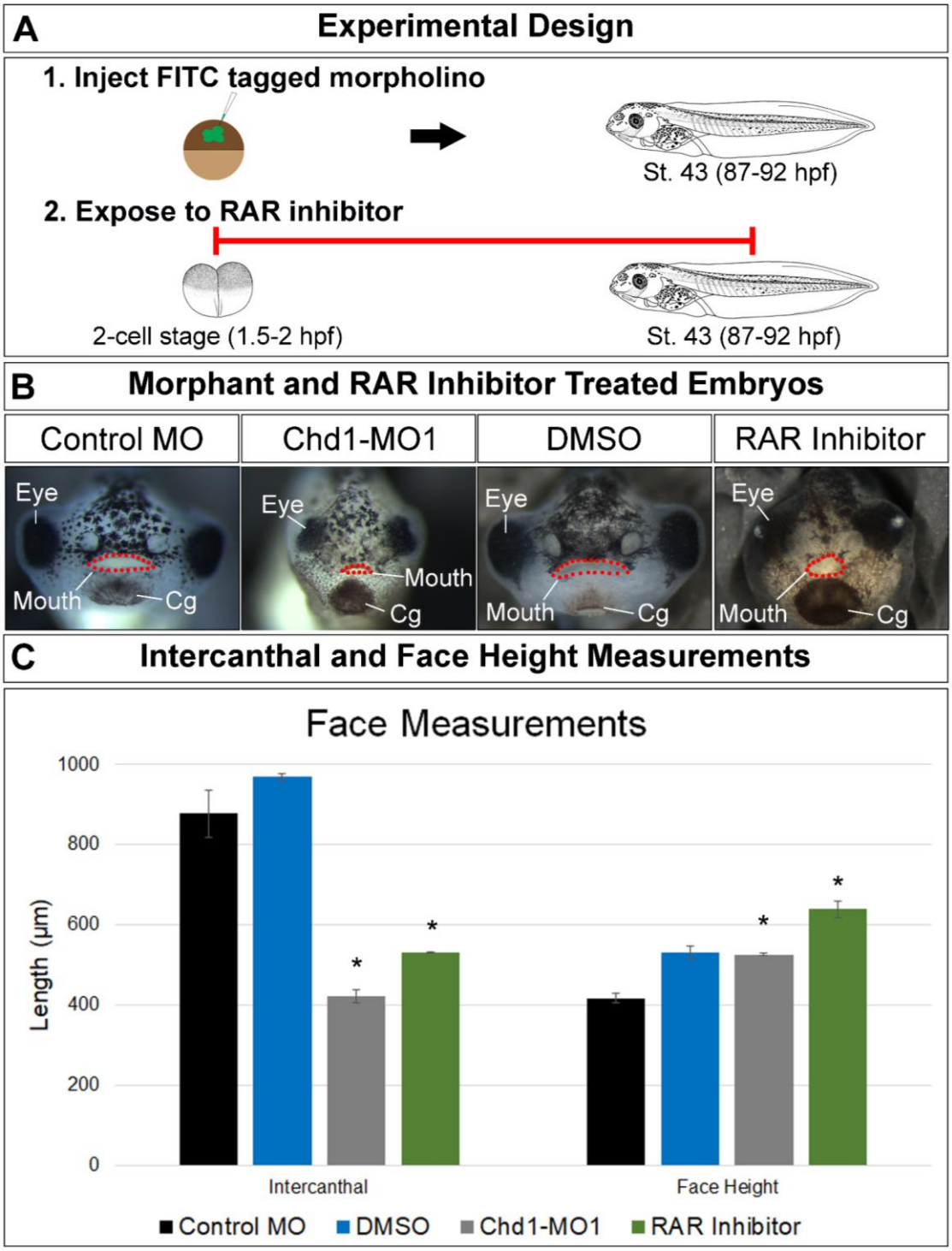

Figure 1.11: *Decreased Chd1 expression and inhibition of RAR results in embryos with narrower faces. (A) Experimental setup for reducing Chd1 expression or inhibiting RAR. (B) Representative embryos Chd1 morphants and embryos exposed to a RAR inhibitor. (C) Quantification of the intercanthal distance and face height in embryos corresponding to (B). * Indicates these are statistically different from their respective controls.*

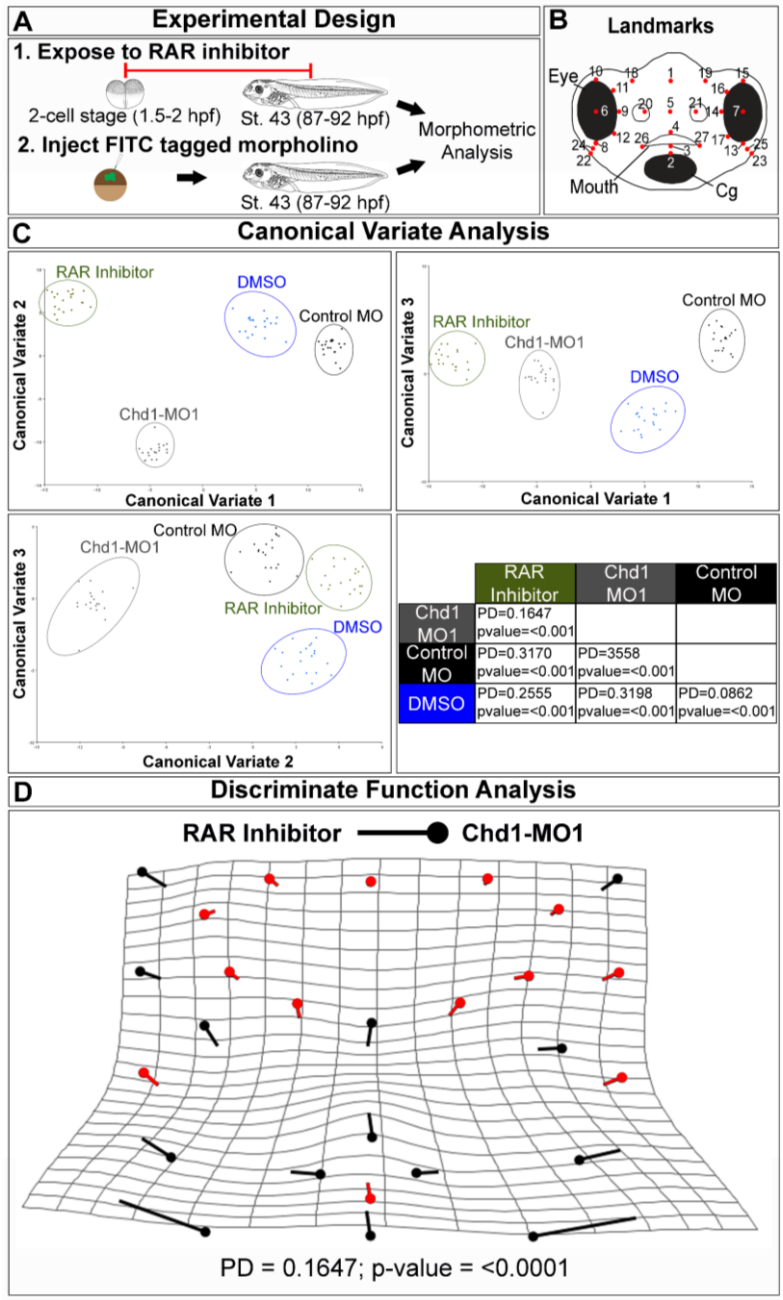

Figure 1.12: *Morphometric comparison of Chd1 morphants and embryos exposed to an RAR inhibitor. (A) Schematic of the experimental design. (B) Landmarks for morphometric analysis. (C) Canonical variate analysis comparing Chd1 morphants, embryos exposed to an RAR inhibitor, and control embryos injected with a control MO or exposed to DMSO. (D) Discriminate function analysis of Chd1 morphants and embryos exposed to an RAR inhibitor shown on a transformation grid.*

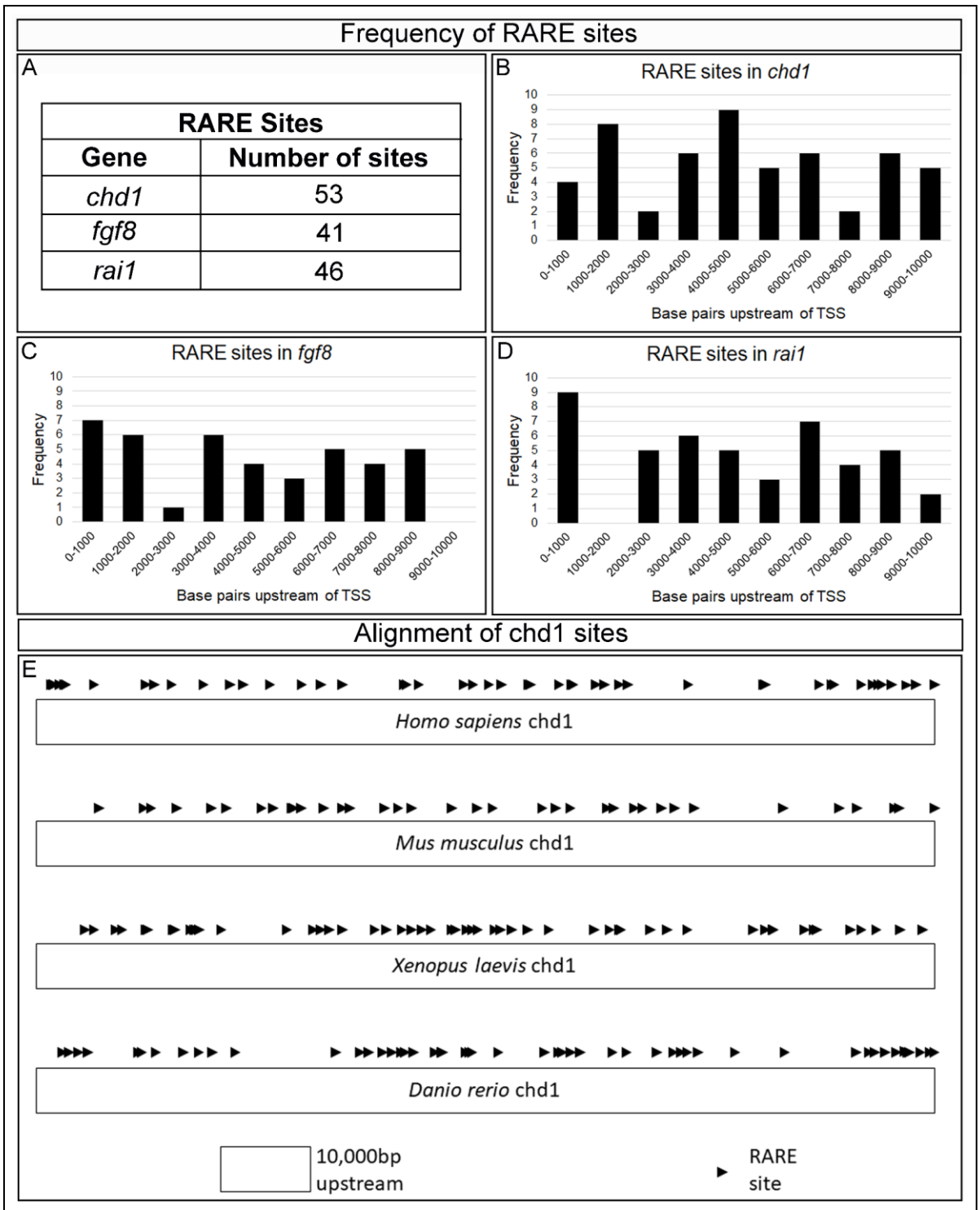

Figure 1.13: *RARE sites are present upstream of the Chd1 transcription start site. (A) Total number of RARE sites upstream of the transcription start site for chd1, fgf8, and rai1. (B-D) Graph showing the location of enrichment of RARE sites upstream of the transcription start site for chd1, fgf8, and rai1. (E) Schematic showing the relative positions of RARE sites upstream of the transcription start site for chd1 in H. sapiens, M. musculus, X. laevis, and D. rerio.*

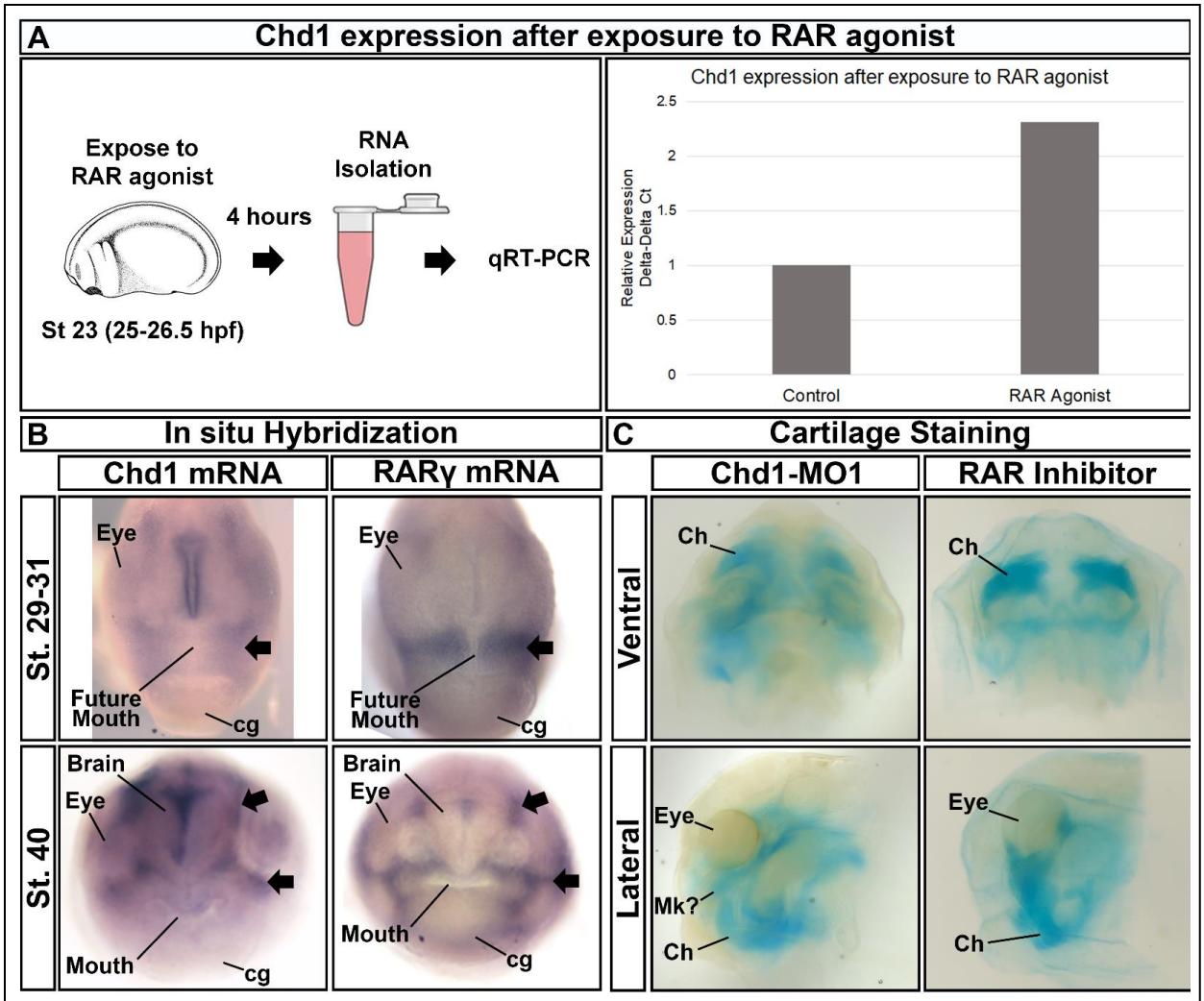

Figure 1.14: *Similarities between Chd1 and retinoic acid signaling (A) Schematic of experiment design for examination of Chd1 expression after exposure to RAR agonist. Bar graph summarizing qRT-PCR results reveals that Chd1 expression is upregulated in response to 4-hour exposure to RAR agonist. (B) Chd1 and RARγ are enriched in similar regions in the embryonic face as indicated by arrows. (C) Decreased Chd1 or exposure to the RAR inhibitor results in reduced and missing cartilages. Ch=Ceratohyal, Mk=Meckel's.*

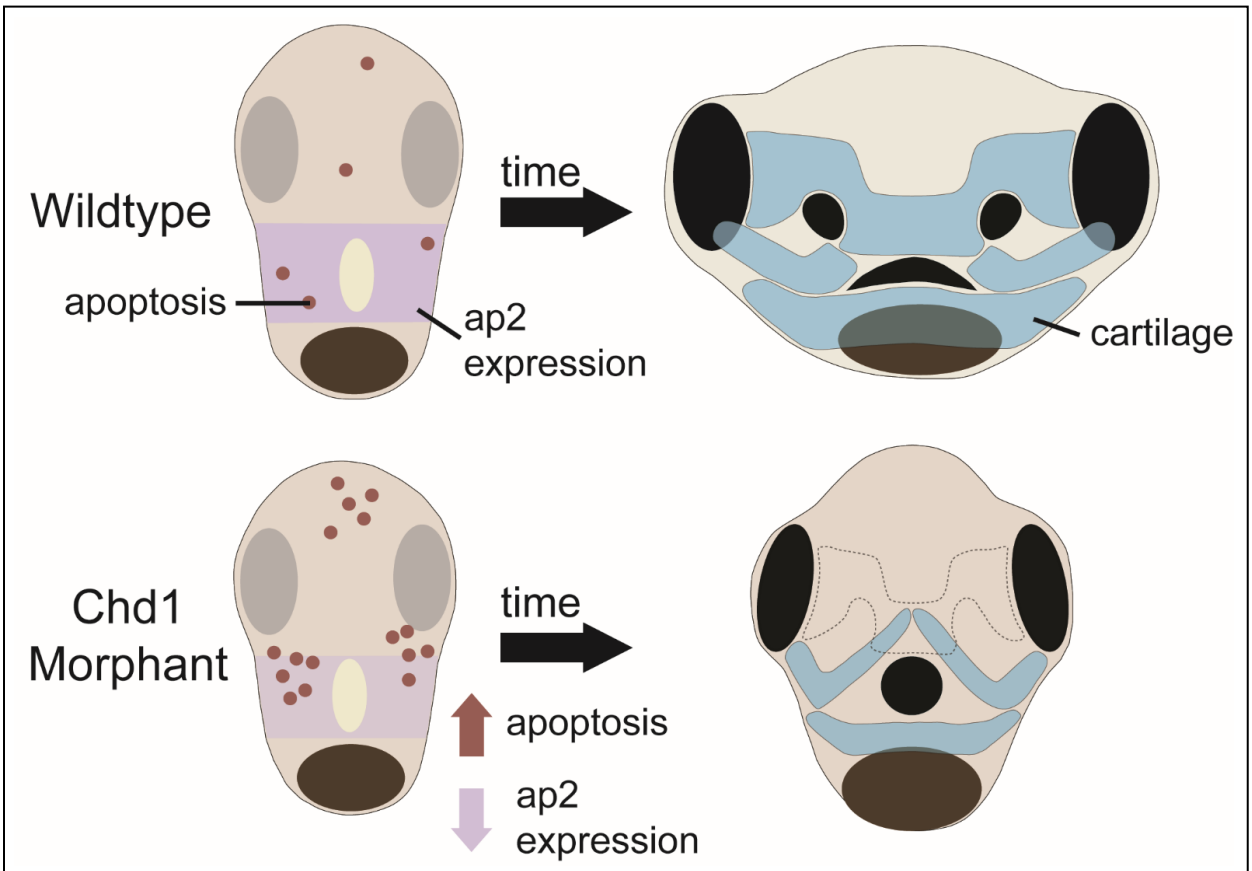

Figure 1.15: *Reduced Chd1 expression results in decreased ap2 expression, an increase in apoptosis, and reduced or missing facial cartilages.*

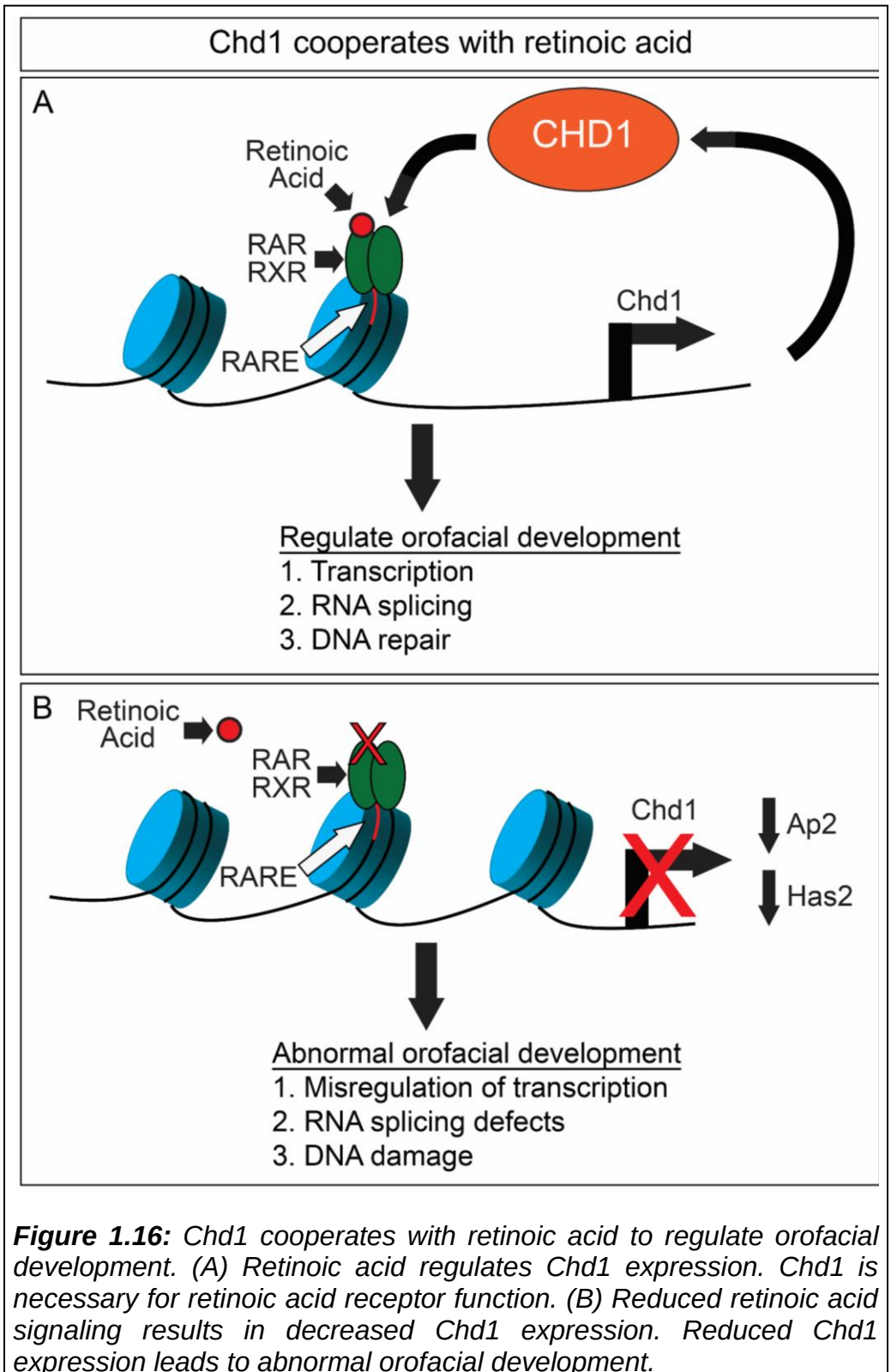

Figure 1.16: *Chd1 cooperates with retinoic acid to regulate orofacial development. (A) Retinoic acid regulates Chd1 expression. Chd1 is necessary for retinoic acid receptor function. (B) Reduced retinoic acid signaling results in decreased Chd1 expression. Reduced Chd1 expression leads to abnormal orofacial development.*

CHAPTER 2 ANALYZING THE CELL CYCLE PROFILE IN *XENOPUS LAEVIS* EMBRYOS

INTRODUCTION

Flow cytometry is a powerful method to analyze cells through the use of fluorescent agents that bind to specific molecules within the cell (See (Kruth, 1982) for review). This method is quantitative and is capable of analyzing thousands of cells relatively quickly. It gives an unbiased view of the cells and can identify small changes that may not be easily identified with staining techniques. In addition, cells can be co-labeled making it possible to examine multiple parameters of individual cells simultaneously.

In the flow cytometer, the cell suspension is injected into the center of a column of sheath fluid. The cells are hydrodynamically focused, thus aligning the cells so that they pass through the interrogation point, the point at which cells are exposed to the laser source, one at a time. The pressure exerted on the sheath fluid sets the flow rate of the cell suspension. High pressure will result in a faster flow rate and allow for quicker data collection. However, the high pressure also increases the diameter of the core stream. If the diameter of the core stream is much larger than the diameter of the cells, then this increases the chances that a cell can enter the interrogation point while the previous cell

has not fully exited the interrogation point. While it may take longer to acquire data with lower pressure, it will reduce the diameter of the core stream. This reduces the chances of two cells in the interrogation point at the same time and as a result, reduces the variability of the results.

Cells in the interrogation point scatter light in all directions, and the scattered light is detected with forward and side scatter detectors. Diffracted light is measured by the forward scatter detector and is proportional to cell size. While refracted light is measured by the side scatter detector and is proportional to cell granularity, or the internal complexity of the cell. The information gathered from these two measurements can be used to differentiate different populations of cells within the cell suspension when plotted on a histogram. In addition, the laser source can be used to excite fluorophores bound to cells in the interrogation to analyze specific characteristics of these labeled cells.

One such example of fluorescent labeling is the utilization of propidium iodide, a fluorescent agent that intercalates with DNA, to investigate the cell cycle profile of cells in a suspension. Propidium iodide has an excitation maxima of 535 nm and a fluorescent emission maxima of 617 nm. This agent does not normally cross the membrane of live cells and is sometimes used to differentiate live and apoptotic cells. For this reason, cells must be permeabilized to allow propidium iodide to access DNA in the cell. One method to do this is by fixation with agents such as alcohols, usually ethanol or methanol. These dissolve lipids in the cell membrane. Live cells can also be labeled by incubating the cells in a buffer containing a small amount of detergent, such as Nonidet P-40, which can partition into the cell membrane bilayer and allow propidium iodide access into the cell.

When labeled cells are in the interrogation point, propidium iodide is excited resulting in the emission of fluorescence is detected by specialized filters and detectors.

The emitted fluorescence is converted into a digital signal by the electronics component of the flow cytometer so that the gathered data can be interpreted by a computer. A photomultiplier tube absorbs photons generated from the emission of fluorescence and releases electrons. This signal is proportionally multiplied generating a current that is converted into a voltage pulse. An analog-to-digital converter converts the voltage pulse into a digital value that is transferred to the computer for data analysis.

The intensity of the fluorescence emitted by excited propidium iodide corresponds to the DNA content in the cell. When the data acquired from these fluorescing cells is plotted on a histogram, the result will typically show two peaks. The first peak corresponds to cells in the G0/G1 phase and the second peak that occurs at twice the intensity of the first peak, corresponds to cells in the G2/M phase, because the increased propidium iodide intensity comes from cells that have doubled their DNA. The population of cells that are represented between these two peaks on the histogram correspond to cells in S phase. The population of cells below the first peak on the X-axis represents cells in the Sub-G1 fraction. This phase corresponds to cells that have lost some of their DNA, which usually happens when cells are undergoing apoptosis. Together, this data provides an overview of the cell cycle profile of the cell population.

The protocol presented here describes a method to utilize propidium iodide labeling and flow cytometry to examine the cell cycle profile of cells obtained from *Xenopus laevis* embryos. More precisely, this method was designed to address the cell cycle profile of cells prepared from the head tissues of these embryos, in order to examine

the cell cycle profile that was representative of this region specifically. This method can be applied to samples that have been exposed to chemical agents or altered with genetic manipulation techniques to access the changes these manipulations may have on cell proliferation relative to controls.

METHODS

Reagents

Collagenase 2

Goat serum, 5% in 1X PBS

1X MBS

1X PBS

0.5X Ringer's Solution (58 mM NaCl, 1.45 mM KCl, 2.5 mM HEPES, pH 7.2)

Staining buffer (100 mM Tris pH 7.5, 154 mM NaCl, 1 mM $CaCl_2$, 0.5 mM $MgCl_2$, 0.2%

BSA, 0.1% Nonidet P-40, 86 µg/mL RNAse A, and 20 µg/mL propidium iodide)

Trypan blue

0.25% Trypsin/EDTA

Equipment

Cell strainer, 40µm

Centrifuge, refrigerated

Eppendorf tubes, 1.5ml

Flow cytometer

Gloves, powder free

Hemocytometer

Micropipettors, 10µl, 1000µl, with corresponding tips

Nutating rocker table

Scalpel, sterile disposable

Tubes, 1.5ml, 50ml

Water bath preset to 37°C

Collecting samples

1. Dissect the embryo heads by making two incisions through the embryo body. Make the first cut at the posterior end of the gut to remove the pressure while making the second cut. Make the second cut at the anterior end of the gut to completely remove the head from the body. When the head has been dissected, transfer it to a tube containing 1X MBS on ice using a glass pipette.

   Alternatively, this method can be applied to whole embryos. Begin with step 2 and collect the whole embryos in 0.5X Ringer's solution.

   There are a few controls that are useful when first starting with a new experiment. (1) Include a control sample of cells only, without treatment or genetic manipulation, and without propidium iodide to determine whether the cells will produce a background signal in the propidium iodide channel. (2) Include a sample

of cells only, without treatment or genetic manipulation, and with propidium iodide to see a normal cell cycle profile. (3) Include a sample with any chemical used for treatment or genetic manipulation only, without propidium iodide to determine whether the addition of these will result in background signal in the propidium iodide channel.

Dissociating tissues into individual cells

---

2. Remove the 1X MBS and replace with calcium free 0.5X Ringer's solution.

   The exclusion of calcium helps to prime cellular dissociation by weakening cellular adhesion. Furthermore, the yolk is soluble in the hypotonic Ringer's solution.

3. Use a 1000µl pipette to gently break up the tissues by pipetting them up and down. The goal is to break up the tissues into small pieces. However, it is important that the tissues are not treated too harshly, because that may cause cell lysis.
4. Allow the tissue pieces to settle, then remove the supernatant and replace with fresh 0.5X Ringer's solution.
5. Mixed the tubes on a nutating rocker table for four minutes at room temperature.
6. Repeat this process two more times allowing the tissue pieces to settle, replacing the 0.5X Ringer's solution and rocking for four minutes.
7. Allow the tissue pieces to settle, and then replace the 0.5X ringer's solution with 1X PBS. Mix the tubes on a nutating rocker table for five minutes at room temperature.

8. Repeat this process one more time allowing the tissue pieces to settle, replacing the 1X PBS, and rocking for five minutes.
9. Allowing the tissue pieces to settle, remove the 1X PBS and replace with 0.25% trypsin/EDTA supplemented with 5mg/ml collagenase 2. This will dissociate the tissues into individual cells.
10. Incubate this solution in a 37°C water bath for twenty minutes. During the incubation, gently invert the tubes a few times every five minutes to help ensure that the cells are dissociating. Do not mix harshly, because the cells are more sensitive in the trypsin solution.
11. Transfer the cell suspensions using a 1000ul pipette and filter them through a 40µm cell strainer into a 50ml conical tube. This will help remove tissue pieces that did not dissociate well.
12. Transfer the cell suspensions to 1.5ml Eppendorf tubes and centrifuge at 3000 rpm for 2 minutes at 4°C.
13. Remove the supernatant and resuspend the cell solution in 750µl of ice cold 5% goat serum in PBS.
14. Centrifuged the cell suspension at 3000 rpm for 2 minutes at 4°C.
15. Remove the supernatant and resuspend the cells in 50µl of 5% goat serum in PBS.
16. Remove a 10µl sample to be used for counting the cells (step 17). Add 500µl of 5% goat serum in PBS to the remaining 40µl of cell suspension and place on ice (for use in step 18) while counting the cells.
17. Stain the cells in the 10µl sample with 30µl of trypan blue and count the cells using a hemocytometer. Live cells will not be permeable to trypan blue and will appear

colorless. While dead cells will take up the trypan blue stain and appear blue. Ideally, there should not be an abundance of dead cells. If there are a lot of dead cells, then the cells were likely treated too harshly resulting in cell lysis. To determine the approximate number of cells in the sample follow the mathematical calculation provided with the hemocytometer slide.

18. Centrifuge the cell suspension at 3000 rpm for 2 minutes at 4°C.
19. Remove the supernatant and resuspend the cells in staining buffer. Add 1ml of staining buffer per 1,000,000 cells.
20. Incubate the cells in staining buffer for one hour on ice before running them on the flow cytometer.

Analyzing the cell samples with the flow cytometer

21. Before running a sample, it is recommended that a quality control is performed every day. This is done by mixing 350µl of 1X PBS with 1 drop of CS&T beads. Open “Cytometer Setup and Tracking” on the computer. Load the sample and run the bead solution on low. This will set the area scaling, laser delay, and optimal MFI to baseline. If the flow cytometer does not pass quality control, try cleaning and priming the flow cytometer, then repeat the quality control.
22. Prior to running the samples on the flow cytometer, filter the cell suspension through a 40µm cell strainer. This will help to eliminate any clumps of cells that may have formed while in the staining buffer.
23. Run sample and set flow rate. The flow rate affects the number of cells passing through the laser at a time. The higher the flow rate, the faster the sample will run,

and the quicker data will be collected. However, if the flow rate is too high, it may allow more than one cell to pass through the laser at the same time. This can lead to variability in the results. Therefore, it is often better to run the sample at a lower flow rate to allow for more precise data collection, particularly when examining DNA content for cell cycle analysis.

24. While the sample is running, isolate single, intact cells for your analysis by using your cells from your control sample. To do this, create a histogram using the software program to visualize area versus width. Adjust the voltage setting so that the population of cells that are tightly clustered together is shown in the middle of the histogram. Draw a gate around this population of cells. The width measurement is proportional to cell size and this population of cells should include single cells. Therefore, the cells that are represented higher on the X-axis compared to the tightly clustered population correlates to cells that are bigger and likely represents cells that occur as doublets (Fig. 2.1A). Doublets should be excluded from the analysis because the DNA content of such cells can be interpreted incorrectly if the flow cytometer recognizes them as one cell.
25. To further isolate single, intact cells, create a histogram to visualize side scatter versus forward scatter. This histogram will plot the cells based on cell size, as measured by forward scatter, and cell granularity, as measured by side scatter. Draw a gate around the population of cells that are tightly clustered together. Cells that are represented lower on the X- and Y-axes of the histogram compared to the tightly clustered population of cells are dead cells and cell fragments that should also be excluded from the analysis. Further, the cells that occur higher on the X-

axis compared to the tightly clustered population of cells can be excluded to ensure that doublets are being removed (Fig. 2.1B).

26. Next, create a histogram for propidium iodide and cell count.
27. Adjust the voltage so that the first peak is at 50 on the X-axis and the second peak is at 100 on the X-axis. Use the control sample to set the voltage. Draw gates to separate the boundaries of each phase, sub-G1, G0/G1, S, and G2/M (Fig. 2.2).
28. Set a stopping gate at 10,000 events. This will analyze 10,000 cells and then stop collecting data so that even numbers of cells are analyzed for each sample. Before choosing to collect data, let the sample run for a few seconds. This will allow the peaks on the histogram to stabilize. Then choose to collect data.
29. After the first sample is finished, remove the sample tube and gently wipe off any residual sample that may remain on the machine with a kimwipe. Load the next sample and allow it to run for a few seconds until the peaks have stabilized. If necessary, adjust the voltage so that the top of the first peak is in exactly the same place with the gate as the first sample. This should only be a small change of about 1-2 units.
30. Repeat step 28 until all samples have been analyzed.

Save the settings used from the first experiment so that they can be used for future replicates. Note that the settings used to get similar results may be slightly different when using different flow cytometers.

Using additional software to analyze the cell cycle profile

Software designed to analyze flow cytometry data is one alternative to using gates to separate the boundaries of each phase of the cell cycle. Software such as FCS express can create overlays to compare samples (Fig. 2.3A) and use models to analyze the cell cycle profile without using gates (Fig. 2.3B). One benefit to using models to analyze the cell cycle profile is that these models take into consideration that there is some overlap between the phases of the cell cycle. Gates, such as those used in the example described previously in this chapter, do not account for this potential overlap. The model used in the example in figure 2.3 only shows percentages for G0/G1, S, and G2/M phases. Cells in the sub-G1 fraction are included in the percent background, aggregates, and debris (BAD) in all cycles. In the example shown, there are some cells included in the BAD fraction of the treated sample that occur in the region of S phase. These may represent cells that were dying before entering G2/M and were not at a point in which they would be included in the sub G1 fraction, and therefore, not appropriately accounted for when analyzed by using gate to separate the boundaries.

DISCUSSION

Flow cytometry is one method that can be utilized to analyze characteristics of cells including the cell cycle profile. While there are other methods that can be utilized to analyze changes in cell proliferation and cell death, such as staining, flow cytometry is quantitative and has the ability to detect small changes making it a powerful method to examine changes in the cell cycle profile between treated and control samples. The protocol presented here describes a method to stain live cells from *X. laevis* with propidium iodide for analysis with flow cytometry. This method demonstrates that it is possible to isolate these cells from specific tissues, as illustrated here in the head tissues from *X. laevis* embryos. The ease of performing chemical genetics in *X. laevis* embryos offers the potential to use the method presented here to investigate the effect of chemical agents on the cell cycle profile.

FIGURES

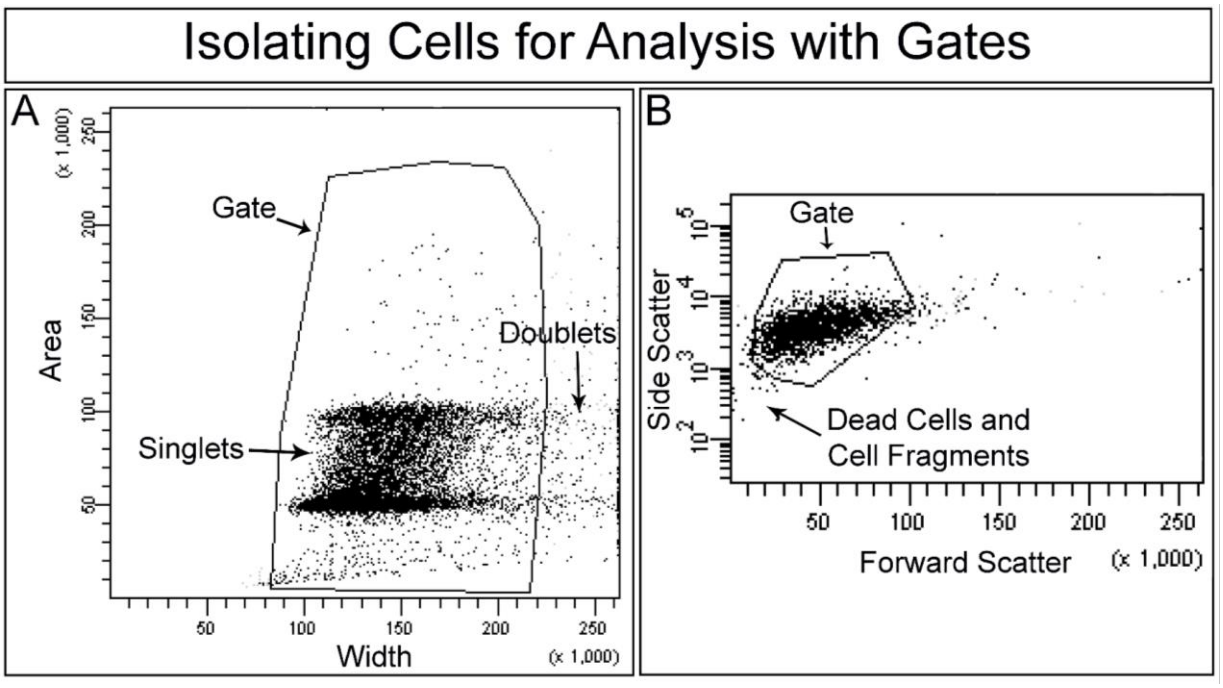

Figure 2.1: Gates will isolate cell populations for further analysis. (A) Histogram plotting area versus width to remove doublets and cell clumps from the analysis. (B) Histogram plotting side scatter versus forward scatter to remove dead cells and cell fragments from the analysis.

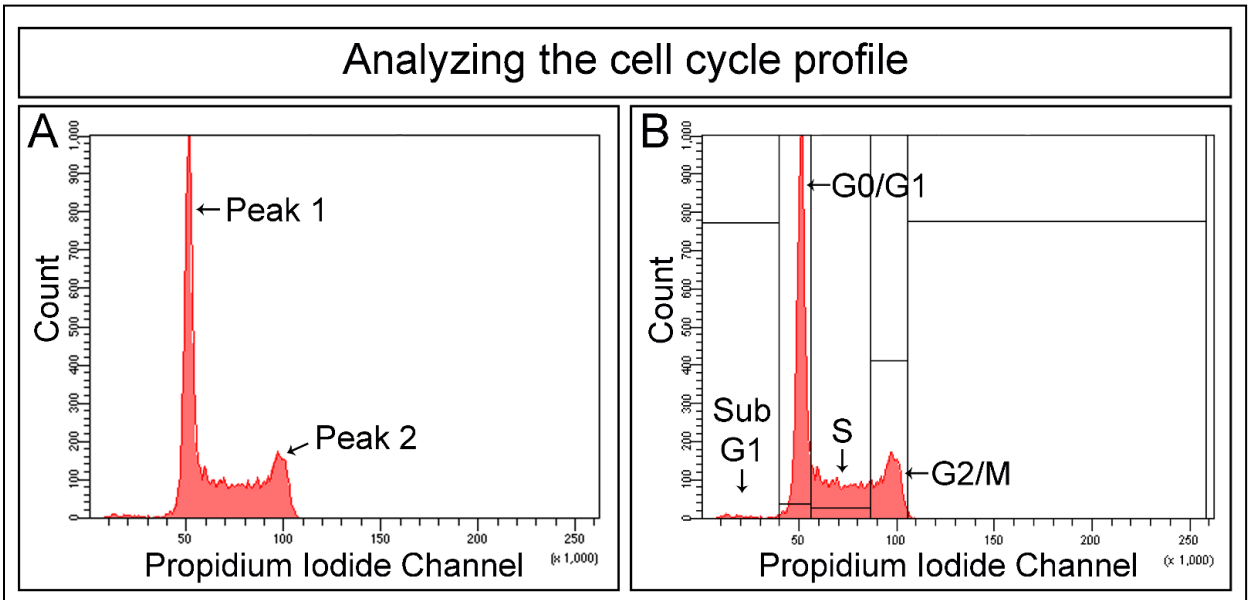

***Figure 2.2*:** Examining the cell cycle profile. (A) Peak 1 and Peak 2 represent cells from two different phases of the cell cycle. (B) Boundaries can be used to quantitate the percentage of cells in each phase of the cell cycle.

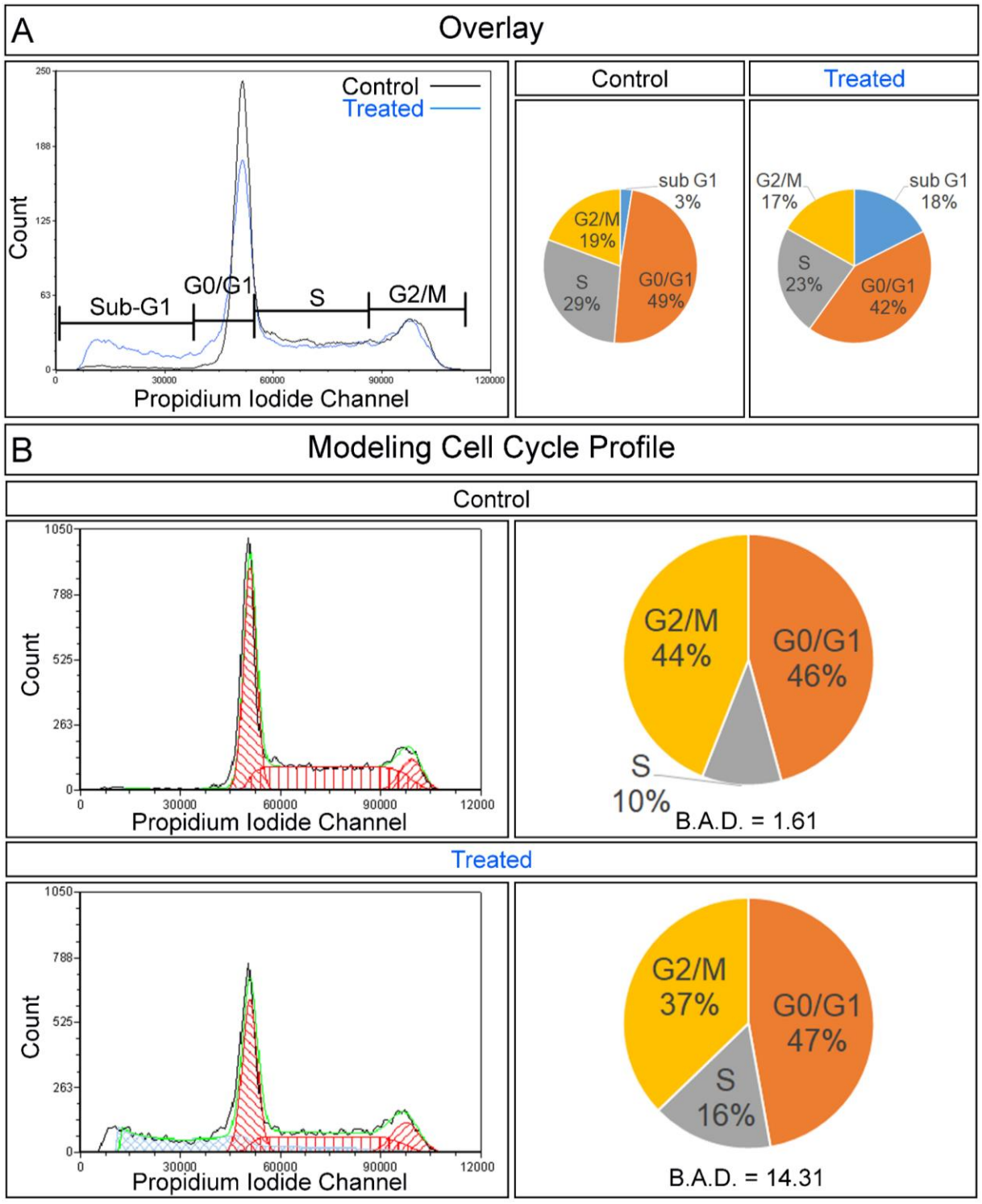

Figure 2.3: *Analyzing the cell cycle profile with FCS Express software. (A) Overlay of control and treated samples. Gates can be applied to the overlay to determine the percentage of cells within each phase of the cell cycle. (B) Software includes models that can be applied as an alternant method to analyze the cell cycle. B.A.D. = Percent background, aggregates, and debris in all cycles.*

REFERENCES

Abe, M., Maeda, T., Wakisaka, S., 2008. Retinoic acid affects craniofacial patterning by changing Fgf8 expression in the pharyngeal ectoderm. Development, growth & differentiation 50, 717-729.

Ackermans, M.M., Zhou, H., Carels, C.E., Wagener, F.A., Von den Hoff, J.W., 2011. Vitamin A and clefting: putative biological mechanisms. Nutrition reviews 69, 613-624.

Alabert, C., Groth, A., 2012. Chromatin replication and epigenome maintenance. Nature reviews. Molecular cell biology 13, 153-167.

Allam, K.A., Wan, D.C., Kawamoto, H.K., Bradley, J.P., Sedano, H.O., Saied, S., 2011. The spectrum of median craniofacial dysplasia. Plastic and reconstructive surgery 127, 812-821.

Altig, R., McDiarmid, R., 1999. Tadpoles: the biology of anuran larvae. University of Chicago Press, Chicago.

Aramaki, M., Kimura, T., Udaka, T., Kosaki, R., Mitsuhashi, T., Okada, Y., Takahashi, T., Kosaki, K., 2007. Embryonic expression profile of chicken CHD7, the ortholog of the causative gene for CHARGE syndrome. Birth defects research. Part A, Clinical and molecular teratology 79, 50-57.

Arends, M.J., Morris, R.G., Wyllie, A.H., 1990. Apoptosis. The role of the endonuclease. The American journal of pathology 136, 593-608.

Aso, T., Lane, W.S., Conaway, J.W., Conaway, R.C., 1995. Elongin (SIII): a multisubunit regulator of elongation by RNA polymerase II. Science (New York, N.Y.) 269, 1439-1443.

Audit, B., Zaghloul, L., Vaillant, C., Chevereau, G., d'Aubenton-Carafa, Y., Thermes, C., Arneodo, A., 2009. Open chromatin encoded in DNA sequence is the signature of 'master' replication origins in human cells. Nucleic acids research 37, 6064-6075.

Badeaux, A.I., Yang, Y., Cardenas, K., Vemulapalli, V., Chen, K., Kusewitt, D., Richie, E., Li, W., Bedford, M.T., 2012. Loss of the methyl lysine effector protein PHF20 impacts the expression of genes regulated by the lysine acetyltransferase MOF. J Biol Chem 287, 429-437.

Bajpai, R., Chen, D.A., Rada-Iglesias, A., Zhang, J., Xiong, Y., Helms, J., Chang, C.P., Zhao, Y., Swigut, T., Wysocka, J., 2010. CHD7 cooperates with PBAF to control multipotent neural crest formation. Nature 463, 958-962.

Bannister, A.J., Zegerman, P., Partridge, J.F., Miska, E.A., Thomas, J.O., Allshire, R.C., Kouzarides, T., 2001. Selective recognition of methylated lysine 9 on histone H3 by the HP1 chromo domain. Nature 410, 120-124.

Basson, M.A., van Ravenswaaij-Arts, C., 2015. Functional Insights into Chromatin Remodelling from Studies on CHARGE Syndrome. Trends in genetics : TIG 31, 600-611.

Bastien, J., Rochette-Egly, C., 2004. Nuclear retinoid receptors and the transcription of retinoid-target genes. Gene 328, 1-16.

Baumgart, S.J., Najafova, Z., Hossan, T., Xie, W., Nagarajan, S., Kari, V., Ditzel, N., Kassem, M., Johnsen, S.A., 2017. CHD1 regulates cell fate determination by activation of differentiation-induced genes. Nucleic acids research 45, 7722-7735.

Bernier, R., Golzio, C., Xiong, B., Stessman, H.A., Coe, B.P., Penn, O., Witherspoon, K., Gerdts, J., Baker, C., Vulto-van Silfhout, A.T., Schuurs-Hoeijmakers, J.H., Fichera, M., Bosco, P., Buono, S., Alberti, A., Failla, P., Peeters, H., Steyaert, J., Vissers, L., Francescatto, L., Mefford, H.C., Rosenfeld, J.A., Bakken, T., O'Roak, B.J., Pawlus, M., Moon, R., Shendure, J., Amaral, D.G., Lein, E., Rankin, J., Romano, C., de Vries, B.B.A., Katsanis, N., Eichler, E.E., 2014. Disruptive CHD8 mutations define a subtype of autism early in development. Cell 158, 263-276.

Betancur, P., Bronner-Fraser, M., Sauka-Spengler, T., 2010. Assembling neural crest regulatory circuits into a gene regulatory network. Annual review of cell and developmental biology 26, 581-603.

Birch, J.L., Tan, B.C., Panov, K.I., Panova, T.B., Andersen, J.S., Owen-Hughes, T.A., Russell, J., Lee, S.C., Zomerdijk, J.C., 2009. FACT facilitates chromatin transcription by RNA polymerases I and III. Embo j 28, 854-865.

Boyle, M.I., Jespersgaard, C., Brondum-Nielsen, K., Bisgaard, A.M., Tumer, Z., 2015. Cornelia de Lange syndrome. Clinical genetics 88, 1-12.

Brickell, P., Thorogood, P., 1997. Retinoic acid and retinoic acid receptors in craniofacial development. Semin Cell Dev Biol 8, 437-443.

Burn, J., 1986. Williams syndrome. Journal of medical genetics 23, 389-395.

Camenisch, T.D., Spicer, A.P., Brehm-Gibson, T., Biesterfeldt, J., Augustine, M.L., Calabro, A., Jr., Kubalak, S., Klewer, S.E., McDonald, J.A., 2000. Disruption of

hyaluronan synthase-2 abrogates normal cardiac morphogenesis and hyaluronan-mediated transformation of epithelium to mesenchyme. The Journal of clinical investigation 106, 349-360.

Carmona-Mora, P., Encina, C.A., Canales, C.P., Cao, L., Molina, J., Kairath, P., Young, J.I., Walz, K., 2010. Functional and cellular characterization of human Retinoic Acid Induced 1 (RAI1) mutations associated with Smith-Magenis Syndrome. BMC molecular biology 11, 63.

Casini, P., Nardi, I., Ori, M., 2012. Hyaluronan is required for cranial neural crest cells migration and craniofacial development. Dev Dyn 241, 294-302.

Cayrou, C., Coulombe, P., Mechali, M., 2010. Programming DNA replication origins and chromosome organization. Chromosome research : an international journal on the molecular, supramolecular and evolutionary aspects of chromosome biology 18, 137-145.

Centers for Disease Control and Prevention, 2018. Birth Defects.

Chai, Y., Maxson, R.E., Jr., 2006. Recent advances in craniofacial morphogenesis. Dev Dyn 235, 2353-2375.

Chaitanya, G.V., Steven, A.J., Babu, P.P., 2010. PARP-1 cleavage fragments: signatures of cell-death proteases in neurodegeneration. Cell communication and signaling : CCS 8, 31.

Cheedipudi, S., Puri, D., Saleh, A., Gala, H.P., Rumman, M., Pillai, M.S., Sreenivas, P., Arora, R., Sellathurai, J., Schroder, H.D., Mishra, R.K., Dhawan, J., 2015. A fine balance: epigenetic control of cellular quiescence by the tumor suppressor PRDM2/RIZ at a bivalent domain in the cyclin a gene. Nucleic acids research 43, 6236-6256.

Collins, N., Poot, R.A., Kukimoto, I., Garcia-Jimenez, C., Dellaire, G., Varga-Weisz, P.D., 2002. An ACF1-ISWI chromatin-remodeling complex is required for DNA replication through heterochromatin. Nature genetics 32, 627-632.

Cordero, D.R., Brugmann, S., Chu, Y., Bajpai, R., Jame, M., Helms, J.A., 2011. Cranial neural crest cells on the move: their roles in craniofacial development. Am J Med Genet A 155a, 270-279.

Dalton, S., 2015. Linking the Cell Cycle to Cell Fate Decisions. Trends in cell biology 25, 592-600.

Darvekar, S., Rekdal, C., Johansen, T., Sjottem, E., 2013. A phylogenetic study of SPBP and RAI1: evolutionary conservation of chromatin binding modules. PLoS One 8, e78907.

De Leersnyder, H., 2013. Smith-Magenis syndrome. Handbook of clinical neurology 111, 295-296.

de Ruijter, A.J., van Gennip, A.H., Caron, H.N., Kemp, S., van Kuilenburg, A.B., 2003. Histone deacetylases (HDACs): characterization of the classical HDAC family. The Biochemical journal 370, 737-749.

Delacroix, L., Moutier, E., Altobelli, G., Legras, S., Poch, O., Choukrallah, M.A., Bertin, I., Jost, B., Davidson, I., 2010. Cell-specific interaction of retinoic acid receptors with target genes in mouse embryonic fibroblasts and embryonic stem cells. Mol Cell Biol 30, 231-244.

DeLaurier, A., Nakamura, Y., Braasch, I., Khanna, V., Kato, H., Wakitani, S., Postlethwait, J.H., Kimmel, C.B., 2012. Histone deacetylase-4 is required during early cranial neural crest development for generation of the zebrafish palatal skeleton. BMC developmental biology 12, 16.

Delcuve, G.P., Khan, D.H., Davie, J.R., 2012. Roles of histone deacetylases in epigenetic regulation: emerging paradigms from studies with inhibitors. Clinical epigenetics 4, 5.

Delmas, V., Stokes, D.G., Perry, R.P., 1993. A mammalian DNA-binding protein that contains a chromodomain and an SNF2/SWI2-like helicase domain. Proc Natl Acad Sci U S A 90, 2414-2418.

Deniz, O., Flores, O., Aldea, M., Soler-Lopez, M., Orozco, M., 2016. Nucleosome architecture throughout the cell cycle. Sci Rep 6, 19729.

DePamphilis, M.L., 2016. Genome Duplication at the Beginning of Mammalian Development. Current topics in developmental biology 120, 55-102.

Dickinson, A., Sive, H., 2007. Positioning the extreme anterior in Xenopus: cement gland, primary mouth and anterior pituitary. Semin Cell Dev Biol 18, 525-533.

Dickinson, A.J., 2016. Using frogs faces to dissect the mechanisms underlying human orofacial defects. Semin Cell Dev Biol 51, 54-63.

Dickinson, A.J., Sive, H.L., 2009. The Wnt antagonists Frzb-1 and Crescent locally regulate basement membrane dissolution in the developing primary mouth. Development 136, 1071-1081.

Dudas, M., Li, W.Y., Kim, J., Yang, A., Kaartinen, V., 2007. Palatal fusion - where do the midline cells go? A review on cleft palate, a major human birth defect. Acta histochemica 109, 1-14.

Dupe, V., Pellerin, I., 2009. Retinoic acid receptors exhibit cell-autonomous functions in cranial neural crest cells. Dev Dyn 238, 2701-2711.

Durand, B., Saunders, M., Leroy, P., Leid, M., Chambon, P., 1992. All-trans and 9-cis retinoic acid induction of CRABPII transcription is mediated by RAR-RXR heterodimers bound to DR1 and DR2 repeated motifs. Cell 71, 73-85.

Eissenberg, J.C., Shilatifard, A., Dorokhov, N., Michener, D.E., 2007. Cdk9 is an essential kinase in Drosophila that is required for heat shock gene expression, histone methylation and elongation factor recruitment. Molecular genetics and genomics : MGG 277, 101-114.

Elmore, S., 2007. Apoptosis: a review of programmed cell death. Toxicologic pathology 35, 495-516.

Endoh, M., Zhu, W., Hasegawa, J., Watanabe, H., Kim, D.K., Aida, M., Inukai, N., Narita, T., Yamada, T., Furuya, A., Sato, H., Yamaguchi, Y., Mandal, S.S., Reinberg, D., Wada, T., Handa, H., 2004. Human Spt6 stimulates transcription elongation by RNA polymerase II in vitro. Mol Cell Biol 24, 3324-3336.

Ferguson, M.W., 1988. Palate development. Development 103 Suppl, 41-60.

Field, Y., Kaplan, N., Fondufe-Mittendorf, Y., Moore, I.K., Sharon, E., Lubling, Y., Widom, J., Segal, E., 2008. Distinct modes of regulation by chromatin encoded through nucleosome positioning signals. PLoS computational biology 4, e1000216.

Finnell, R.H., Shaw, G.M., Lammer, E.J., Brandl, K.L., Carmichael, S.L., Rosenquist, T.H., 2004. Gene-nutrient interactions: importance of folates and retinoids during early embryogenesis. Toxicology and applied pharmacology 198, 75-85.

Finnin, M.S., Donigian, J.R., Cohen, A., Richon, V.M., Rifkind, R.A., Marks, P.A., Breslow, R., Pavletich, N.P., 1999. Structures of a histone deacetylase homologue bound to the TSA and SAHA inhibitors. Nature 401, 188-193.

Flanagan, J.F., Mi, L.Z., Chruszcz, M., Cymborowski, M., Clines, K.L., Kim, Y., Minor, W., Rastinejad, F., Khorasanizadeh, S., 2005. Double chromodomains cooperate to recognize the methylated histone H3 tail. Nature 438, 1181-1185.

Fujita, K., Ogawa, R., Kawawaki, S., Ito, K., 2014. Roles of chromatin remodelers in maintenance mechanisms of multipotency of mouse trunk neural crest cells in the formation of neural crest-derived stem cells. Mech Dev 133, 126-145.

Gaspar-Maia, A., Alajem, A., Polesso, F., Sridharan, R., Mason, M.J., Heidersbach, A., Ramalho-Santos, J., McManus, M.T., Plath, K., Meshorer, E., Ramalho-Santos, M., 2009. Chd1 regulates open chromatin and pluripotency of embryonic stem cells. Nature 460, 863-868.

Gibbons, R.J., Higgs, D.R., 2000. Molecular-clinical spectrum of the ATR-X syndrome. American journal of medical genetics 97, 204-212.

Gibson, W.T., Hood, R.L., Zhan, S.H., Bulman, D.E., Fejes, A.P., Moore, R., Mungall, A.J., Eydoux, P., Babul-Hirji, R., An, J., Marra, M.A., Chitayat, D., Boycott, K.M., Weaver, D.D., Jones, S.J., 2012. Mutations in EZH2 cause Weaver syndrome. American journal of human genetics 90, 110-118.

Gu, L., Hitzel, J., Moll, F., Kruse, C., Malik, R.A., Preussner, J., Looso, M., Leisegang, M.S., Steinhilber, D., Brandes, R.P., Fork, C., 2016. The Histone Demethylase PHF8 Is Essential for Endothelial Cell Migration. PLoS One 11, e0146645.

Guzman-Ayala, M., Sachs, M., Koh, F.M., Onodera, C., Bulut-Karslioglu, A., Lin, C.J., Wong, P., Nitta, R., Song, J.S., Ramalho-Santos, M., 2015. Chd1 is essential for the high transcriptional output and rapid growth of the mouse epiblast. Development 142, 118-127.

Haberland, M., Mokalled, M.H., Montgomery, R.L., Olson, E.N., 2009a. Epigenetic control of skull morphogenesis by histone deacetylase 8. Genes & development 23, 1625-1630.

Haberland, M., Montgomery, R.L., Olson, E.N., 2009b. The many roles of histone deacetylases in development and physiology: implications for disease and therapy. Nature reviews. Genetics 10, 32-42.

Hall, J.A., Georgel, P.T., 2007. CHD proteins: a diverse family with strong ties. Biochemistry and cell biology = Biochimie et biologie cellulaire 85, 463-476.

Harakalova, M., van den Boogaard, M.J., Sinke, R., van Lieshout, S., van Tuil, M.C., Duran, K., Renkens, I., Terhal, P.A., de Kovel, C., Nijman, I.J., van Haelst, M., Knoers, N.V., van Haaften, G., Kloosterman, W., Hennekam, R.C., Cuppen, E., Ploos van Amstel, H.K., 2012. X-exome sequencing identifies a HDAC8 variant in a large pedigree with X-linked intellectual disability, truncal obesity, gynaecomastia, hypogonadism and unusual face. Journal of medical genetics 49, 539-543.

Hendzel, M.J., Wei, Y., Mancini, M.A., Van Hooser, A., Ranalli, T., Brinkley, B.R., Bazett-Jones, D.P., Allis, C.D., 1997. Mitosis-specific phosphorylation of histone H3 initiates primarily within pericentromeric heterochromatin during G2 and spreads in an ordered fashion coincident with mitotic chromosome condensation. Chromosoma 106, 348-360.

Huang, N., vom Baur, E., Garnier, J.M., Lerouge, T., Vonesch, J.L., Lutz, Y., Chambon, P., Losson, R., 1998. Two distinct nuclear receptor interaction domains in NSD1, a novel SET protein that exhibits characteristics of both corepressors and coactivators. Embo j 17, 3398-3412.

Ignatius, M.S., Unal Eroglu, A., Malireddy, S., Gallagher, G., Nambiar, R.M., Henion, P.D., 2013. Distinct functional and temporal requirements for zebrafish Hdac1 during neural crest-derived craniofacial and peripheral neuron development. PLoS One 8, e63218.

Imai, Y., Suzuki, Y., Matsui, T., Tohyama, M., Wanaka, A., Takagi, T., 1995. Cloning of a retinoic acid-induced gene, GT1, in the embryonal carcinoma cell line P19: neuron-specific expression in the mouse brain. Brain research. Molecular brain research 31, 1-9.

Iseki, S., 2011. Disintegration of the medial epithelial seam: is cell death important in palatogenesis? Development, growth & differentiation 53, 259-268.

Jacox, L.A., Dickinson, A.J., Sive, H., 2014. Facial transplants in Xenopus laevis embryos. J Vis Exp.

Jiang, R., Bush, J.O., Lidral, A.C., 2006. Development of the upper lip: morphogenetic and molecular mechanisms. Dev Dyn 235, 1152-1166.

Kaiser, F.J., Ansari, M., Braunholz, D., Concepcion Gil-Rodriguez, M., Decroos, C., Wilde, J.J., Fincher, C.T., Kaur, M., Bando, M., Amor, D.J., Atwal, P.S., Bahlo, M., Bowman, C.M., Bradley, J.J., Brunner, H.G., Clark, D., Del Campo, M., Di Donato, N., Diakumis, P., Dubbs, H., Dyment, D.A., Eckhold, J., Ernst, S., Ferreira, J.C., Francey, L.J., Gehlken, U., Guillen-Navarro, E., Gyftodimou, Y., Hall, B.D., Hennekam, R., Hudgins, L., Hullings, M., Hunter, J.M., Yntema, H., Innes, A.M., Kline, A.D., Krumina, Z., Lee, H., Leppig, K., Lynch, S.A., Mallozzi, M.B., Mannini, L., McKee, S., Mehta, S.G., Micule, I., Mohammed, S., Moran, E., Mortier, G.R., Moser, J.A., Noon, S.E., Nozaki, N., Nunes, L., Pappas, J.G., Penney, L.S., Perez-Aytes, A., Petersen, M.B., Puisac, B., Revencu, N., Roeder, E., Saitta, S., Scheuerle, A.E., Schindeler, K.L., Siu, V.M., Stark, Z., Strom, S.P., Thiese, H., Vater, I., Willems, P., Williamson, K., Wilson, L.C., Hakonarson, H., Quintero-Rivera, F., Wierzba, J., Musio, A., Gillessen-Kaesbach, G., Ramos, F.J., Jackson, L.G., Shirahige, K., Pie, J., Christianson, D.W., Krantz, I.D., Fitzpatrick, D.R., Deardorff, M.A., 2014. Loss-of-function HDAC8 mutations cause a phenotypic spectrum of Cornelia de Lange syndrome-like features, ocular hypertelorism, large fontanelle and X-linked inheritance. Hum Mol Genet 23, 2888-2900.

Kari, V., Mansour, W.Y., Raul, S.K., Baumgart, S.J., Mund, A., Grade, M., Sirma, H., Simon, R., Will, H., Dobbelstein, M., Dikomey, E., Johnsen, S.A., 2016. Loss of CHD1 causes DNA repair defects and enhances prostate cancer therapeutic responsiveness. EMBO reports 17, 1609-1623.

Kelley, D.E., Stokes, D.G., Perry, R.P., 1999. CHD1 interacts with SSRP1 and depends on both its chromodomain and its ATPase/helicase-like domain for proper association with chromatin. Chromosoma 108, 10-25.

Kennedy, A.E., Dickinson, A.J., 2012. Median facial clefts in Xenopus laevis: roles of retinoic acid signaling and homeobox genes. Dev Biol 365, 229-240.

Kennedy, A.E., Dickinson, A.J., 2014a. Quantification of orofacial phenotypes in Xenopus. J Vis Exp, e52062.

Kennedy, A.E., Dickinson, A.J., 2014b. Quantitative analysis of orofacial development and median clefts in Xenopus laevis. Anat Rec (Hoboken) 297, 834-855.

Klingenberg, C.P., Wetherill, L., Rogers, J., Moore, E., Ward, R., Autti-Ramo, I., Fagerlund, A., Jacobson, S.W., Robinson, L.K., Hoyme, H.E., Mattson, S.N., Li, T.K., Riley, E.P., Foroud, T., 2010. Prenatal alcohol exposure alters the patterns of facial asymmetry. Alcohol (Fayetteville, N.Y.) 44, 649-657.

Koh, F.M., Lizama, C.O., Wong, P., Hawkins, J.S., Zovein, A.C., Ramalho-Santos, M., 2015. Emergence of hematopoietic stem and progenitor cells involves a Chd1-dependent increase in total nascent transcription. Proc Natl Acad Sci U S A 112, E1734-1743.

Kruth, H.S., 1982. Flow cytometry: rapid biochemical analysis of single cells. Analytical biochemistry 125, 225-242.

Lalevee, S., Anno, Y.N., Chatagnon, A., Samarut, E., Poch, O., Laudet, V., Benoit, G., Lecompte, O., Rochette-Egly, C., 2011. Genome-wide in silico identification of new conserved and functional retinoic acid receptor response elements (direct repeats separated by 5 bp). J Biol Chem 286, 33322-33334.

Landry, J., Sharov, A.A., Piao, Y., Sharova, L.V., Xiao, H., Southon, E., Matta, J., Tessarollo, L., Zhang, Y.E., Ko, M.S., Kuehn, M.R., Yamaguchi, T.P., Wu, C., 2008. Essential role of chromatin remodeling protein Bptf in early mouse embryos and embryonic stem cells. PLoS genetics 4, e1000241.

Lauberth, S.M., Nakayama, T., Wu, X., Ferris, A.L., Tang, Z., Hughes, S.H., Roeder, R.G., 2013. H3K4me3 interactions with TAF3 regulate preinitiation complex assembly and selective gene activation. Cell 152, 1021-1036.

Lee, J.Y., Lake, R.J., Kirk, J., Bohr, V.A., Fan, H.Y., Hohng, S., 2017. NAP1L1 accelerates activation and decreases pausing to enhance nucleosome remodeling by CSB. Nucleic acids research 45, 4696-4707.

Lee, M.S., Bonner, J.R., Bernard, D.J., Sanchez, E.L., Sause, E.T., Prentice, R.R., Burgess, S.M., Brody, L.C., 2012. Disruption of the folate pathway in zebrafish causes developmental defects. BMC developmental biology 12, 12.

Levy, M.A., Kernohan, K.D., Jiang, Y., Berube, N.G., 2015. ATRX promotes gene expression by facilitating transcriptional elongation through guanine-rich coding regions. Hum Mol Genet 24, 1824-1835.

Liu, Z., Zhou, Z., Chen, G., Bao, S., 2007. A putative transcriptional elongation factor hIws1 is essential for mammalian cell proliferation. Biochemical and biophysical research communications 353, 47-53.

Lohnes, D., Mark, M., Mendelsohn, C., Dolle, P., Dierich, A., Gorry, P., Gansmuller, A., Chambon, P., 1994. Function of the retinoic acid receptors (RARs) during development (I). Craniofacial and skeletal abnormalities in RAR double mutants. Development 120, 2723-2748.

Lombardi, P.M., Cole, K.E., Dowling, D.P., Christianson, D.W., 2011. Structure, mechanism, and inhibition of histone deacetylases and related metalloenzymes. Current opinion in structural biology 21, 735-743.

Lu, X., Meng, X., Morris, C.A., Keating, M.T., 1998. A novel human gene, WSTF, is deleted in Williams syndrome. Genomics 54, 241-249.

Maina, P.K., Shao, P., Jia, X., Liu, Q., Umesalma, S., Marin, M., Long, D., Jr., Concepcion-Roman, S., Qi, H.H., 2017. Histone demethylase PHF8 regulates hypoxia signaling through HIF1alpha and H3K4me3. Biochimica et biophysica acta 1860, 1002-1012.

Marfella, C.G., Imbalzano, A.N., 2007. The Chd family of chromatin remodelers. Mutat Res 618, 30-40.

Mark, M., Ghyselinck, N.B., Chambon, P., 2004. Retinoic acid signalling in the development of branchial arches. Current opinion in genetics & development 14, 591-598.

Mayekar, M.K., Gardner, R.G., Arndt, K.M., 2013. The recruitment of the Saccharomyces cerevisiae Paf1 complex to active genes requires a domain of Rtf1 that directly interacts with the Spt4-Spt5 complex. Mol Cell Biol 33, 3259-3273.

Mayor, R., Theveneau, E., 2013. The neural crest. Development 140, 2247-2251.

McLean, J.E., Neidhardt, E.A., Grossman, T.H., Hedstrom, L., 2001. Multiple inhibitor analysis of the brequinar and leflunomide binding sites on human dihydroorotate dehydrogenase. Biochemistry 40, 2194-2200.

Mechali, M., 2010. Eukaryotic DNA replication origins: many choices for appropriate answers. Nature reviews. Molecular cell biology 11, 728-738.

Messina, G., Atterrato, M.T., Prozzillo, Y., Piacentini, L., Losada, A., Dimitri, P., 2017. The human Cranio Facial Development Protein 1 (Cfdp1) gene encodes a protein required for the maintenance of higher-order chromatin organization. Sci Rep 7, 45022.

Metcalfe, K., 1999. Williams syndrome: an update on clinical and molecular aspects. Archives of disease in childhood 81, 198-200.

Micucci, J.A., Layman, W.S., Hurd, E.A., Sperry, E.D., Frank, S.F., Durham, M.A., Swiderski, D.L., Skidmore, J.M., Scacheri, P.C., Raphael, Y., Martin, D.M., 2014. CHD7 and retinoic acid signaling cooperate to regulate neural stem cell and inner ear development in mouse models of CHARGE syndrome. Hum Mol Genet 23, 434-448.

Milite, C., Feoli, A., Viviano, M., Rescigno, D., Cianciulli, A., Balzano, A.L., Mai, A., Castellano, S., Sbardella, G., 2016. The emerging role of lysine methyltransferase SETD8 in human diseases. Clinical epigenetics 8, 102.

Milne, T.A., Briggs, S.D., Brock, H.W., Martin, M.E., Gibbs, D., Allis, C.D., Hess, J.L., 2002. MLL targets SET domain methyltransferase activity to Hox gene promoters. Molecular cell 10, 1107-1117.

Minoux, M., Holwerda, S., Vitobello, A., Kitazawa, T., Kohler, H., Stadler, M.B., Rijli, F.M., 2017. Gene bivalency at Polycomb domains regulates cranial neural crest positional identity. Science (New York, N.Y.) 355.

Miotto, B., Struhl, K., 2010. HBO1 histone acetylase activity is essential for DNA replication licensing and inhibited by Geminin. Molecular cell 37, 57-66.

Muchardt, C., Reyes, J.C., Bourachot, B., Leguoy, E., Yaniv, M., 1996. The hbrm and BRG-1 proteins, components of the human SNF/SWI complex, are phosphorylated and excluded from the condensed chromosomes during mitosis. Embo j 15, 3394-3402.

Nagata, S., 2000. Apoptotic DNA fragmentation. Exp Cell Res 256, 12-18.

Nagata, S., Nagase, H., Kawane, K., Mukae, N., Fukuyama, H., 2003. Degradation of chromosomal DNA during apoptosis. Cell death and differentiation 10, 108-116.

Niederreither, K., Dolle, P., 2008. Retinoic acid in development: towards an integrated view. Nature reviews. Genetics 9, 541-553.

Nieuwkoop, P.D., Faber, J., 1994. Normal table of Xenopus laevis (Daudin) : a systematical and chronological survey of the development from the fertilized egg till the end of metamorphosis. Garland Pub.

Panchenko, M.V., 2016. Structure, function and regulation of jade family PHD finger 1 (JADE1). Gene 589, 1-11.

Park, J.W., Cai, J., McIntosh, I., Jabs, E.W., Fallin, M.D., Ingersoll, R., Hetmanski, J.B., Vekemans, M., Attie-Bitach, T., Lovett, M., Scott, A.F., Beaty, T.H., 2006. High throughput SNP and expression analyses of candidate genes for non-syndromic oral clefts. Journal of medical genetics 43, 598-608.

Pauli, S., Bajpai, R., Borchers, A., 2017. CHARGEd with neural crest defects. American journal of medical genetics. Part C, Seminars in medical genetics 175, 478-486.

Pillai, R., Coverdale, L.E., Dubey, G., Martin, C.C., 2004. Histone deacetylase 1 (HDAC-1) required for the normal formation of craniofacial cartilage and pectoral fins of the zebrafish. Dev Dyn 231, 647-654.

Platt, R.J., Zhou, Y., Slaymaker, I.M., Shetty, A.S., Weisbach, N.R., Kim, J.A., Sharma, J., Desai, M., Sood, S., Kempton, H.R., Crabtree, G.R., Feng, G., Zhang, F., 2017. Chd8 Mutation Leads to Autistic-like Behaviors and Impaired Striatal Circuits. Cell reports 19, 335-350.

Qi, H.H., Sarkissian, M., Hu, G.Q., Wang, Z., Bhattacharjee, A., Gordon, D.B., Gonzales, M., Lan, F., Ongusaha, P.P., Huarte, M., Yaghi, N.K., Lim, H., Garcia, B.A., Brizuela, L., Zhao, K., Roberts, T.M., Shi, Y., 2010. Histone H4K20/H3K9 demethylase PHF8 regulates zebrafish brain and craniofacial development. Nature 466, 503-507.

Ratnakumar, K., Bernstein, E., 2013. ATRX: the case of a peculiar chromatin remodeler. Epigenetics 8, 3-9.

Rhinn, M., Dolle, P., 2012. Retinoic acid signalling during development. Development 139, 843-858.

Rinon, A., Lazar, S., Marshall, H., Buchmann-Moller, S., Neufeld, A., Elhanany-Tamir, H., Taketo, M.M., Sommer, L., Krumlauf, R., Tzahor, E., 2007. Cranial neural crest cells regulate head muscle patterning and differentiation during vertebrate embryogenesis. Development 134, 3065-3075.

Rose, C., 2009. Generating, growing and transforming skeletal shape: insights from amphibian pharyngeal arch cartilages. BioEssays : news and reviews in molecular, cellular and developmental biology 31, 287-299.

Rosenfeld, M.G., Lunyak, V.V., Glass, C.K., 2006. Sensors and signals: a coactivator/corepressor/epigenetic code for integrating signal-dependent programs of transcriptional response. Genes & development 20, 1405-1428.

Rowbotham, S.P., Barki, L., Neves-Costa, A., Santos, F., Dean, W., Hawkes, N., Choudhary, P., Will, W.R., Webster, J., Oxley, D., Green, C.M., Varga-Weisz, P., Mermoud, J.E., 2011. Maintenance of silent chromatin through replication requires SWI/SNF-like chromatin remodeler SMARCAD1. Molecular cell 42, 285-296.

Saavalainen, K., Pasonen-Seppanen, S., Dunlop, T.W., Tammi, R., Tammi, M.I., Carlberg, C., 2005. The human hyaluronan synthase 2 gene is a primary retinoic acid and epidermal growth factor responding gene. J Biol Chem 280, 14636-14644.

Savory, J.G., Edey, C., Hess, B., Mears, A.J., Lohnes, D., 2014. Identification of novel retinoic acid target genes. Dev Biol 395, 199-208.

Schwarz, D., Varum, S., Zemke, M., Scholer, A., Baggiolini, A., Draganova, K., Koseki, H., Schubeler, D., Sommer, L., 2014. Ezh2 is required for neural crest-derived cartilage and bone formation. Development 141, 867-877.

Siggens, L., Cordeddu, L., Ronnerblad, M., Lennartsson, A., Ekwall, K., 2015. Transcription-coupled recruitment of human CHD1 and CHD2 influences chromatin accessibility and histone H3 and H3.3 occupancy at active chromatin regions. Epigenetics Chromatin 8, 4.

Simic, R., Lindstrom, D.L., Tran, H.G., Roinick, K.L., Costa, P.J., Johnson, A.D., Hartzog, G.A., Arndt, K.M., 2003. Chromatin remodeling protein Chd1 interacts with transcription elongation factors and localizes to transcribed genes. EMBO J 22, 1846-1856.

Simoes-Costa, M., Bronner, M.E., 2015. Establishing neural crest identity: a gene regulatory recipe. Development 142, 242-257.

Simpson, R.T., 1990. Nucleosome positioning can affect the function of a cis-acting DNA element in vivo. Nature 343, 387-389.

Sims, R.J., 3rd, Chen, C.F., Santos-Rosa, H., Kouzarides, T., Patel, S.S., Reinberg, D., 2005. Human but not yeast CHD1 binds directly and selectively to histone H3 methylated at lysine 4 via its tandem chromodomains. J Biol Chem 280, 41789-41792.

Sive, H.L., Grainger, R.M., Harland, R.M., 2000. Early development of Xenopus laevis : a laboratory manual. Cold Spring Harbor Laboratory Press, Cold Spring Harbor, N.Y. :.

Skene, P.J., Hernandez, A.E., Groudine, M., Henikoff, S., 2014. The nucleosomal barrier to promoter escape by RNA polymerase II is overcome by the chromatin remodeler Chd1. eLife 3, e02042.

Sperber, G.H., Sperber, S.M., Guttmann, G.D., 2010. Craniofacial embryogenetics and development. People's Medical Publishing House, Shelton, Conn.

Sperry, E.D., Hurd, E.A., Durham, M.A., Reamer, E.N., Stein, A.B., Martin, D.M., 2014. The chromatin remodeling protein CHD7, mutated in CHARGE syndrome, is necessary for proper craniofacial and tracheal development. Dev Dyn 243, 1055-1066.

Spicer, A.P., Tien, J.Y., 2004. Hyaluronan and morphogenesis. Birth defects research. Part C, Embryo today : reviews 72, 89-108.

Stokes, D.G., Tartof, K.D., Perry, R.P., 1996. CHD1 is concentrated in interbands and puffed regions of Drosophila polytene chromosomes. Proc Natl Acad Sci U S A 93, 7137-7142.

Strobl-Mazzulla, P.H., Sauka-Spengler, T., Bronner-Fraser, M., 2010. Histone demethylase JmjD2A regulates neural crest specification. Developmental cell 19, 460-468.

Suzuki, A., Sangani, D.R., Ansari, A., Iwata, J., 2016. Molecular mechanisms of midfacial developmental defects. Dev Dyn 245, 276-293.

Suzuki, S., Nozawa, Y., Tsukamoto, S., Kaneko, T., Manabe, I., Imai, H., Minami, N., 2015. CHD1 acts via the Hmgpi pathway to regulate mouse early embryogenesis. Development 142, 2375-2384.

Swartz, M.E., Sheehan-Rooney, K., Dixon, M.J., Eberhart, J.K., 2011. Examination of a palatogenic gene program in zebrafish. Dev Dyn 240, 2204-2220.

Szabo-Rogers, H.L., Smithers, L.E., Yakob, W., Liu, K.J., 2010. New directions in craniofacial morphogenesis. Dev Biol 341, 84-94.

Tahir, R., Kennedy, A., Elsea, S.H., Dickinson, A.J., 2014. Retinoic acid induced-1 (Rai1) regulates craniofacial and brain development in Xenopus. Mech Dev 133, 91-104.

Tai, H.H., Geisterfer, M., Bell, J.C., Moniwa, M., Davie, J.R., Boucher, L., McBurney, M.W., 2003. CHD1 associates with NCoR and histone deacetylase as well as with RNA splicing proteins. Biochemical and biophysical research communications 308, 170-176.

Taylor, W.R., Van Dyke, G.C., 1985. Revised procedures for staining and clearing small fishes and other vertebrates for bone and cartilage study. Cybium 9, 107-120.

Tien, J.Y., Spicer, A.P., 2005. Three vertebrate hyaluronan synthases are expressed during mouse development in distinct spatial and temporal patterns. Dev Dyn 233, 130-141.

Urvalek, A., Laursen, K.B., Gudas, L.J., 2014. The roles of retinoic acid and retinoic acid receptors in inducing epigenetic changes. Sub-cellular biochemistry 70, 129-149.

Urvalek, A.M., Gudas, L.J., 2014. Retinoic acid and histone deacetylases regulate epigenetic changes in embryonic stem cells. J Biol Chem 289, 19519-19530.

van der Velden, Y.U., Wang, L., Querol Cano, L., Haramis, A.P., 2013. The polycomb group protein ring1b/rnf2 is specifically required for craniofacial development. PLoS One 8, e73997.

Wan, M., Liang, J., Xiong, Y., Shi, F., Zhang, Y., Lu, W., He, Q., Yang, D., Chen, R., Liu, D., Barton, M., Songyang, Z., 2013. The trithorax group protein Ash2l is essential for pluripotency and maintaining open chromatin in embryonic stem cells. J Biol Chem 288, 5039-5048.

Wedden, S.E., Ralphs, J.R., Tickle, C., 1988. Pattern formation in the facial primordia. Development 103 Suppl, 31-40.

White, R.M., Cech, J., Ratanasirintrawoot, S., Lin, C.Y., Rahl, P.B., Burke, C.J., Langdon, E., Tomlinson, M.L., Mosher, J., Kaufman, C., Chen, F., Long, H.K., Kramer, M., Datta, S., Neuberg, D., Granter, S., Young, R.A., Morrison, S., Wheeler, G.N., Zon, L.I., 2011. DHODH modulates transcriptional elongation in the neural crest and melanoma. Nature 471, 518-522.

Williams, S.R., Aldred, M.A., Der Kaloustian, V.M., Halal, F., Gowans, G., McLeod, D.R., Zondag, S., Toriello, H.V., Magenis, R.E., Elsea, S.H., 2010. Haploinsufficiency of HDAC4 causes brachydactyly mental retardation syndrome, with brachydactyly type E, developmental delays, and behavioral problems. American journal of human genetics 87, 219-228.

Wu, J.R., Gilbert, D.M., 1996. A distinct G1 step required to specify the Chinese hamster DHFR replication origin. Science (New York, N.Y.) 271, 1270-1272.

Yoshida, M., Horinouchi, S., Beppu, T., 1995. Trichostatin A and trapoxin: novel chemical probes for the role of histone acetylation in chromatin structure and function. BioEssays : news and reviews in molecular, cellular and developmental biology 17, 423-430.

Zentner, G.E., Layman, W.S., Martin, D.M., Scacheri, P.C., 2010. Molecular and phenotypic aspects of CHD7 mutation in CHARGE syndrome. Am J Med Genet A 152a, 674-686.

Zhang, Z., Jones, A.E., Wu, W., Kim, J., Kang, Y., Bi, X., Gu, Y., Popov, I.K., Renfrow, M.B., Vassylyeva, M.N., Vassylyev, D.G., Giles, K.E., Chen, D., Kumar, A., Fan, Y., Tong, Y., Liu, C.F., An, W., Chang, C., Luo, J., Chow, L.T., Wang, H., 2017. Role of

remodeling and spacing factor 1 in histone H2A ubiquitination-mediated gene silencing. Proc Natl Acad Sci U S A 114, E7949-e7958.

Zhou, J., Chau, C.M., Deng, Z., Shiekhattar, R., Spindler, M.P., Schepers, A., Lieberman, P.M., 2005. Cell cycle regulation of chromatin at an origin of DNA replication. Embo j 24, 1406-1417.

APPENDIX: DEVELOPING METHODS TO UNCOVER MECHANISMS REGULATED BY CHD1

The misexpression of some genes in Chd1 morphants prompted a closer examination of how these genes are misexpressed. *Chd1*$^{-/-}$ ESCs have lower transcriptional output (Guzman-Ayala et al., 2015), and this raised the question of whether transcriptional output was reduced in *X. laevis* Chd1 morphants. Further, Chd1 interacts with transcriptional elongation factors including the PAF and FACT complexes (Simic et al., 2003) and facilitates release of RNA polymerase II into productive elongation (Skene et al., 2014). This prompted an investigation into whether transcriptional elongation was affected in Chd1 morphants.

RNA isolated from 30 embryo heads was analyzed with qRT-PCR to examine whether or not reduced Chd1 expression results in defects in transcriptional elongation. Embryos were injected with 65-75ng of Chd1-MO, or an equal amount of control morpholino at the 1-cell stage, and then raised to stage 29-30 (35-37.5 hpf). At this stage, the heads of these embryos were dissected and collected for isolation of RNA. Next, two sets of primers were used for qRT-PCR to determine whether there were differences in the expression levels of the 5' and 3' regions of ap2, has2, and msx2. These genes were chosen because their expression was reduced in Chd1 morphants. One set of primers

was designed to target the 5’ end of each gene and the second set of primers was designed to target the 3’ end of each gene. The expression levels from the 5’ primer set were compared to the expression levels from the 3’ primer set following qRT-PCR. If the expression levels from the 3’ primer set were different than the expression levels from the 5’ primer set in Chd1 morphants, then this would suggest that transcriptional elongation was misregulated. Overall, there was little change between 5’ and 3’ expression of *ap2*, *has2*, and *msx2* when these were normalized to *gapdh* expression. This may suggest that transcriptional elongation was not affected in the genes with decreased Chd1 expression. However, this experimental design may not have been sensitive enough to detect if there were truly any changes.

An important factor in the design of this assay was that housekeeping gene was not affected by loss of Chd1. Close inspection of *gapdh* revealed that there was very little change in expression of this housekeeping gene in Chd1 morphants. However, if *gapdh* was also affected in Chd1 morphants, then this assay would not detect changes in transcriptional elongation when the genes were normalized to *gapdh*. If a suitable housekeeping gene was not available, one alternative approach would be to use spike-in RNAs for normalization.

TABLES AND FIGURES

Table A.1: *Primer sequences for qRT-PCR*

Primer Name	Primer Sequence
Ap2-F-5’	CGCAGTGCTACAGGTTATTC
Ap2-R-5’	CCGCTTCAAATCTCACAGTC
Ap2-F-3’	ACGTTGAGGACCAGAGTATC
Ap2-R-3’	GAACACCTCGTTGGGATTG
Has2-F-5’	TCTCCTTTGGACTCTATGGG
Has2-R-5’	GGTGTTCCAGAAAGGCAA
Has2-F-3’	GGTCTTCATGTCCCTCTACT
Has2-R-3’	CCAACCTGCCTTGTTGAT
Msx2-F-5’	TCCCAGGAGGATCAAAGAG
Msx2-R-5’	GAAAGGGAGGCTGGAGAT
Msx2-F-3’	CTCCAGGAAGCGGAAATAG
Msx2-R-3’	CAGCCTGAATAGGAGAGTTG
Gapdh-F-5’	GCGGCAAAGTTCAAGTCA
Gapdh-R-5’	TCTCAGCCTTAACGGTTCC
Gapdh-F-3’	ATCAAGGCCGCCATTAAG
Gapdh-R-3’	CAAAGATGGAGGAGTGAGTG

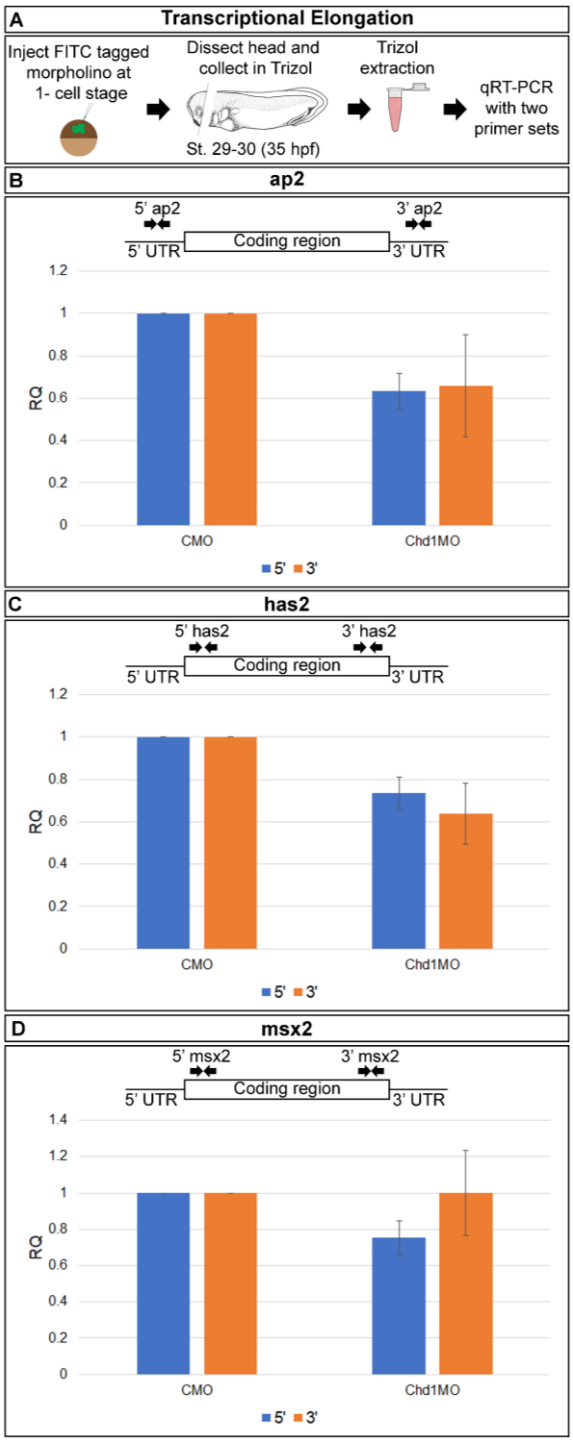

Figure A.1: *Decreased Chd1 expression does not affect transcriptional elongation. (A)Schematic of experimental design for testing for defects in transcriptional elongation. (B-D) Decreased Chd1 does not affect transcriptional elongation of ap2, has2, and msx2.*

VITA

Brent Hardin Wyatt was born on November 8, 1982 in Charlotte, North Carolina and is an America citizen. He graduated from Harding High School, Charlotte, North Carolina in 2001. He received his Bachelor of Science in Biology from East Carolina University, Greenville, North Carolina in 2009. He received his Master of Science in Molecular Biology and Biotechnology from East Carolina University, Greenville, North Carolina in 2013.